NASA CR-54968
APS-5211-R

BRAYTON CYCLE
3.2-INCH RADIAL COMPRESSOR
PERFORMANCE EVALUATION

prepared for

National Aeronautics and Space Administration

Contract NAS3-6463

GARRETT

AIRESEARCH MANUFACTURING COMPANY OF ARIZONA
A DIVISION OF THE GARRETT CORPORATION
PHOENIX, ARIZONA

MP-13432

Requests for copies of this report should be referred to

National Aeronautics and Space Administration
Office of Scientific and Technical Information
Attention: ATSS
Washington, D.C. 20546

NASA CR-54968
APS-5211-R

BRAYTON CYCLE
3.2-INCH RADIAL COMPRESSOR
PERFORMANCE EVALUATION

prepared for
National Aeronautics and Space Administration

by

AiResearch Manufacturing Company of Arizona
G. L. Perrone
H. H. Milligan

May 1966

Contract NAS3-6463

Technical Management
NASA Lewis Research Center
Cleveland, Ohio 44135
Space Power Systems Division
Jack A. Heller
Technical Specialist
Fluid Systems Components Division
Calvin L. Ball

GARRETT

AIRESEARCH MANUFACTURING COMPANY OF ARIZONA
A DIVISION OF THE GARRETT CORPORATION
PHOENIX, ARIZONA

FORWARD

This report describes the evaluation program conducted by the AiResearch Manufacturing Company of Arizona, a division of The Garrett Corporation, on Contract NAS3-6463, Brayton Cycle 3.2-inch Radial Compressor Performance Evaluation for the Lewis Research Center of the National Aeronautics and Space Administration. The objective of the program is to determine the performance characteristics of a small radial compressor operating at high speed over a wide compressor Reynolds number range.

TABLE OF CONTENTS

LIST OF FIGURES

LIST OF FIGURES (CONTD.)

LIST OF FIGURES (CONTD.)

BRAYTON CYCLE
3.2-INCH RADIAL COMPRESSOR
PERFORMANCE EVALUATION

SUMMARY

29906

A test program was undertaken to determine the overall and component efficiencies of an existing compressor stage (3.2 inch diameter impeller) over a wide range of Reynolds numbers. A redesigned diffuser was also tested to determine design capability in improving peak performance at low compressor inlet pressure conditions. Results indicate that although the diffuser efficiency was slightly increased at the lower Reynolds numbers, some improvement could also be noted at all pressure levels. Reasonable correlation is obtainable for stage efficiency versus Reynolds number.

The program confirmed that it is possible to predict the performance of a given compressor geometry in one fluid from data taken in another fluid.

Test results indicate that an improvement in the art of temperature sensing, at low fluid flows and pressures, is desired.

Cauthen

INTRODUCTION

The NASA-Lewis Research Center is currently engaged in an investigation of Brayton-cycle space-power systems that use solar or nuclear energy as the heat source and an inert gas as the working fluid. Optimum Brayton-cycle systems with output powers above 10 kw_e have reasonable turbomachinery designs with nominal cycle pressures. However, the low power systems require low compressor inlet pressures. The effect of low Reynolds numbers on radial-flow compressor performance was not well established, as with axial flow compressors, and required further evaluation in order to achieve better predictability criteria.

Results of performance tests on Brayton-cycle compressors with nominal inlet pressures have shown that high efficiencies (up to 80 percent total-to-total) can be obtained. However, with the same test hardware utilized at low inlet pressures, test results indicate that efficiencies are reduced due to the Reynolds number effects. Consideration was given to the generation of a new diffuser, designed specifically for the lower Reynolds number range. The ability to design a diffuser for low Reynolds number operation was subject to some doubt. Actual design and test would thus demonstrate this capability.

An advantage of the Brayton cycle is the flexibility of testing the turbomachinery on air and, with the air performance results, predicting the performance that would be achieved on an inert gas such as argon. Prediction procedures based on matching velocity triangles at the inducer and vane diffuser inlet have been established and verified by test results with compressors at nominal inlet pressures. Verification of the performance prediction procedures has not been accomplished with low compressor inlet pressures (down to 2 psia).

Therefore a two-part test program was undertaken, the first to determine the effects of Reynolds number on the performance of a given compressor configuration and the second, to determine if improvements in performance in the low Reynolds number range could be achieved by designing the diffuser for this range. The tests were to be conducted by utilizing an existing 3.2-inch diameter radial compressor assembly, previously evaluated under Air Force Contract AF33(657)-11721.

The Compressor Assembly Part 369740, and two additional Diffusers, Parts 369748-10 and -20, were authorized for use in the program as required. As part of the program, a new Diffuser Part 871034 was designed and fabricated for low range evaluation.

The design characteristics of the test compressor as received were:

Inlet pressure, psia	31
Inlet temperature, $^{\circ}$R	540
Speed, rpm	64,000
Argon flow rate, lbs per sec.	1.216
Pressure ratio	2.06
Impeller outside diameter, inches	3.2

PROGRAM REQUIREMENTS

Testing with Existing Hardware

With the use of the existing impeller, diffuser, and scroll, performance tests were to be conducted using air as the working fluid at inlet pressures of 24.0, 15.0, 7.0, 4.0, and 2.0 psia each at shaft speeds of 70, 80, 90, and 100 percent of design speed. A minimum of 7 data points were to be observed at each combination of speed and inlet pressure. Check runs with argon as the working fluid were to be conducted at an equivalent design speed and inlet pressures of 24.0, 15.0, and 7.0 psia each at weight flows corresponding to surge, peak efficiency, and choke.

The compressor was to be instrumented so that at least three values of static and total pressures, and total temperatures at the inlet and discharge could be measured. In addition, one diffuser passage was to be instrumented so that a performance breakdown between the impeller, diffuser, and scroll could be estimated.

The air performance data at the five pressure levels was to be utilized to calculate the equivalent performance in argon. The validity of the performance predictions was to be checked by comparing the argon data with the computed argon performance.

Low Reynolds Number Diffuser

A new diffuser, optimized for the Reynolds number corresponding to a 4 psia inlet pressure, was to be designed and fabricated. One flow passage of the new diffuser was to be instrumented to provide diffuser data so that a performance breakdown between the impeller, diffuser, and scroll could be provided.

Testing with the new diffuser was to be identical with the testing outlined for the existing hardware except that the argon check runs were to be performed at compressor inlet pressures of 15.0 and 7.0 psia only.

NOMENCLATURE

CPR	Coefficient of pressure recovery $= \dfrac{P_{s_3} - P_{s_2}}{P_2 - P_{s_2}}$
D_T	Impeller tip diameter, inches
N	Physical shaft speed, rpm = 64,000 for air; 62,000 for argon
	$N/\sqrt{\theta}$ = 62,745 for air testing; 60,783 for argon testing
P	Pressure, psia or in. Hg Abs. as noted
r_c	Compressor pressure ratio $= P_3/P_1$
Re	Compressor Reynolds number $= \dfrac{\rho_1 U_T D_T}{12\mu}$
ΔT	Impeller temperature rise, $^{\circ}F$
T	Total temperature, $^{\circ}R$
U_T	Impeller tip speed, ft. per sec.
W	Weight flow rate, lbs. per sec.
β	Flow angle measured from the radial direction, degrees
γ	Ratio of specific heats = 1.395 for air; 1.666 for argon
δ	P/14.696
θ	T/518.7
μ	Gas viscosity, lbs per ft-sec.
ρ	Gas density, lbs per cu. ft.

η_C Compressor efficiency $= \dfrac{r_c^{\frac{\gamma-1}{\gamma}} - 1}{\left(\frac{\Delta T}{T_1}\right)_{actual}}$

η_D Diffuser efficiency $= \dfrac{\left(\frac{P_{s_3}}{P_{s_2}}\right)^{\frac{\gamma-1}{\gamma}} - 1}{\frac{T_{s_3}}{T_{s_2}} - 1}$

Subscripts

1 Compressor inlet conditions

2 Diffuser inlet conditions

3 Diffuser - scroll exit conditions

is Isentropic

s Static conditions

APPARATUS, INSTRUMENTATION, AND PROCEDURE

Figure 1 shows the existing compressor scroll and diffuser, together with the impeller mounted in the ball-bearing test package. Components of the entire test package are shown in Figure 2.

Compressor tests were conducted using a closed loop with both air and argon test fluids. The test system, located at the AiResearch test facilities in Phoenix, Arizona, is shown in Figure 3 during installation and in Figure 4 with the compressor installed and the loop insulated.

The loop is fabricated from stainless steel tubing of a nominal 4-inch diameter with appropriate transitions to the inlet and discharge of the compressor and other components in the loop. Welded joints were used throughout with the exception of flanged joints at the compressor and motorized control valve.

The components of the loop consisted of:

1. Measuring orifice section
2. Motorized valve
3. Filter
4. Vacuum pump
5. Compressor
6. Drive turbine
7. Heat exchanger (cooler)
8. Cooling turbine and heat exchanger
9. Instrumentation

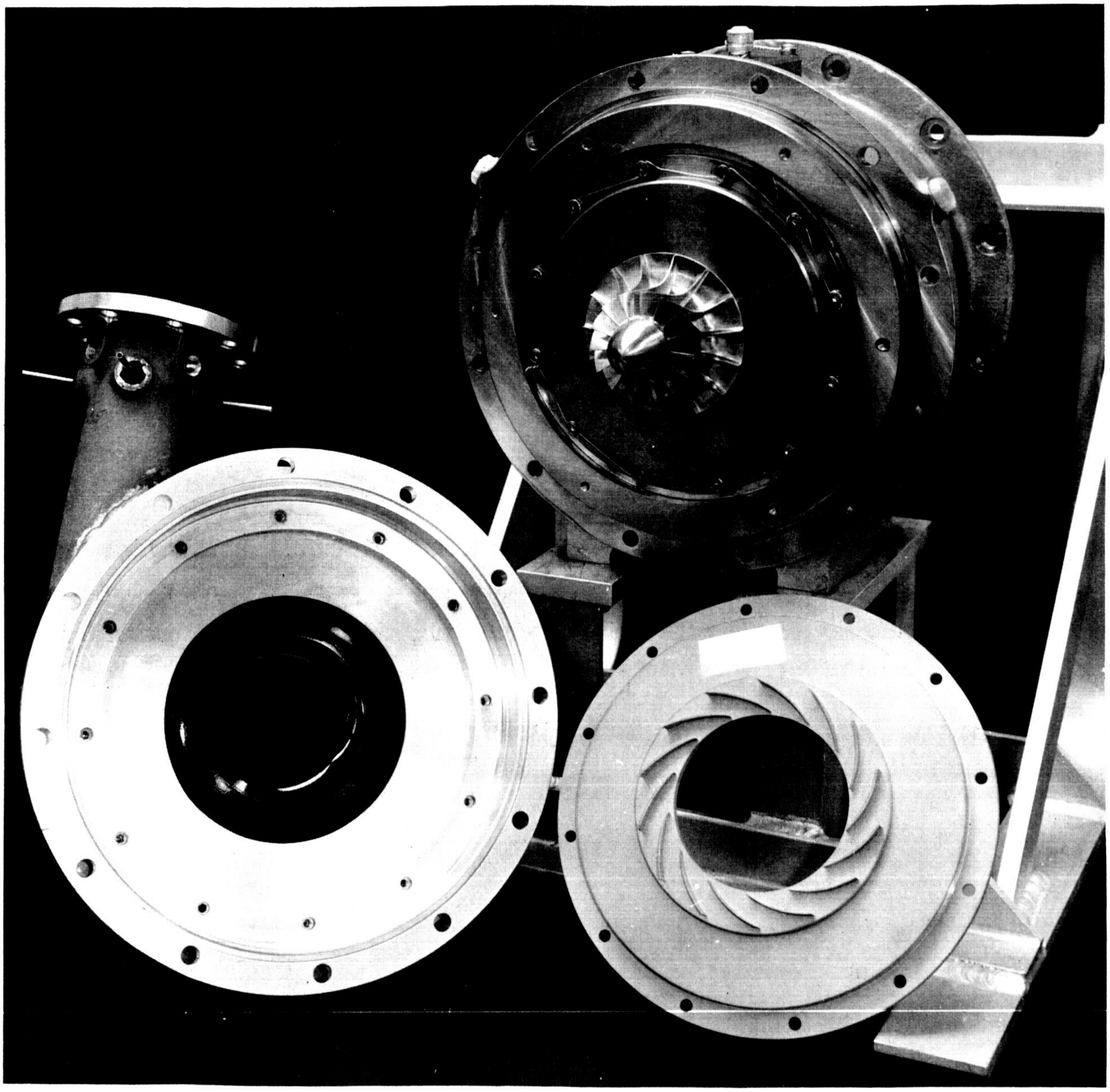

EXISTING RESEARCH COMPRESSOR PACKAGE
FIGURE 1

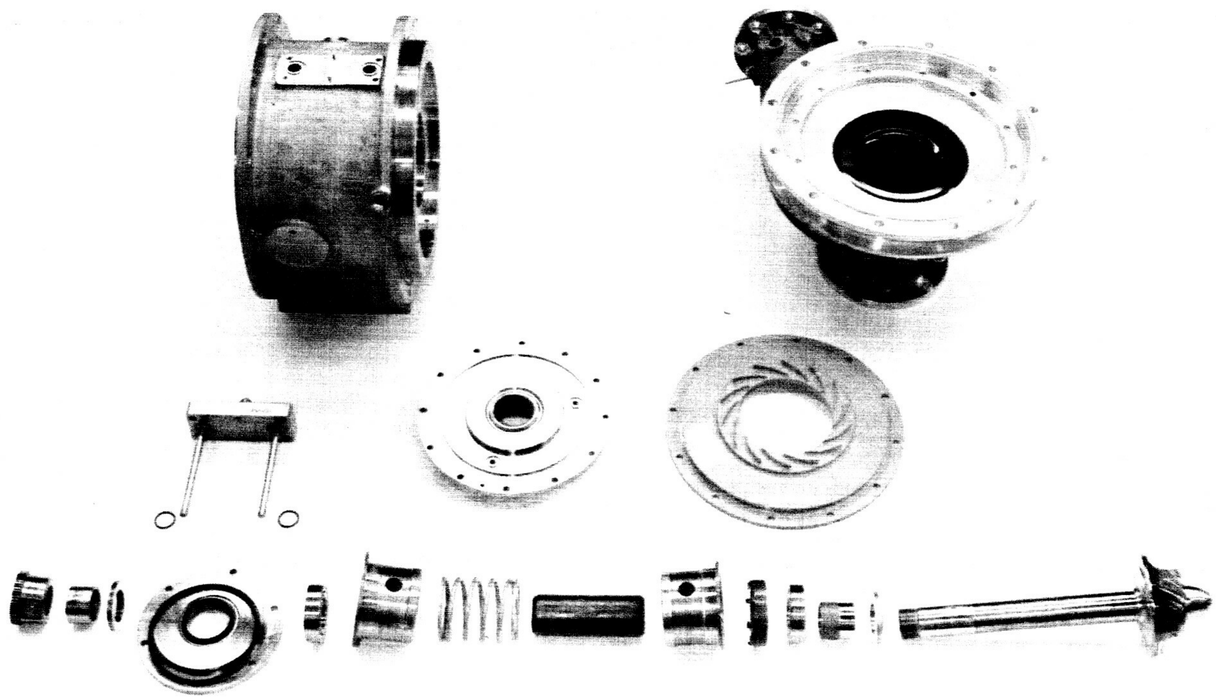

RESEARCH COMPRESSOR PACKAGE COMPONENTS

FIGURE 2

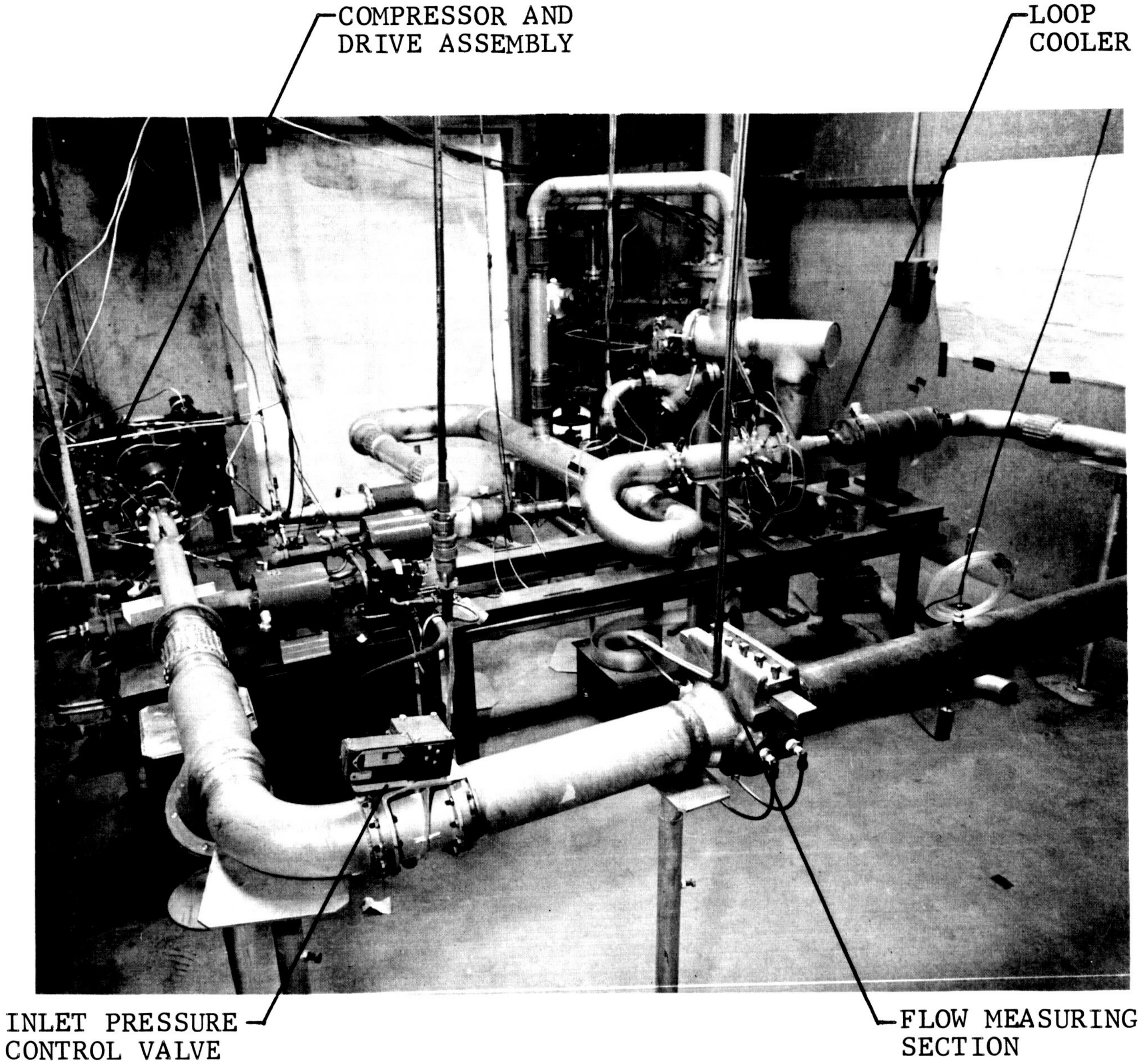

CLOSED BRAYTON-CYCLE TURBOMACHINERY TEST LOOP

FIGURE 3

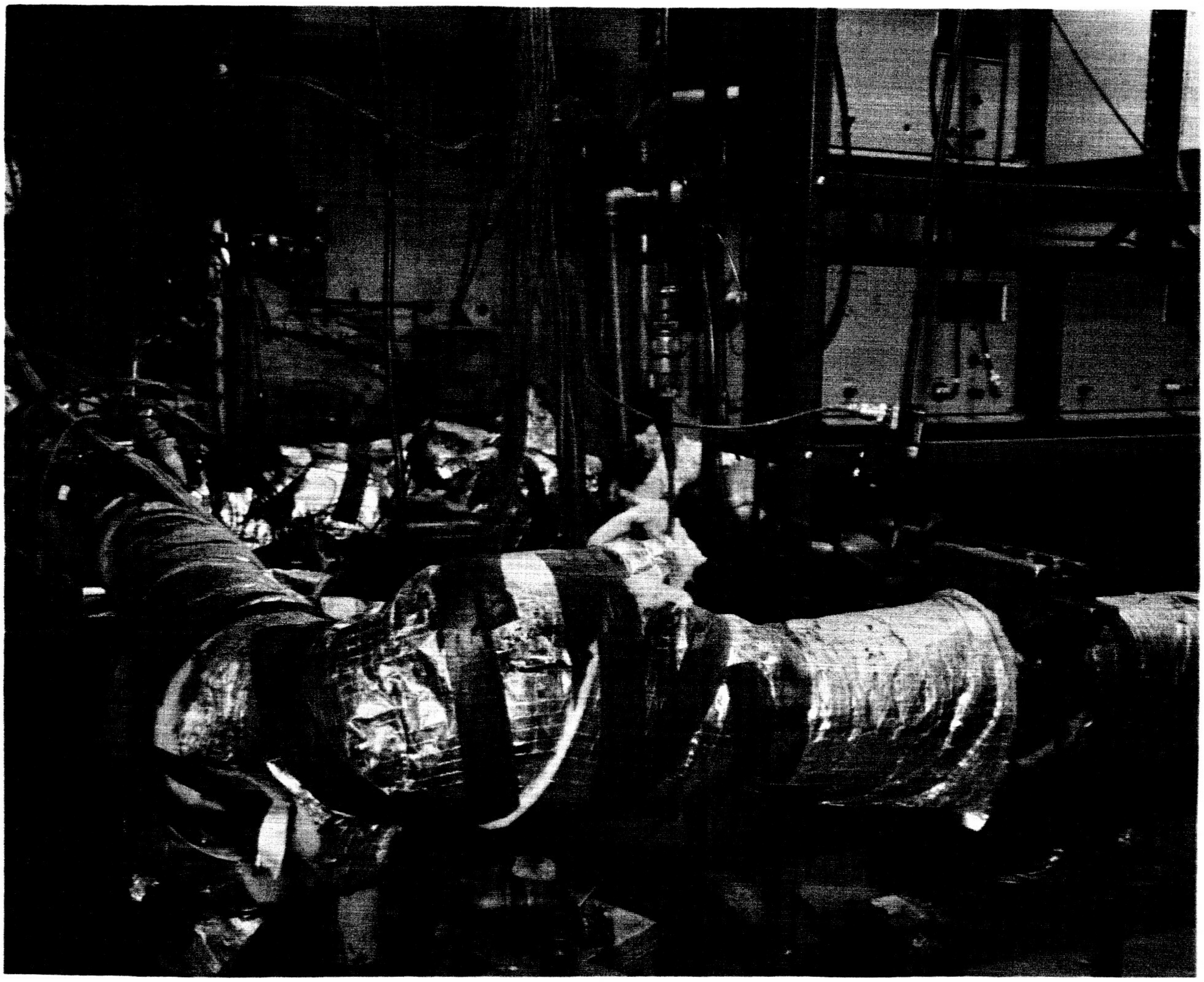

COMPRESSOR TEST LOOP WITH
COMPRESSOR INSTALLED AND LOOP INSULATED

FIGURE 4

A 4-inch measuring section was used with a range of orifice plates in order to maintain a reasonably constant pressure drop as flows were varied during the tests.

The motorized valve was used to control the pressure ratio across the test compressor and set each test condition.

The filter was used as a precaution against the induction of any particle which might damage the impeller blades. The filter body was also the station for evacuation of the loop by the vacuum pump.

The vacuum pump was used to purge the loop of air and to control the pressure level of the argon during the test. (As the pressure ratio of the compressor was varied, the loop pressures would change, which would require the addition or removal of gas to maintain a constant compressor inlet pressure.)

The compressor under test was installed in the loop by use of flanged joints. Such an arrangement permitted the easy removal of the compressor from the loop for changes of the diffuser. The compressor and inlet and discharge ducting were insulated with 1 inch of foil-backed Fiberglas during all testing to facilitate accurate temperature-rise measurement.

The compressor was driven through a quill shaft by an air turbine motor. The speed of the turbine was controlled by a pneumatically controlled valve installed in the plant air system.

A water-cooled gas heat-exchanger was installed in the loop to control the compressor inlet gas temperature. Motorized valves on the water side of the heat exchanger permitted control of the compressor inlet gas temperature to within $\pm 1^{\circ}F$.

At compressor flows and pressure ratios where full flow of the plant water supply would not control the loop gas temperature to the desired values, chilled water from a second air-to-water heat exchanger was piped through the loop heat exchanger. The water was chilled by air from an air-driven cooling turbine.

The basic compressor instrumentation consisted of thermocouples, static pressure taps, and total pressure probes in the inlet and discharge of the compressor. The location and number of this instrumentation can be seen in Figure 5. In addition, static pressure taps and total pressure probes were installed in one compressor diffuser passage so that diffuser performance could be evaluated. A total of 4 thermocouples were also installed at four locations in the diffuser discharge. The location and number of this instrumentation is shown in Figures 5 and 6. The remaining data to be measured consisted of total pressure, temperature, and orifice ΔP at the closed loop orifice section and shaft speed of the compressor. All data was recorded on a Systron Digital Recorder system.

The compressor inlet duct contained six chromel-alumel thermocouples with duct immersions given in Table I. Five of these thermocouples were connected to an AiResearch designed Temperature Scanner device which sensed each temperature and relayed a millivolt signal to the digital recorder. The sixth thermocouple was connected to the test cell Brown indicator to permit control of the compressor inlet temperature by the test technician.

COMPRESSOR TEST PACKAGE
INSTRUMENTATION
FIGURE 5

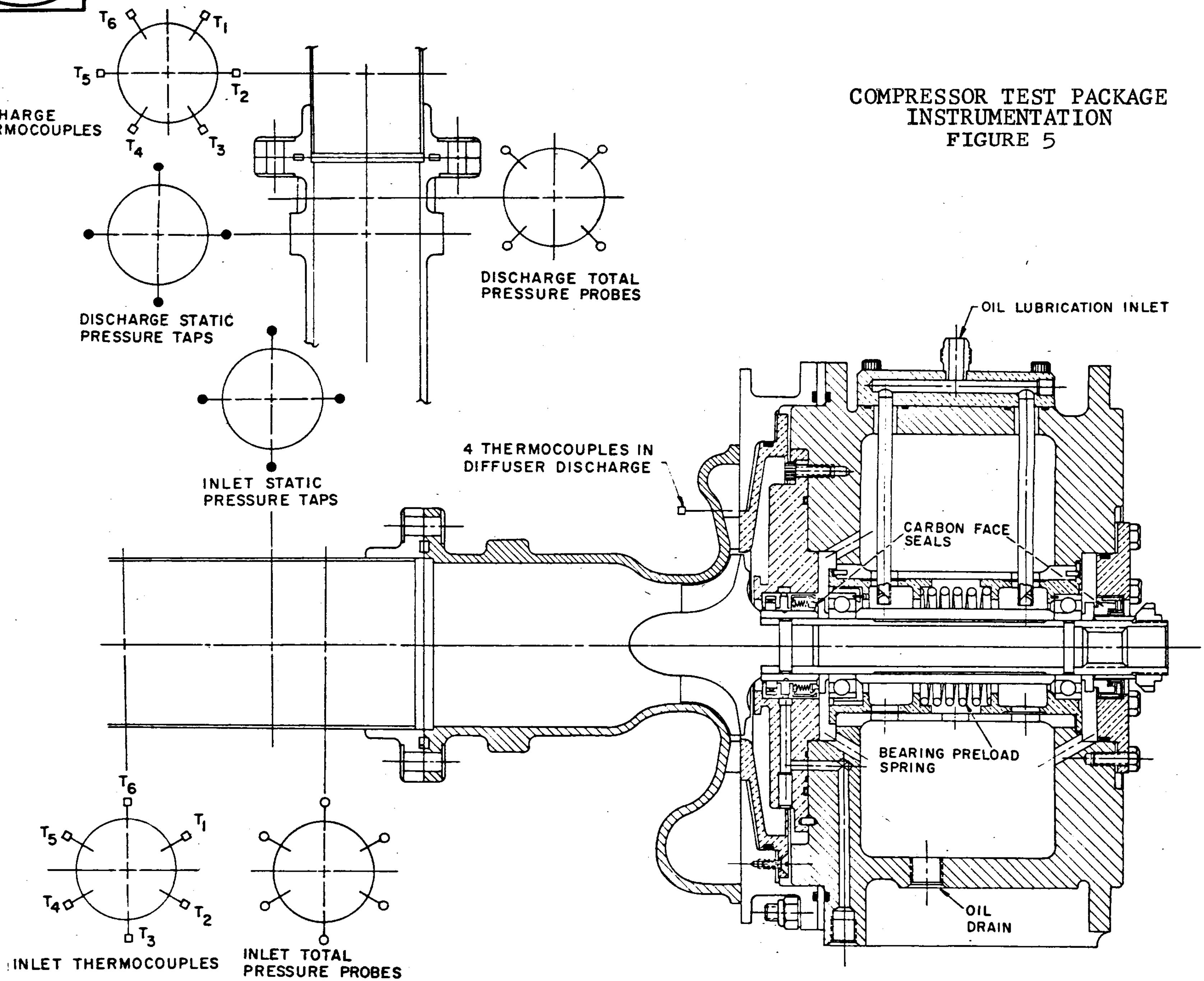

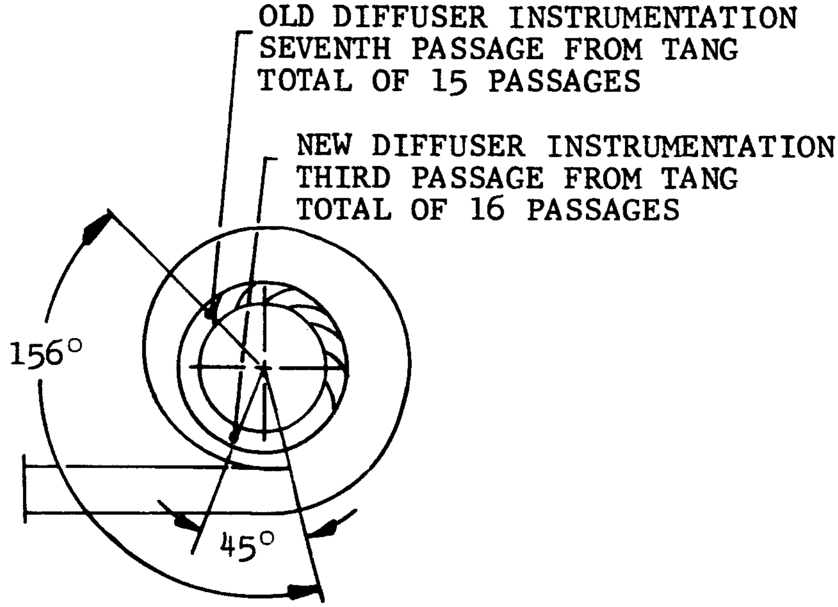

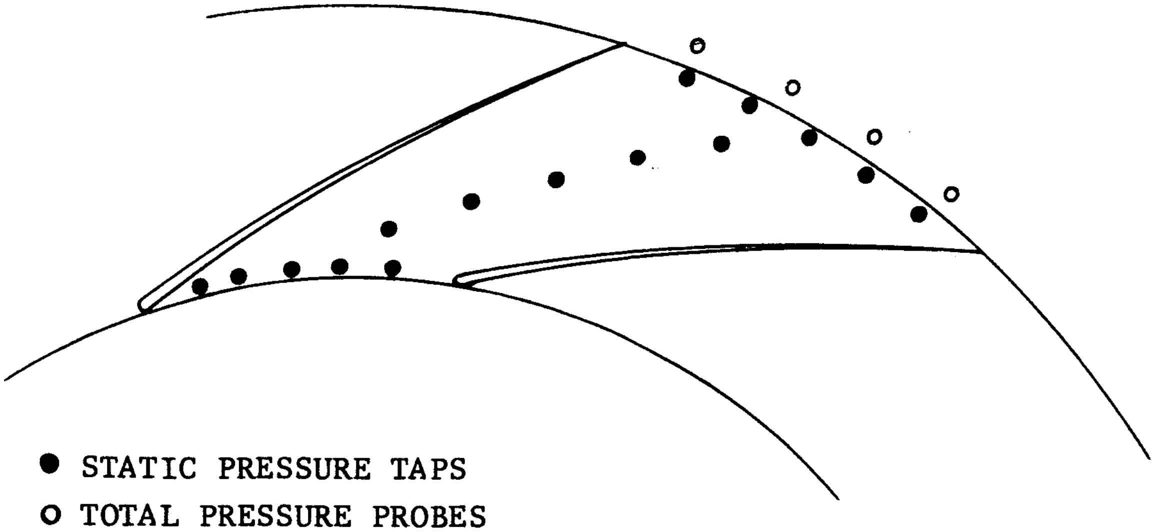

DIFFUSER PASSAGE INSTRUMENTATION
TYPICAL BOTH DIFFUSERS
AS NOTED

FIGURE 6

TABLE I

THERMOCOUPLE IMMERSION DEPTHS

INLET DUCT

Thermocouple		Depth(Inch)
1	MANUAL ON PANEL	0.09
2		0.36
3		0.82
4		0.09
5		0.36
6		0.82

DISCHARGE DUCT

Thermocouple		Depth(Inch)
1	MANUAL ON PANEL	0.41
2		0.27
3		0.55
4		0.41
5		0.27
6		0.55

Four static pressure taps in the inlet duct were manifolded together and the average static pressure was routed to an AiResearch Pressure Scanner device which relayed a millivolt signal to the digital recorder. Six total pressure probes in the inlet duct were individually connected to the Pressure Scanner device. In addition, a separate differential pressure transducer was connected between the manifolded static pressures and one of the total pressure probes to provide a ΔP measurement to the digital recorder.

The compressor diffuser and scroll were instrumented for both static and total pressures. The diffuser was instrumented to provide 15 static pressures between adjoining blades, and 4 total pressures and 4 temperatures at the outer radius of the diffuser passage as shown in Figures 5 and 6. Two separate sets of diffuser instrumentation were provided: for the reference diffuser (Part 369738-20, 31-psia design), and the new diffuser (Part 871034, 4-psia design).

The compressor discharge duct contained 4 static pressure taps manifolded together and 4 total pressure probes individually connected to the Pressure Scanner. The delta pressure between the manifolded static pressures and one total pressure port was measured by a separate differential pressure transducer. All pressure measurements were recorded by the digital recorder.

As in the compressor inlet duct, six chromel-alumel thermocouples were installed in the compressor discharge duct. Five were connected to the temperature scanner device and the sixth to the test cell Brown indicator. Thermocouple immersion depths are shown in Table I.

A differential pressure transducer with a range of 0-50 inches of water was used at the loop orifice plate to measure the orifice pressure drop. Accuracy of this transducer was within ±1/2 percent of full scale. Repeatability was consistent as displayed by the choke flows recorded. The transducer output was recorded by the digital recorder.

The pressure scanner valve device consisted of a 50 port Scanivalve (shown in Figure 7) which incorporates an absolute pressure zero to 150 in. Hg pressure transducer. An accurate calibration of this item is shown in Figure 34.

Pressure measurements were accurate to within 0.04-inch mercury and were in reference to a secondary standard mercurial barometer corrected for temperature and geographic location. The automatic solenoid-operated Scanivalve samples each test pressure on command from the digital recorder technician and delivers a millivolt signal to the recorder for each pressure sensed. The volume of the valve and transducer is so minute that no error is introduced in stepping from one pressure to another.

The temperature scanner device, also shown in Figure 7, consists of an automatic, solenoid-operated rotary switch connected between the digital recorder and each thermocouple in the test setup. The scanner device contains a constant 150°F oil bath junction, in which all chromel-alumel thermocouple leads are connected to copper leads, creating two additional secondary thermocouples. These secondary thermocouples, immersed in a constant (150 ±0.1°F) oil bath, generate zero-millivolt output when the thermocouple is also at 150°F, but create a negative-millivolt output when the thermocouple is less than 150°F and a positive millivolt output when the thermocouple is higher than 150°F. The output of each thermocouple circuit is delivered to the digital recorder at the command of the recorder technician. The 150°F bath provides a continuous calibration for each scan of temperatures.

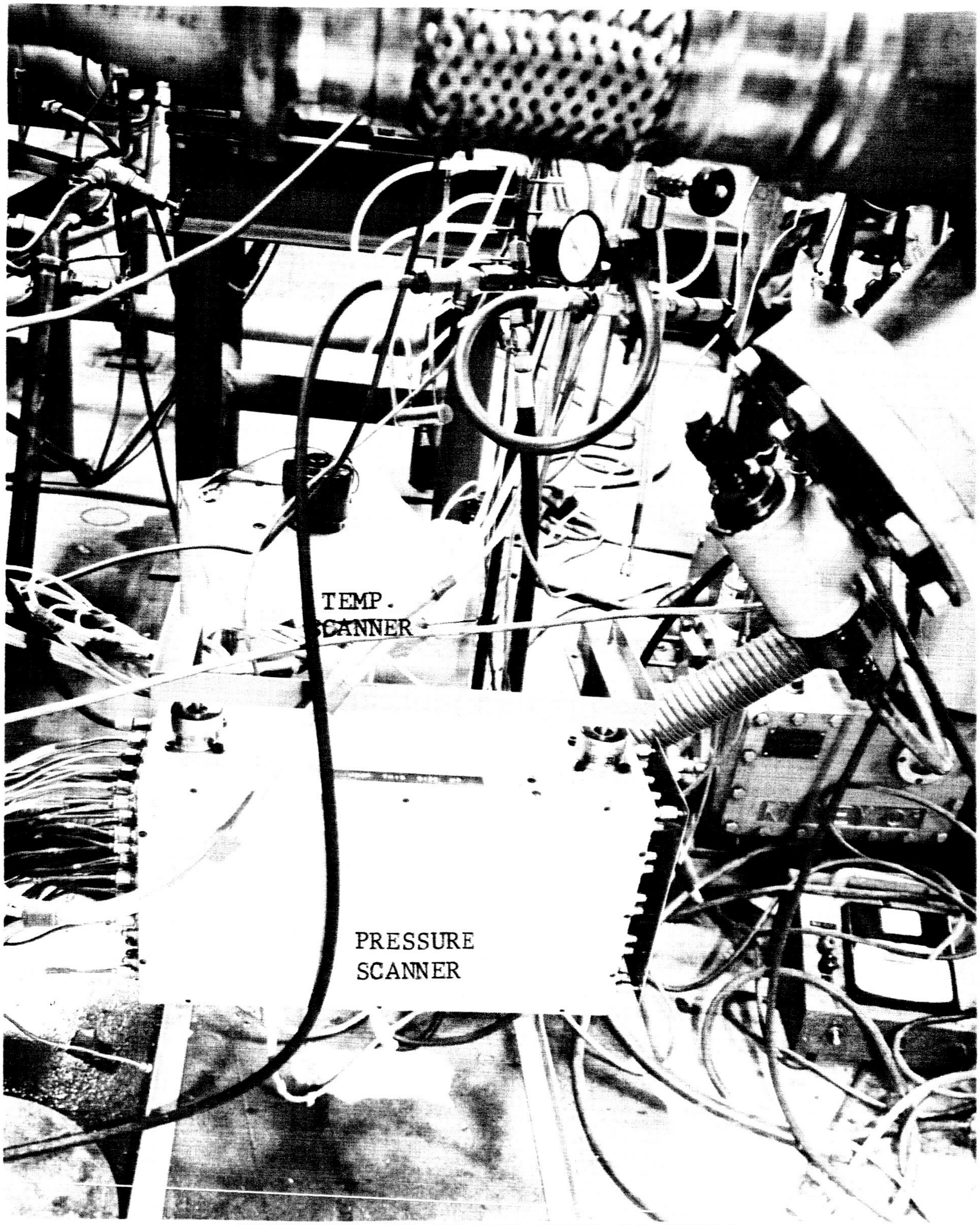

PRESSURE AND TEMPERATURE SCANNERS

FIGURE 7

The specially designed scanner valves were used for proper sequencing of the instrument signals to the digital recorder. This method greatly improves accuracy in data recording. Several com-plate scans of all the instrumentation can be made in a fraction of the time required for a single manual readout; thus, human error is minimized. Furthermore, set data-point conditions need not be held as long to get a complete reading, and the errors due to loop transients are reduced.

COMPRESSOR TESTING

Performance mapping of the subject compressor was conducted in two phases. In Phase I, the original compressor design (Assembly Part 369740 and utilizing Diffuser Part 369748-20) was tested in air at impeller inlet total pressures of 2, 4, 7, 15, and 24 psia. At each pressure level, data was obtained at 100 percent, 90 percent, 80 percent and 70 percent of design physical speed (64,000 rpm) with the impeller inlet total temperature held constant at 540°R.

Following the air testing, partial mapping of the unit was conducted in argon with impeller inlet pressures of 7, 15, and 24 psia at a fixed physical speed of 62,000 rpm which was determined to be the approximate equivalent design speed in argon in accordance with AiResearch velocity triangle matching procedures for estimating argon performance from air data. In the argon mapping, a minimum of the choke, surge and approximate peak overall efficiency points were obtained for each of the three pressure levels investigated.

For each data point the following data was obtained:

Barometric pressure in test cell

Impeller inlet static pressure

Impeller inlet total pressure

Impeller exit static pressure (measured at the diffuser inlet)

Diffuser static pressure distribution (measured along diffuser mean line)

Diffuser exit static pressure

Diffuser exit total pressure

Scroll exit static pressure

Compressor exit total pressure
(measured at scroll exit)

Impeller inlet total temperature

Compressor exit total temperature

Flow orifice inlet total pressure

Flow orifice ΔP

Flow orifice inlet total temperature

Rotational speed

Details concerning the type, number, and exact location of all instrumentation are given in the previous section.

A complete set of data was recorded on digital output tapes with a minimum of two scans of all data taken at each data point.

Plots of the overall performance resulting from Phase I air testing are presented in Figures 8 through 12. On each plot for a fixed inlet pressure, the recorded overall total pressure ratio, total temperature rise, and overall efficiency based on temperature rise are shown. (The dashed lines shown on some of these maps will be discussed later.)

A breakdown of the impeller efficiency, diffuser plus scroll efficiency, diffuser pressure recovery, and diffuser inlet flow angles is given for the air 100 percent speed line for each pressure level in Figure 13 through 17. Definitions of all terms can be found on page 4.

Because of the physical difficulty of installing total pressure probes between the impeller and diffuser, it was necessary to calculate the total pressure at the diffuser inlet. This can be accomplished with good accuracy by assuming a reasonable value for the

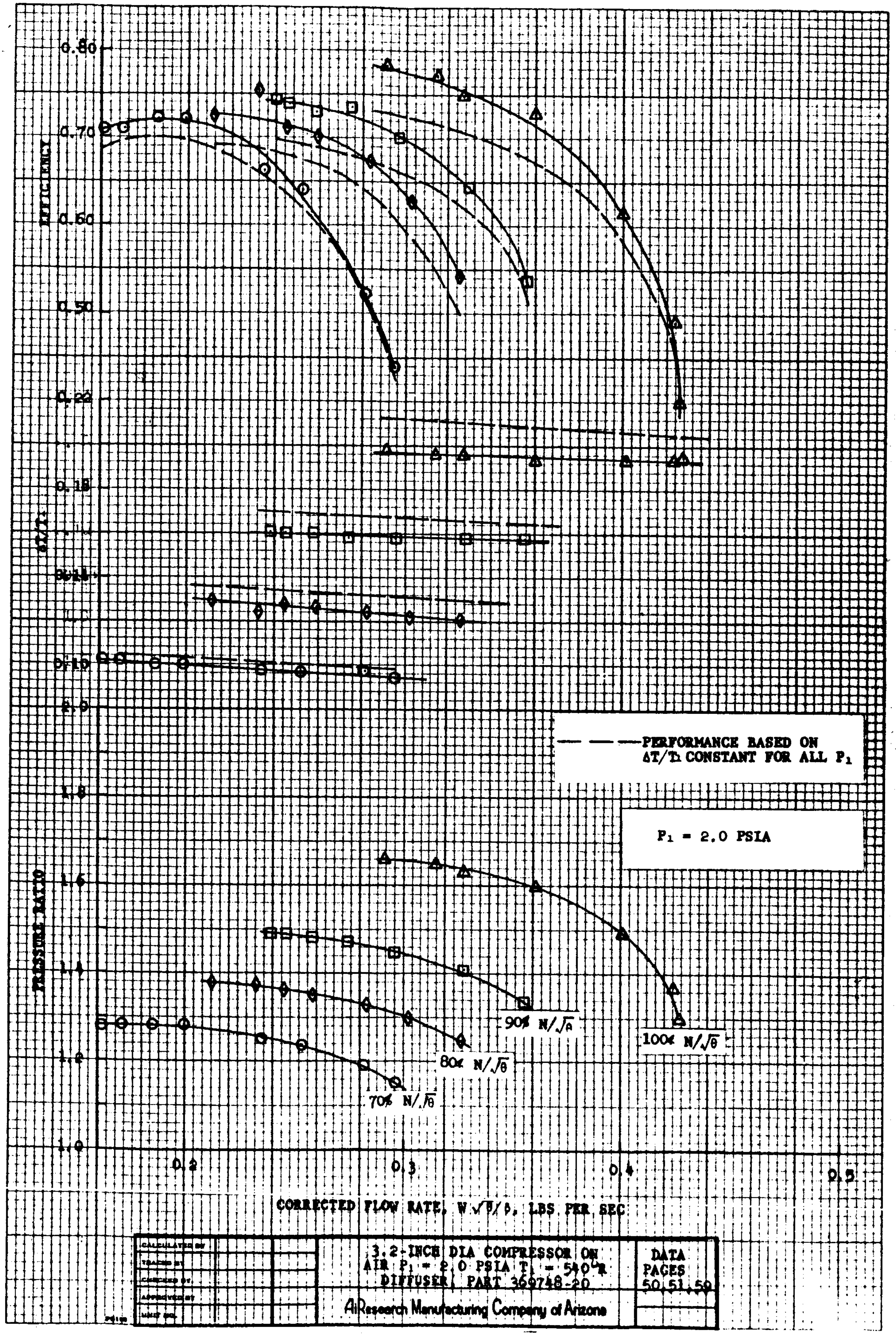

EFFICIENCY
0.80
0.70
0.60
0.50
$\Delta T/T_1$
PRESSURE RATIO
2.0
1.8
1.6
1.4
1.2
1.0
0.2
0.3
0.4
0.5
— — — PERFORMANCE BASED ON $\Delta T/T_1$ CONSTANT FOR ALL P_1
P_1 = 2.0 PSIA
100% $N/\sqrt{\theta}$
90% $N/\sqrt{\theta}$
80% $N/\sqrt{\theta}$
70% $N/\sqrt{\theta}$
CORRECTED FLOW RATE, $W\sqrt{\theta}/\delta$, LBS PER SEC
3.2-INCH DIA COMPRESSOR ON AIR P_1 = 2.0 PSIA T_1 = 540°R DIFFUSER, PART 369748-20
DATA PAGES 50,51,59
AiResearch Manufacturing Company of Arizona

FIGURE 8

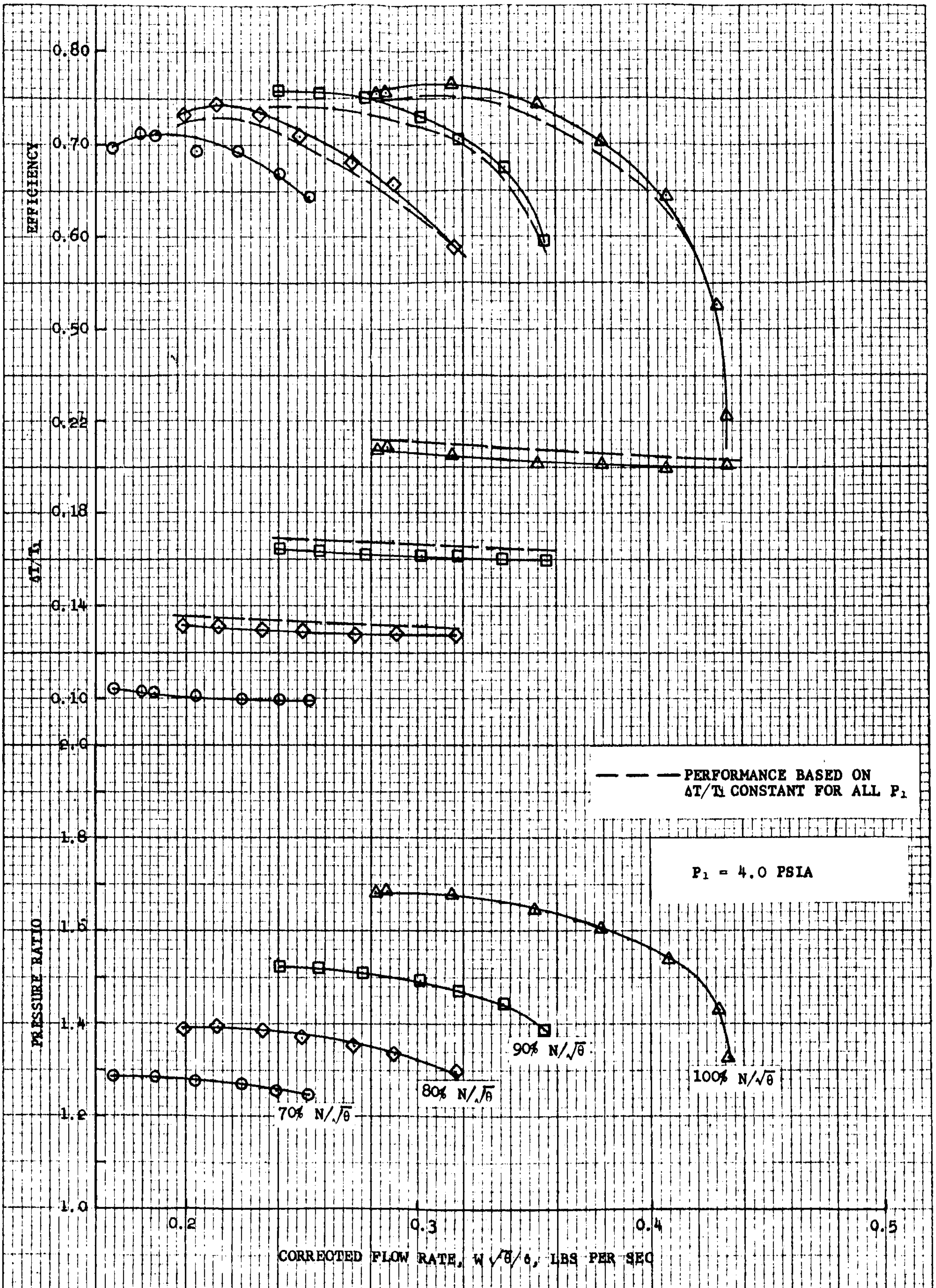

CALCULATED BY			3.2-INCH DIA COMPRESSOR ON AIR P_1 = 4.0 PSIA T_1 = 540°R DIFFUSER, PART 369748-20	DATA PAGES 51, 52, 58, 59
TRACED BY				
CHECKED BY				
APPROVED BY			AiResearch Manufacturing Company of Arizona	
UNIT NO.				

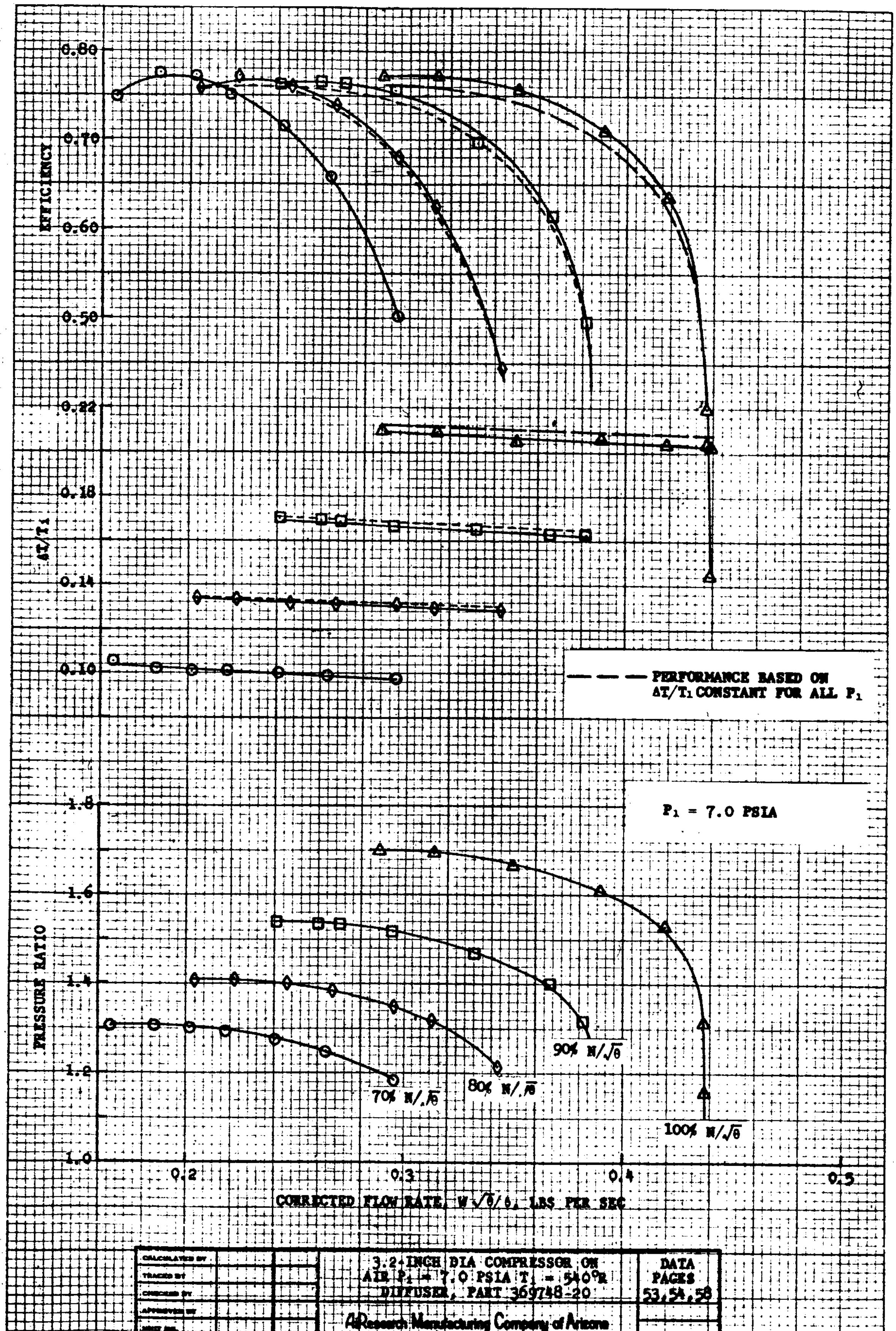
EFFICIENCY
0.80
0.70
0.60
0.50
0.22
0.18
0.14
0.10
ΔT/T₁
PERFORMANCE BASED ON ΔT/T₁ CONSTANT FOR ALL P₁
P₁ = 7.0 PSIA
PRESSURE RATIO
1.8
1.6
1.4
1.2
1.0
70% N/√θ
80% N/√θ
90% N/√θ
100% N/√θ
0.2
0.3
0.4
0.5
CORRECTED FLOW RATE, W√θ/δ, LBS PER SEC
CALCULATED BY
TRACED BY
CHECKED BY
APPROVED BY
3.2-INCH DIA COMPRESSOR ON AIR P₁ = 7.0 PSIA T₁ = 540°R DIFFUSER, PART 369748-20
DATA PAGES 53,54,58
AiResearch Manufacturing Company of Arizona

FIGURE 10

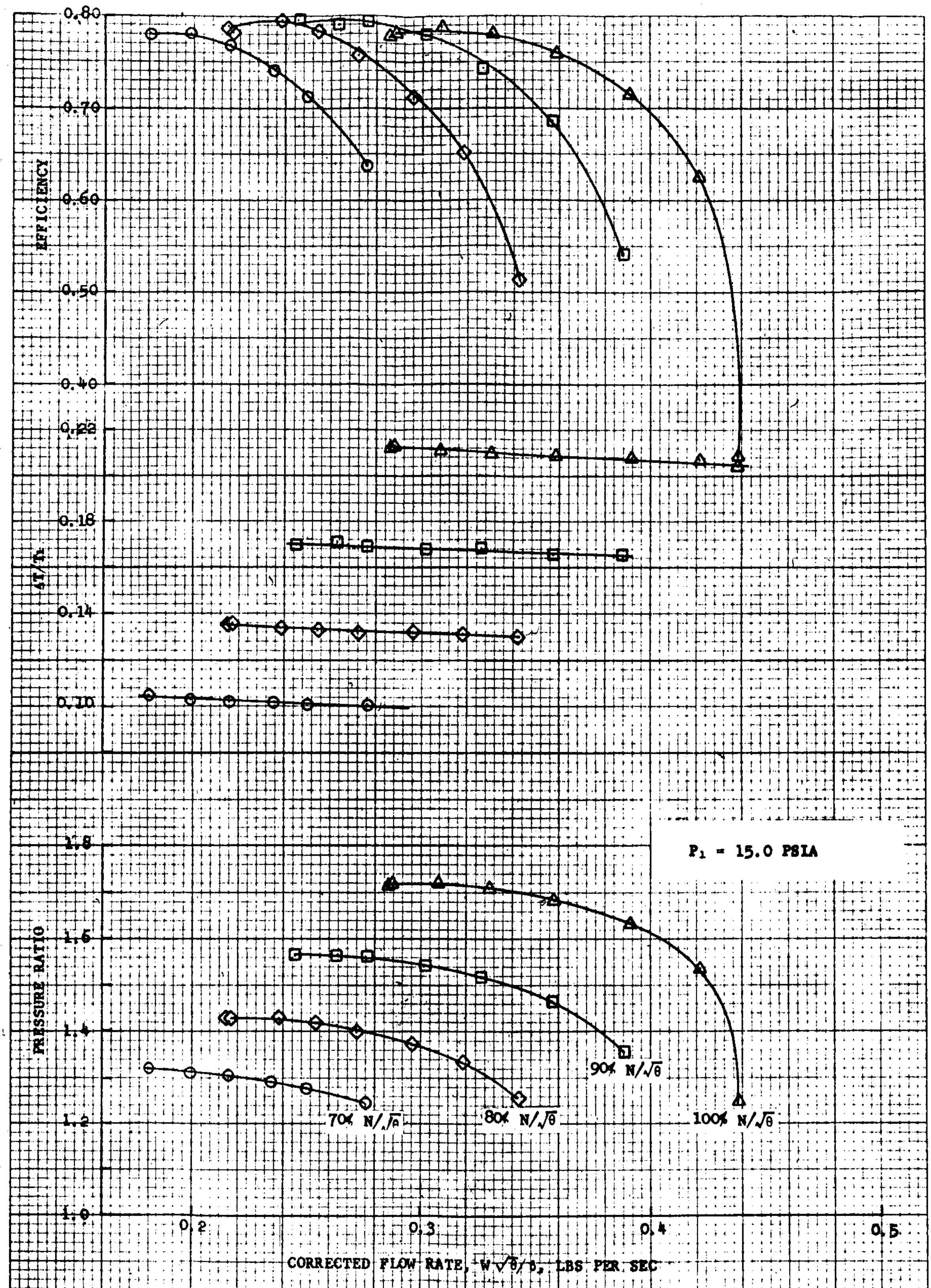

CALCULATED BY TRACED BY CHECKED BY APPROVED BY UNIT NO.	3.2-INCH DIA COMPRESSOR ON AIR P_1 = 15.0 PSIA T_1 = 540°R DIFFUSER PART 369748-20 AiResearch Manufacturing Company of Arizona	DATA PAGES 54,55,57, 58

FIGURE 11

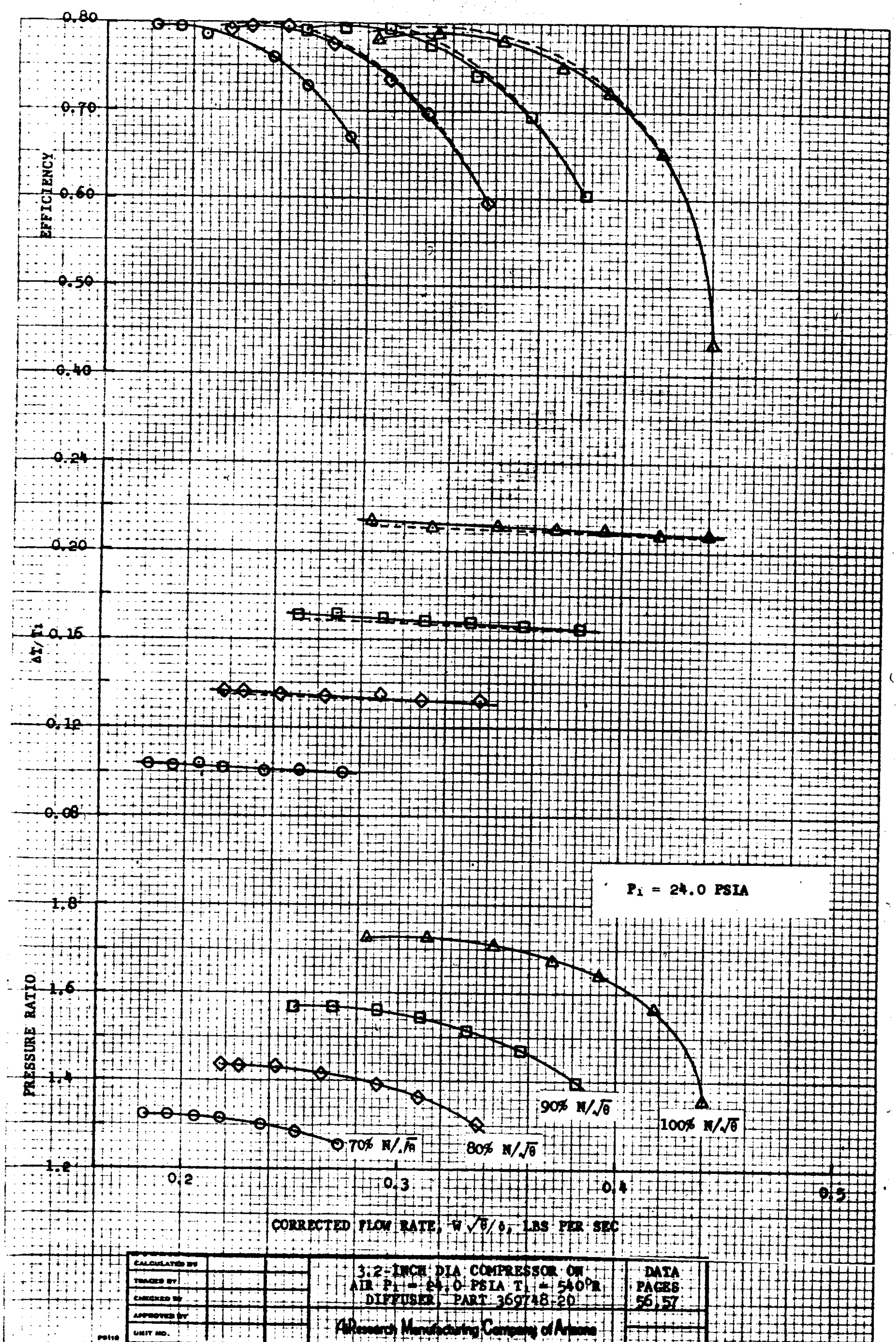
0.80
0.70
0.60
0.50
0.40
EFFICIENCY
0.24
0.20
0.16
0.12
0.08
ΔT/T₁
1.8
1.6
1.4
1.2
PRESSURE RATIO
Pᵢ = 24.0 PSIA
70% N/√θ
80% N/√θ
90% N/√θ
100% N/√θ
0.2
0.3
0.4
0.5
CORRECTED FLOW RATE, W √θ/δ, LBS PER SEC
3.2-INCH DIA COMPRESSOR ON AIR Pᵢ = 24.0 PSIA Tᵢ = 540°R DIFFUSER, PART 369748-20
DATA PAGES 56,57
AiResearch Manufacturing Company of Arizona

FIGURE 12

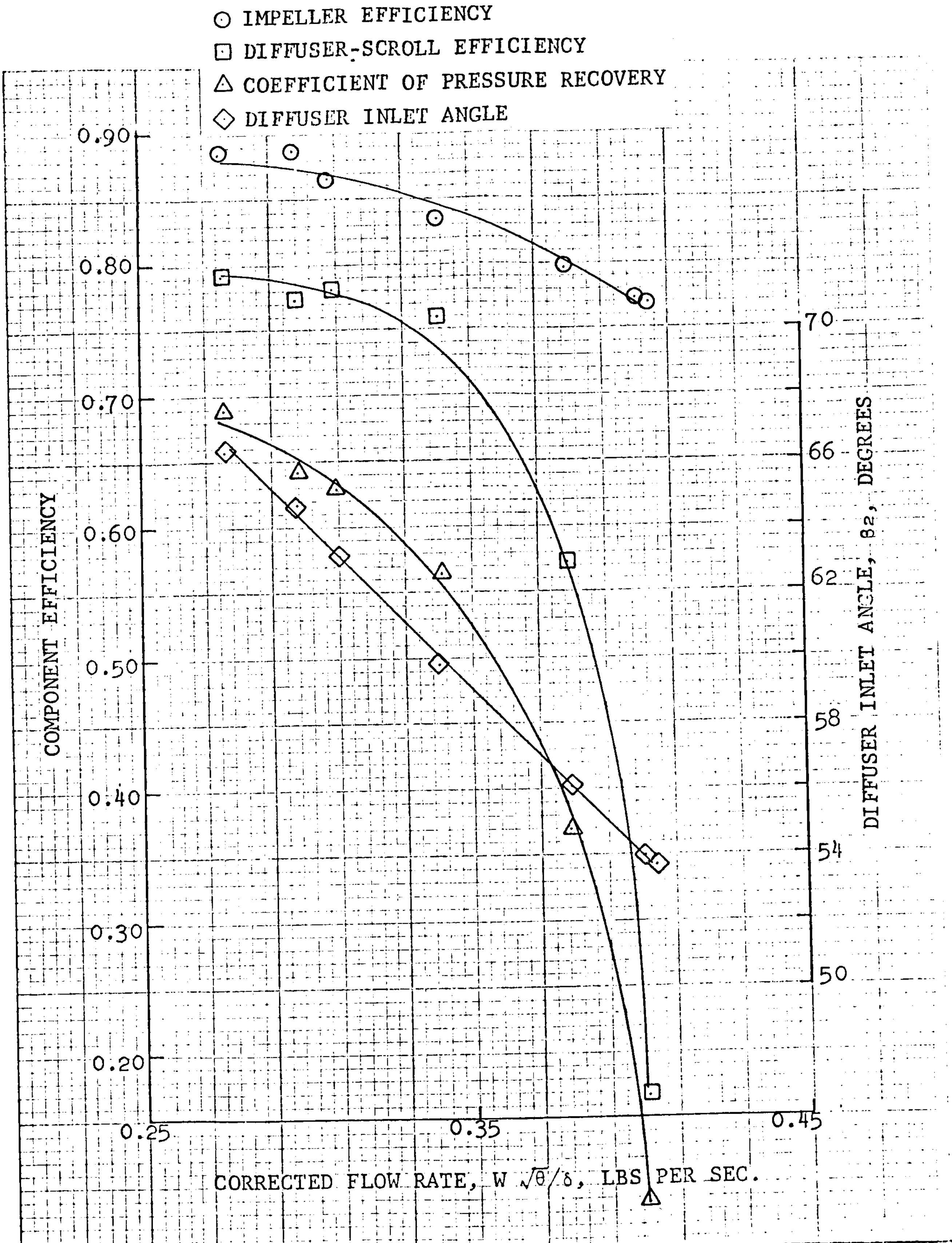

CALCULATED BY			3.2-INCH DIAMETER COMPRESSOR ON AIR P_1 = 2 PSIA T_1 = 540°R DIFFUSER PART 369748-20	N√θ=100 DATA PAGE
TRACED BY				
CHECKED BY				59
APPROVED BY			AiResearch Manufacturing Company of Arizona	
UNIT NO.				

FIGURE 13

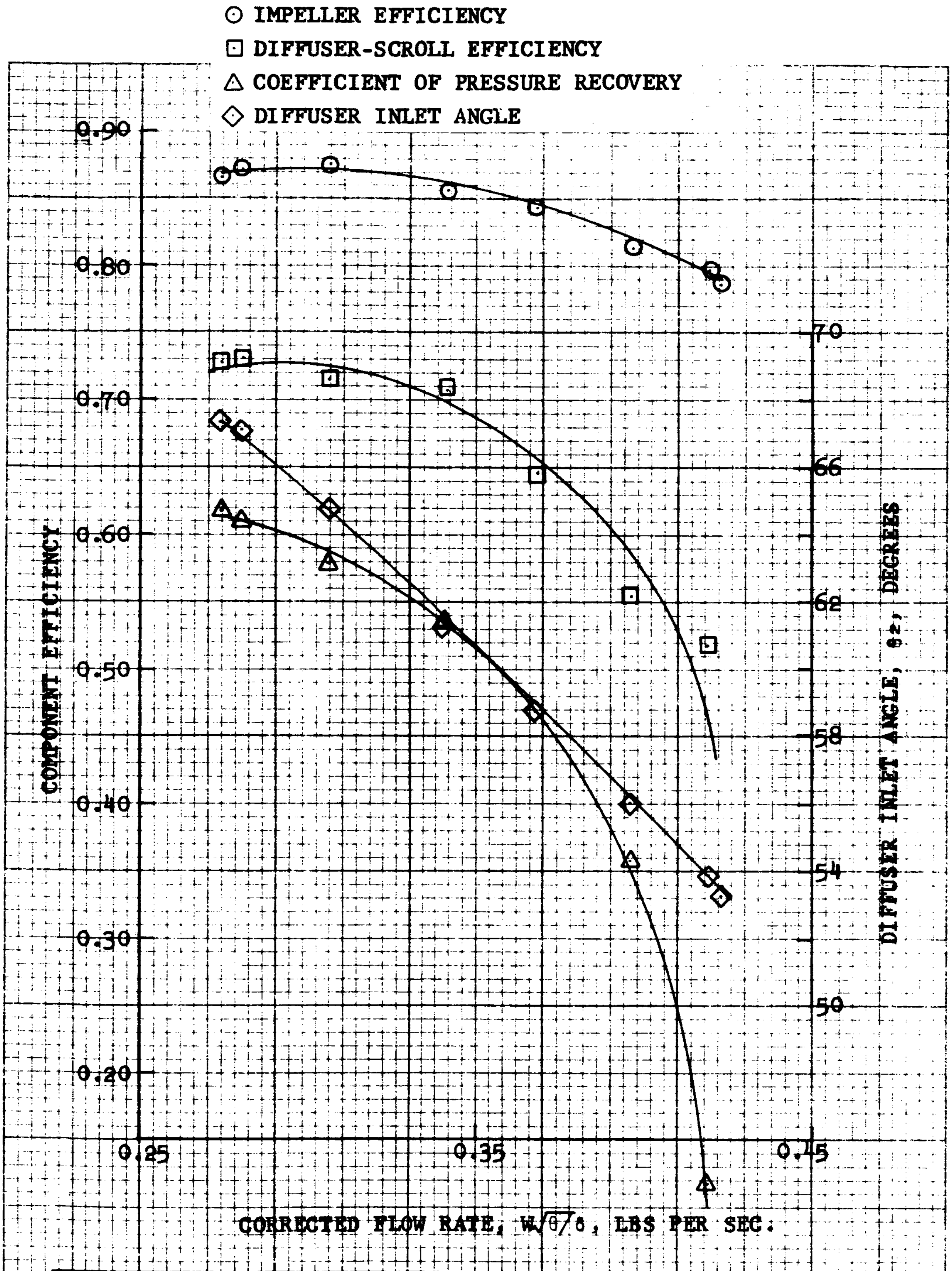

CALCULATED BY		3.2-INCH DIAMETER COMPRESSOR ON AIR $N/\sqrt{\theta}$=100	
TRACED BY		P_1 = 4.0 PSIA T_1 = 540°R	DATA
CHECKED BY		DIFFUSER PART 369748-20	PAGE
APPROVED BY			58
UNIT NO.		AiResearch Manufacturing Company of Arizona	

FIGURE 14

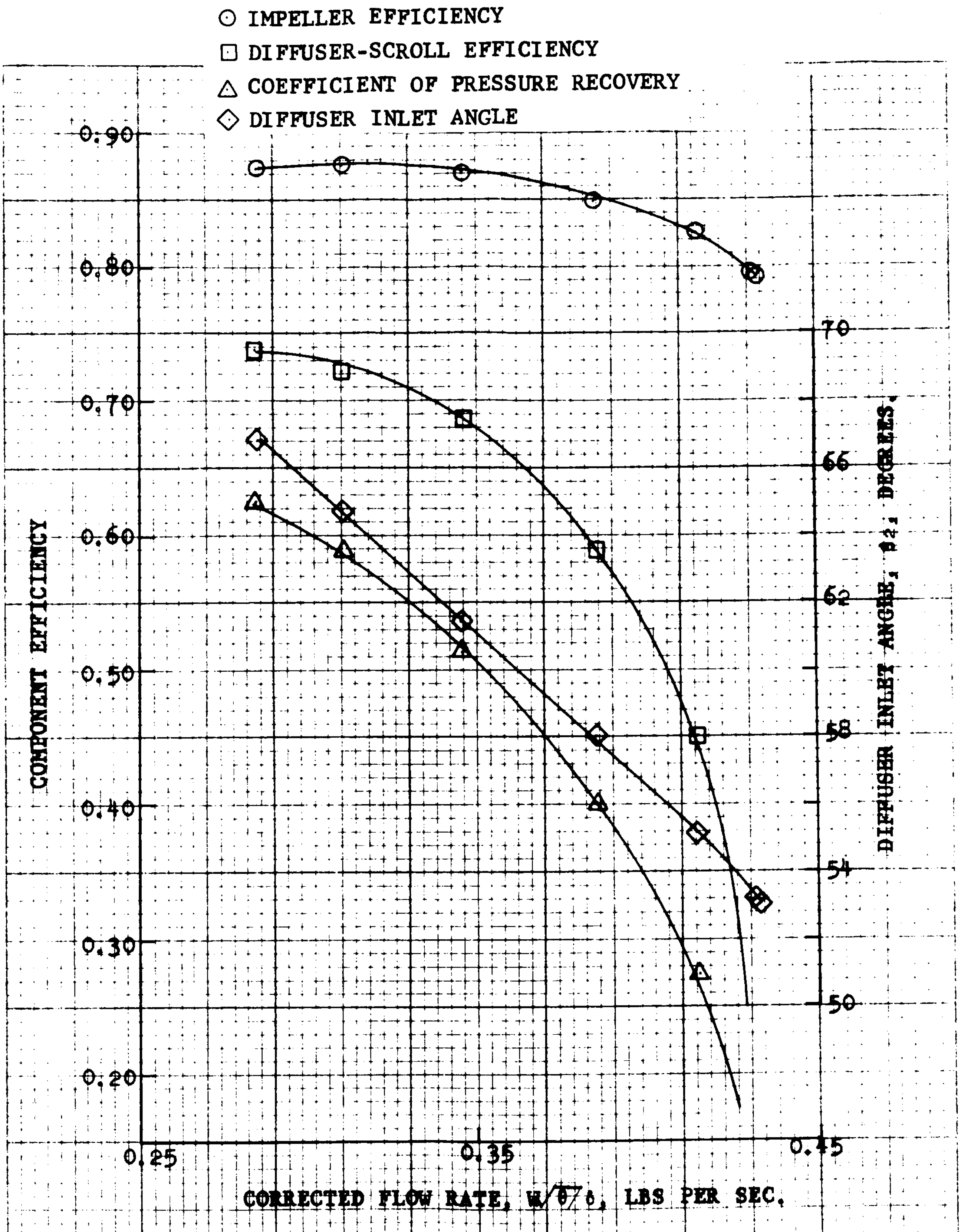

CALCULATED BY	3.2-INCH DIAMTER COMPRESSOR ON AIR P_1 = 7.0 PSIA T_1 = 540°R DIFFUSER PART 369748-20	$N/\sqrt{\theta}$=100
TRACED BY		DATA PAGE
CHECKED BY		60
APPROVED BY	AiResearch Manufacturing Company of Arizona	
UNIT NO.		

FIGURE 15

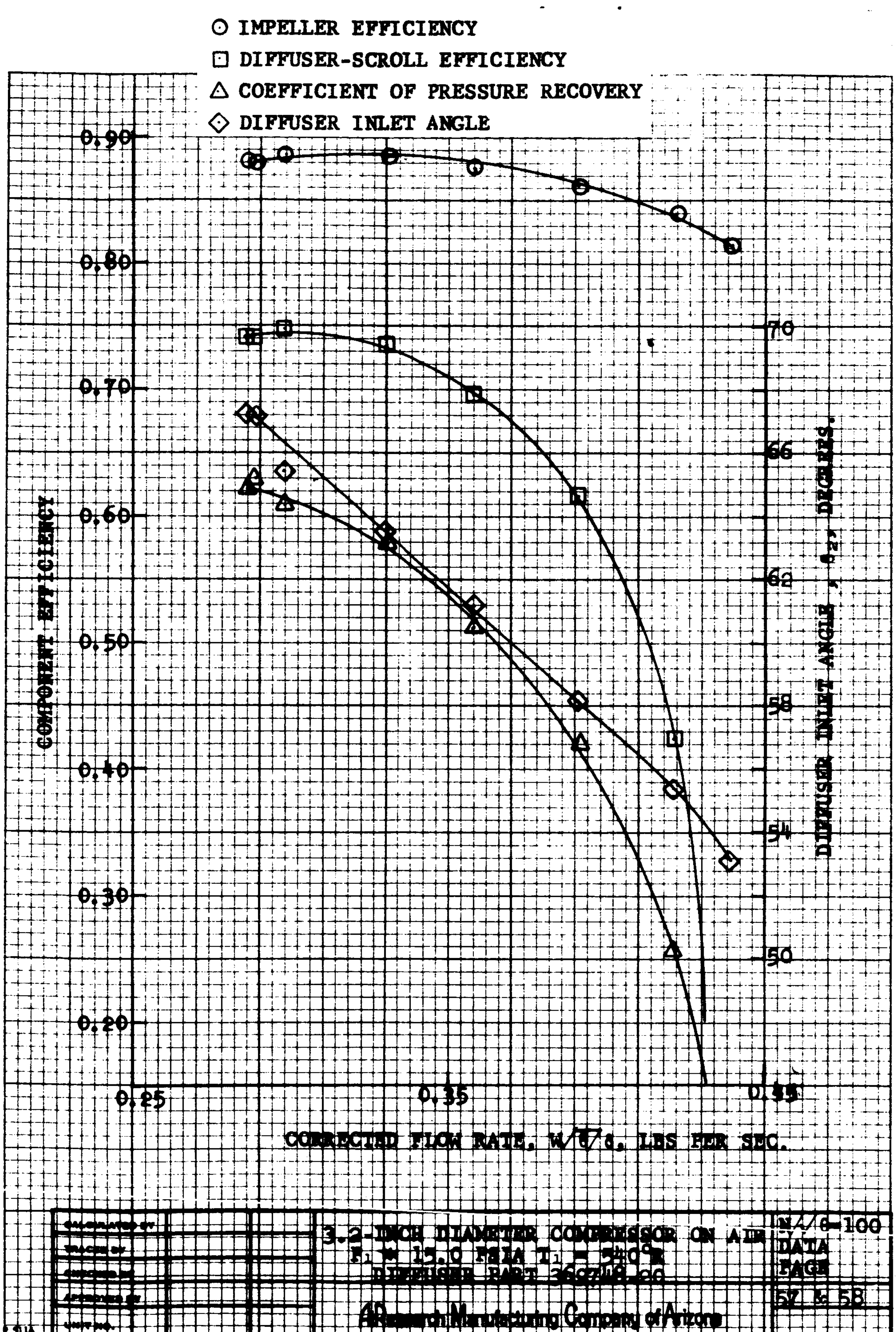

IMPELLER EFFICIENCY
DIFFUSER-SCROLL EFFICIENCY
COEFFICIENT OF PRESSURE RECOVERY
DIFFUSER INLET ANGLE
COMPONENT EFFICIENCY
0.90
0.80
0.70
0.60
0.50
0.40
0.30
0.20
DIFFUSER INLET ANGLE, DEGREES
70
66
62
58
54
50
0.25
0.35
CORRECTED FLOW RATE, LBS PER SEC.
3.2-INCH DIAMETER COMPRESSOR ON AIR
DATA PAGE
57 & 58
AiResearch Manufacturing Company of Arizona

FIGURE 16

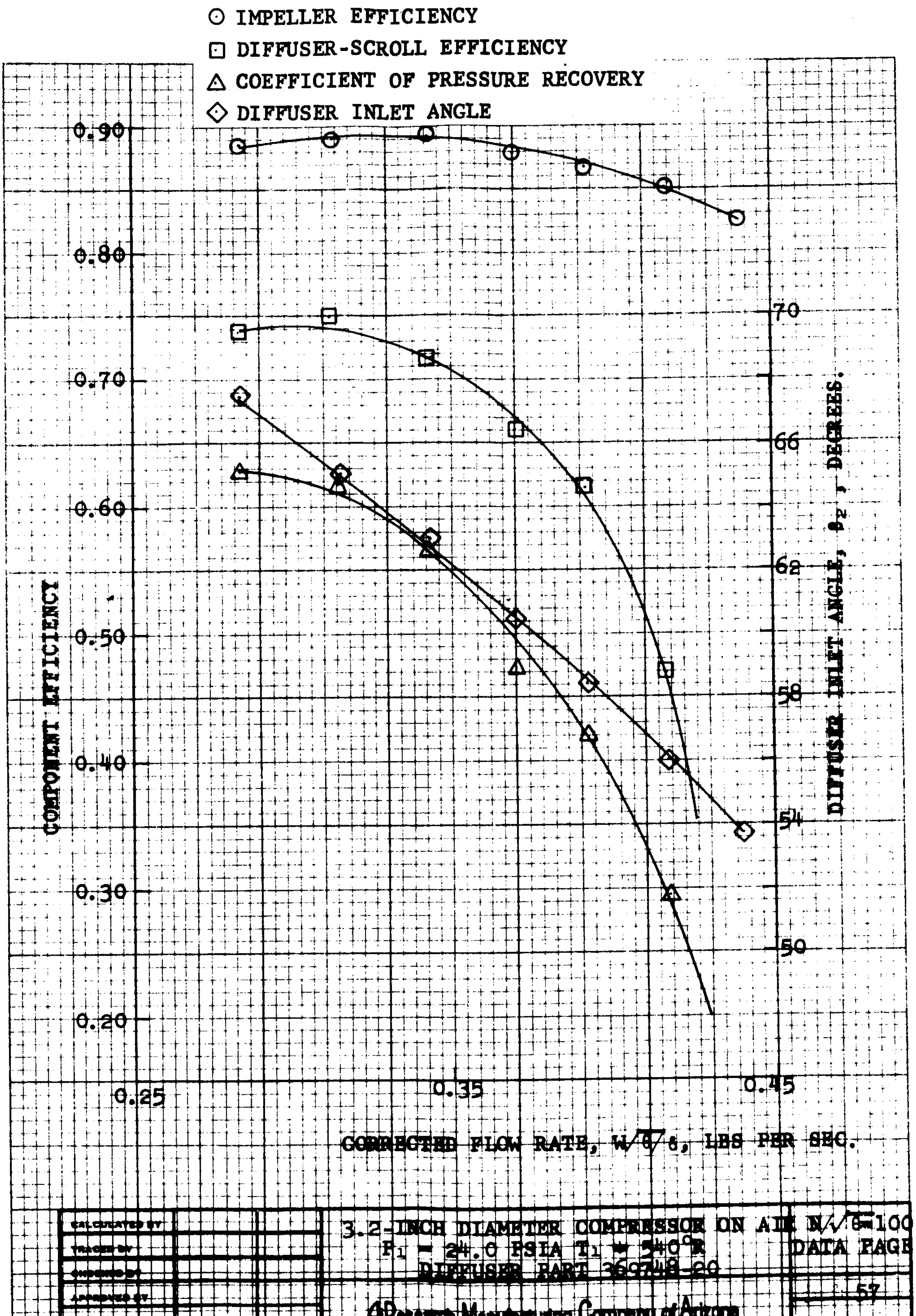

IMPELLER EFFICIENCY
DIFFUSER-SCROLL EFFICIENCY
COEFFICIENT OF PRESSURE RECOVERY
DIFFUSER INLET ANGLE
0.90
0.80
0.70
0.60
0.50
0.40
0.30
0.20
COMPONENT EFFICIENCY
70
66
62
58
54
50
DIFFUSER INLET ANGLE, θ_2, DEGREES.
0.25
0.35
0.45
CORRECTED FLOW RATE, $W\sqrt{\theta}/\delta$, LBS PER SEC.
3.2-INCH DIAMETER COMPRESSOR ON AIR $N/\sqrt{\theta}$=100
P_1 = 24.0 PSIA T_1 = 540°R
DIFFUSER PART 369748-20
DATA PAGE
57
AiResearch Manufacturing Company of Arizona

FIGURE 17

boundary layer clogging at the diffuser inlet (0.90 for this investigation) and using the continuity and angular momentum relationships along with the observed data to determine the diffuser inlet Mach number and flow direction. Finally, from the observed average static pressure at the diffuser inlet, a total pressure is obtained.

The observed static pressure distribution along the diffuser mean line is given for each air data point in Appendix I. The average static pressure at the scroll exit is also shown in these figures in order that scroll performance may be determined. On each graph the speed and inlet pressure are constant while the static pressure distributions are shown as the compressor is taken from operation points near the choke region to points near the surge region.

Phase II of the testing was conducted using the hardware identical to that of Phase I with the exception of a newly designed Diffuser Part 871034 in which the area ratio and distribution was modified in the attempt to improve diffuser efficiency at low Reynolds numbers (pressure levels at 4 psia particularly). Figure 18 shows the comparison between the two diffusers subjected to test. (A comparison of the performance of the two diffusers will be discussed in the section on analysis and interpretation of results.)

It should be noted that in the interest of economy, no change in the existing scroll was made in order to make it compatible with the redesigned diffuser passages.

The Phase II test program and data obtained were identical with that of Phase I with the exception of the 7 psia argon check points which were not required in Phase II.

Throughout all testing, efforts were made to maintain impeller shroud clearances at constant values in order to eliminate this factor from the observed performance. Shroud clearances were all set to the same measured value, at room temperature, during compressor assembly.

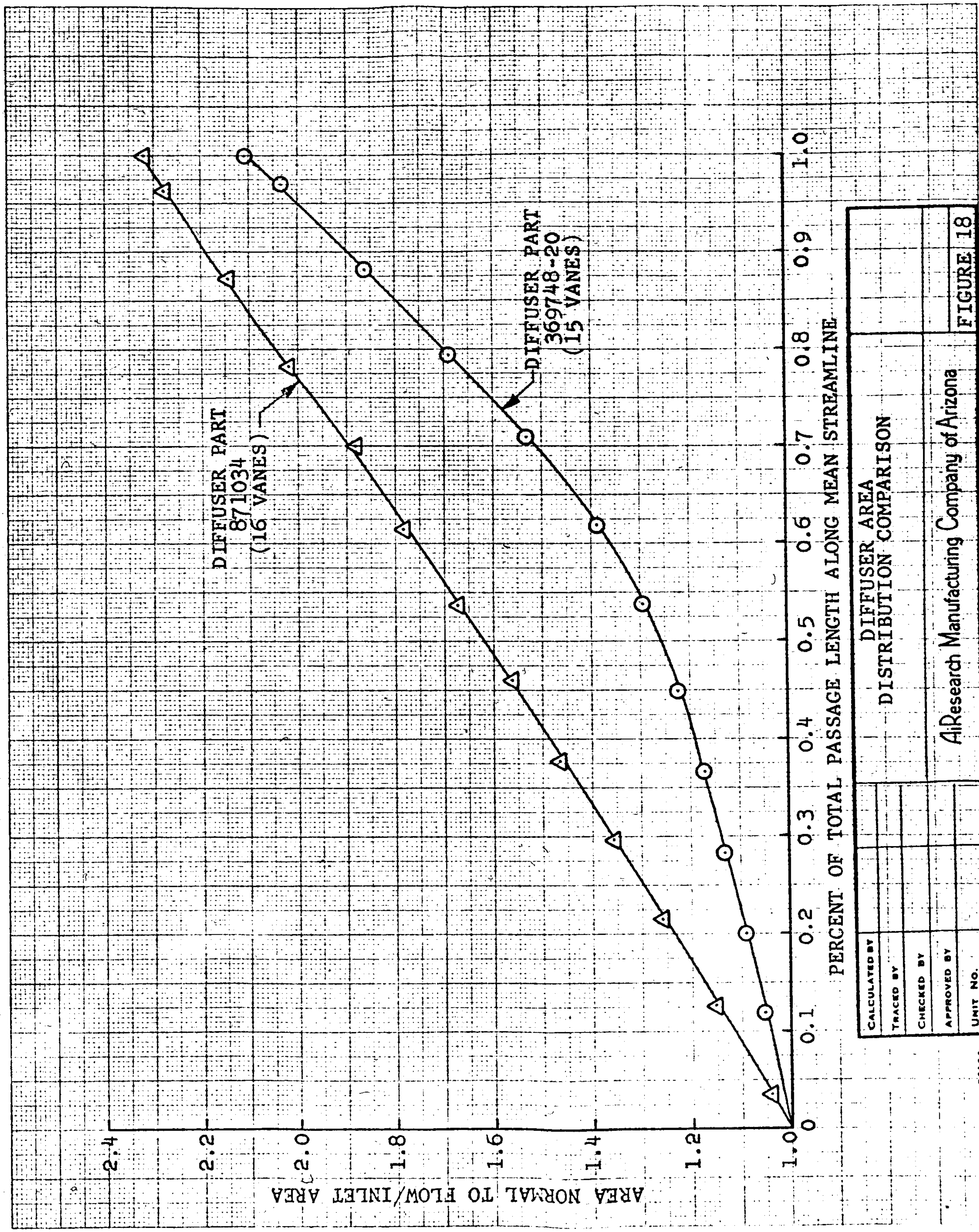

FIGURE 18
DIFFUSER AREA DISTRIBUTION COMPARISON

Plots of the observed overall performance resulting from Phase II testing are presented in Figure 19 through 23. (Here again the dashed lines will be discussed later in the analysis section.) The breakdown of impeller efficiency, diffuser plus scroll efficiency, diffuser pressure recovery, and diffuser inlet flow angles is given for the air 100 percent speed line for each pressure level in Figures 24 through 28.

The argon check point overall stage data for 100 percent equivalent speed at 7, 15, and 24 psia for Phase I and 15 and 24 psia for Phase II is shown on Figures 29 through 33. The solid lines shown are the estimated argon performance based on the previously recorded 100 percent speed air data. Excellent agreement between the predicted and observed performance is apparent for pressure ratios, efficiency, temperature rise and flow near the surge and peak efficiency points; however, the predicted choke flow is generally high. A reasonable level of confidence is therefore justified in the ability to predict at least the performance near peak efficiencies in argon from test results on identical compressors run in air.

It should be noted that while technical difficulties prevented any reliable argon data from being taken at 4 psia and 2 psia inlet pressures, there is every reason to believe that performance predictions from corresponding air data would have been successful.

It should be noted at this point that the transducer used to read out all pressures was not linear at the lower pressures. The digital readout was adjusted so that at approximately 30 in. Hg abs the readout agreed exactly with a reference standard manometer. Subsequent calibration of the transducer revealed that, as the measured pressure dropped, an increasing error between the digital

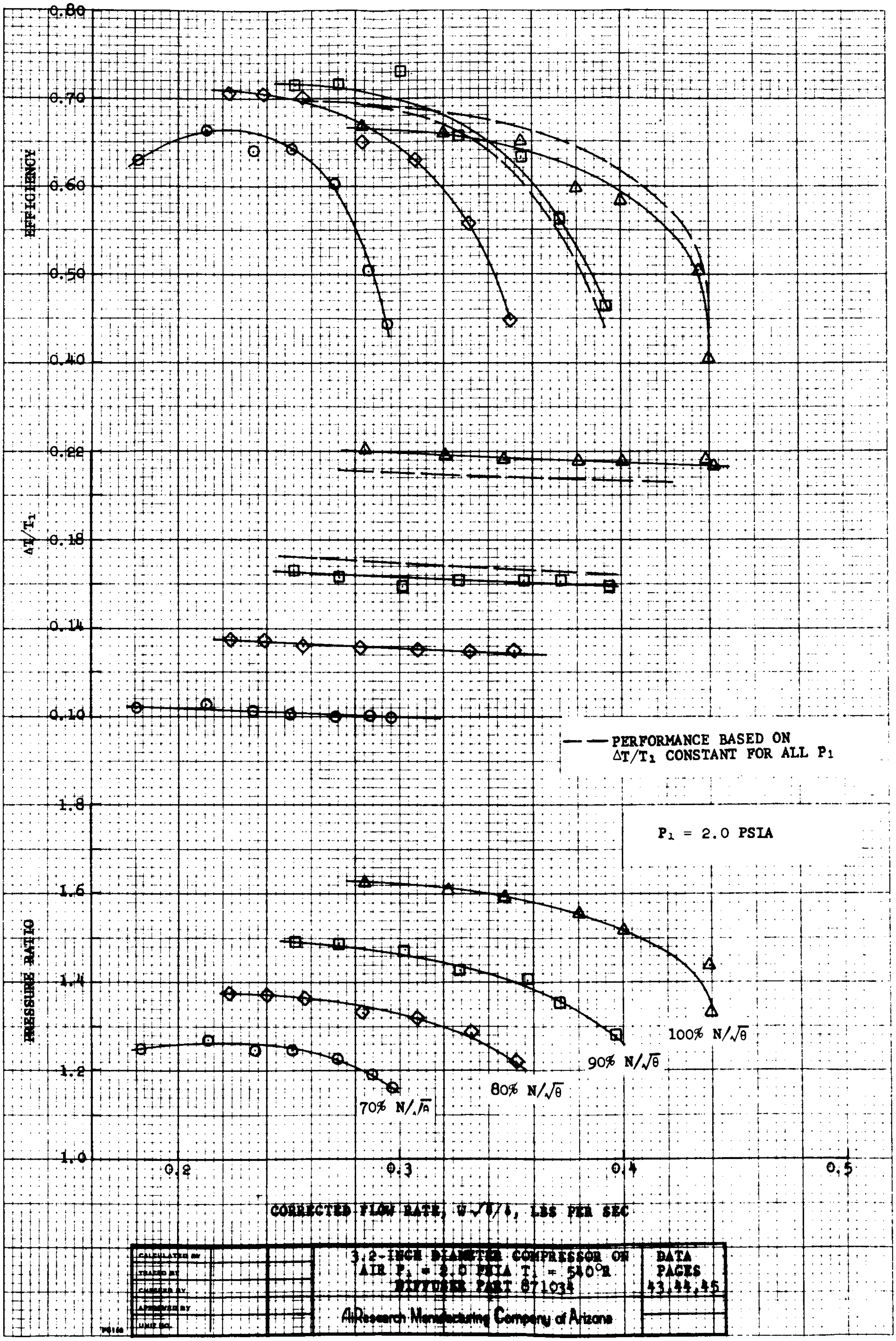
EFFICIENCY
0.80
0.70
0.60
0.50
0.40
$\Delta T/T_1$
0.22
0.18
0.14
0.10
PRESSURE RATIO
1.8
1.6
1.4
1.2
1.0
0.2
0.3
0.4
0.5
CORRECTED FLOW RATE, $W\sqrt{\theta}/\delta$, LBS PER SEC
PERFORMANCE BASED ON $\Delta T/T_1$ CONSTANT FOR ALL P_1
P_1 = 2.0 PSIA
100% $N/\sqrt{\theta}$
90% $N/\sqrt{\theta}$
80% $N/\sqrt{\theta}$
70% $N/\sqrt{\theta}$
3.2-INCH DIAMETER COMPRESSOR ON AIR P_1 = 2.0 PSIA T_1 = 540°R DIFFUSER PART 871034
DATA PAGES 43,44,45
AiResearch Manufacturing Company of Arizona

FIGURE 19

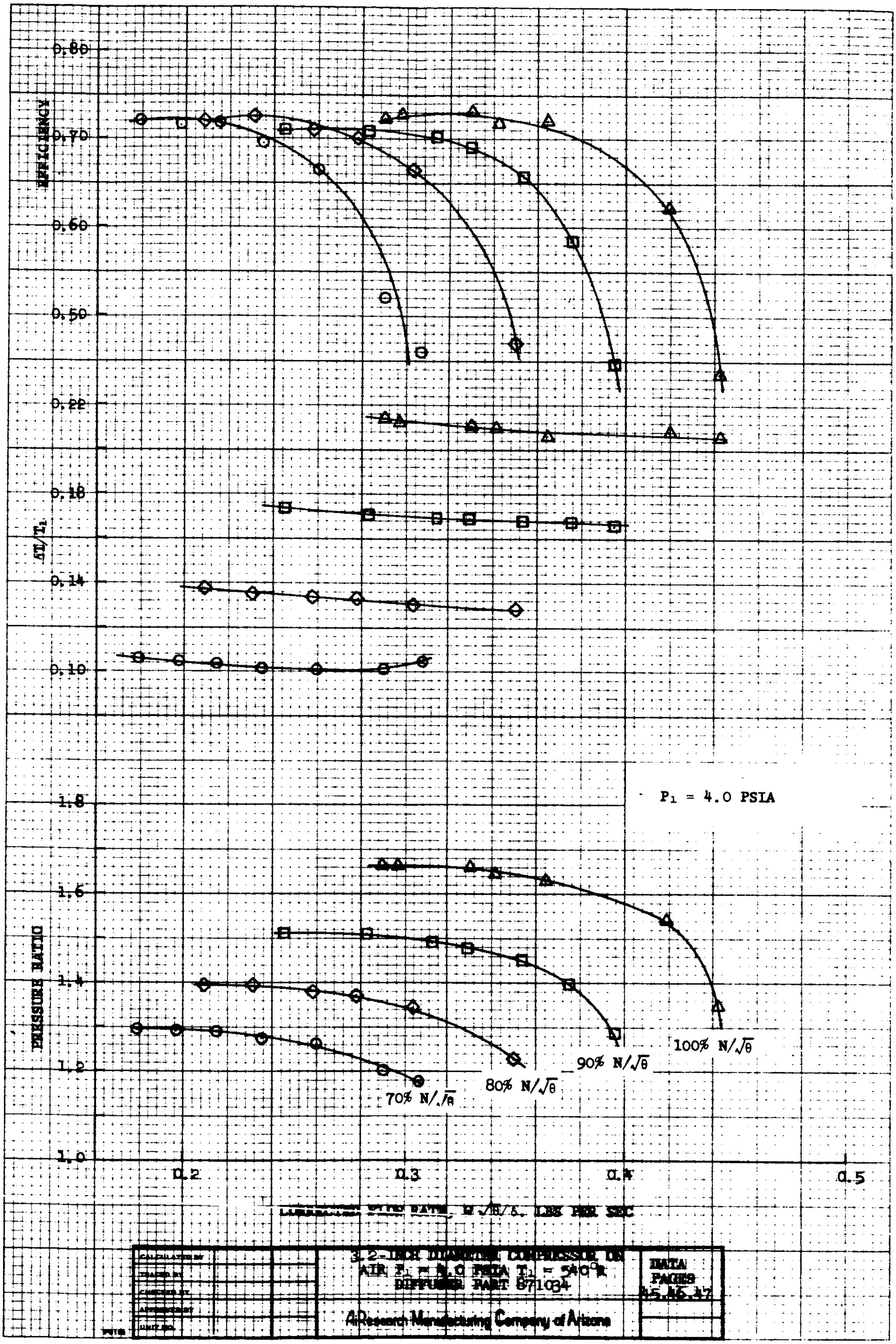
EFFICIENCY
0.80
0.70
0.60
0.50
0.22
0.18
0.14
0.10
ΔT/T1
P1 = 4.0 PSIA
1.8
1.6
1.4
1.2
1.0
PRESSURE RATIO
100% N/√θ
90% N/√θ
80% N/√θ
70% N/√θ
0.2
0.3
0.4
0.5
W √θ/δ, LBS PER SEC
3.2-INCH DIAMETER COMPRESSOR ON
AIR P1 = 4.0 PSIA T1 = 540°R
DIFFUSER PART 871034
DATA
PAGES
45,46,47
AiResearch Manufacturing Company of Arizona

FIGURE 20

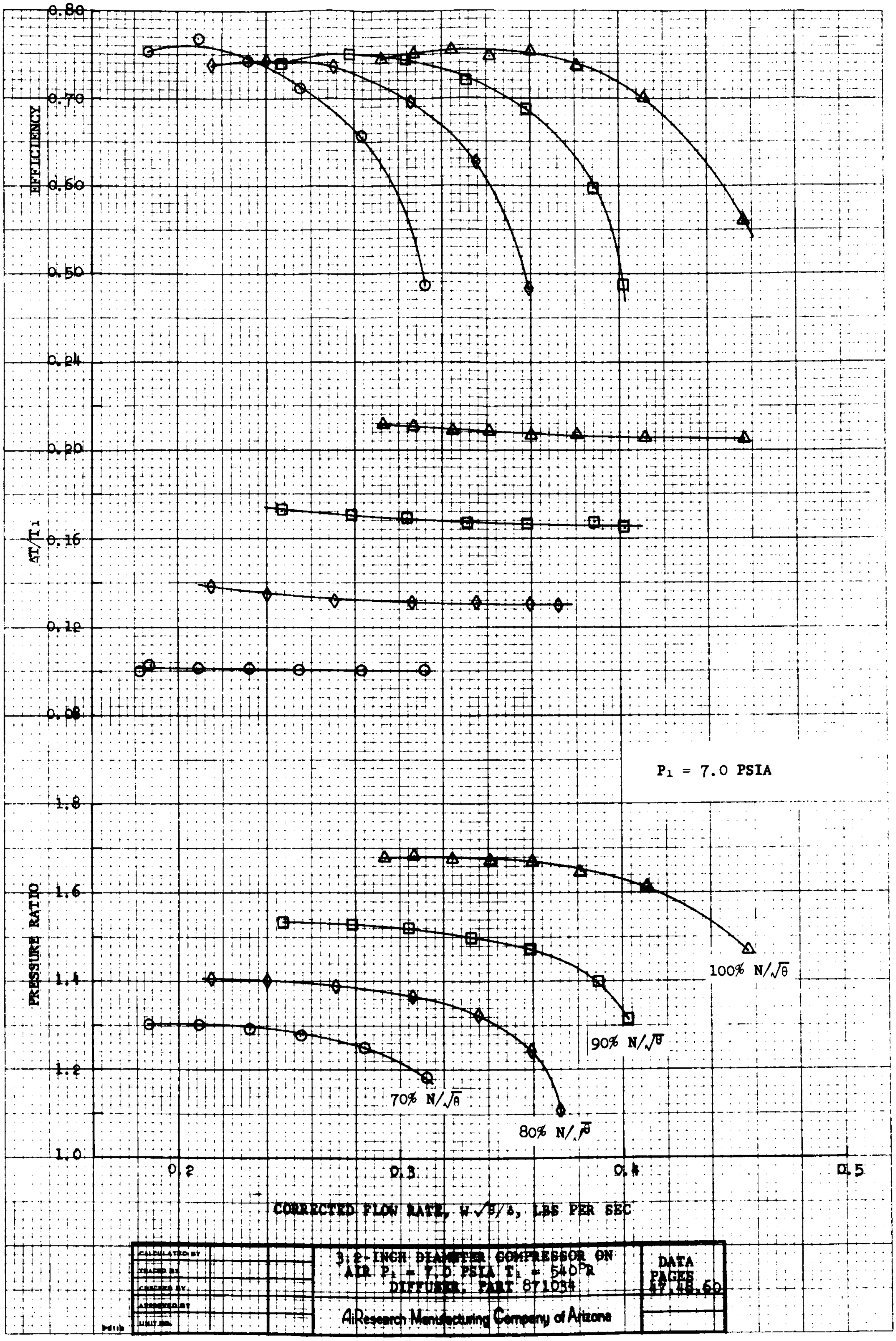

FIGURE 21
APS-5211-R

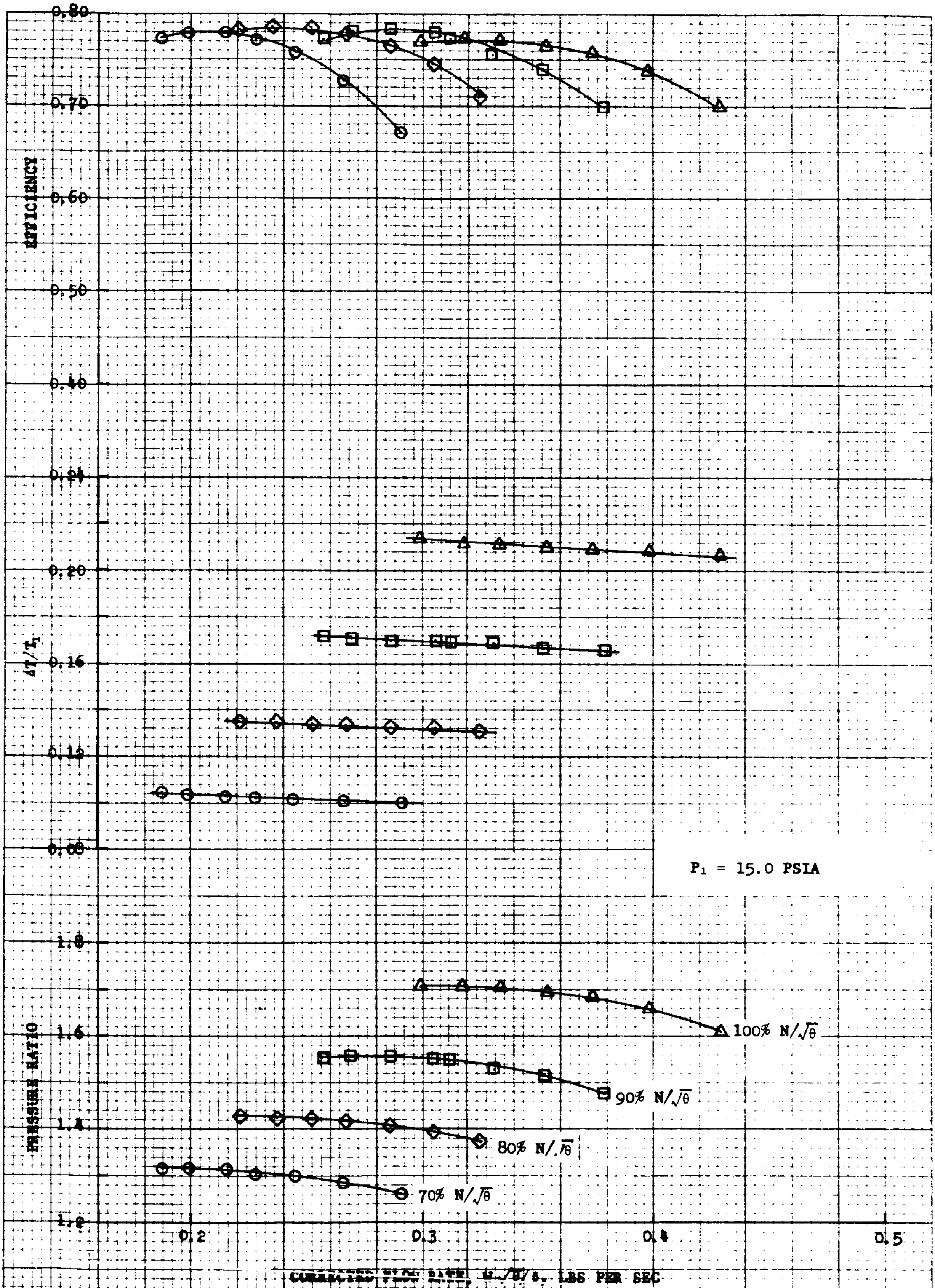

3.2-INCH DIAMETER COMPRESSOR ON AIR P_1 = 15.0 PSIA T_1 = 540°R DIFFUSER, PART 871034

DATA PAGES 60,61,62

AiResearch Manufacturing Company of Arizona

FIGURE 22

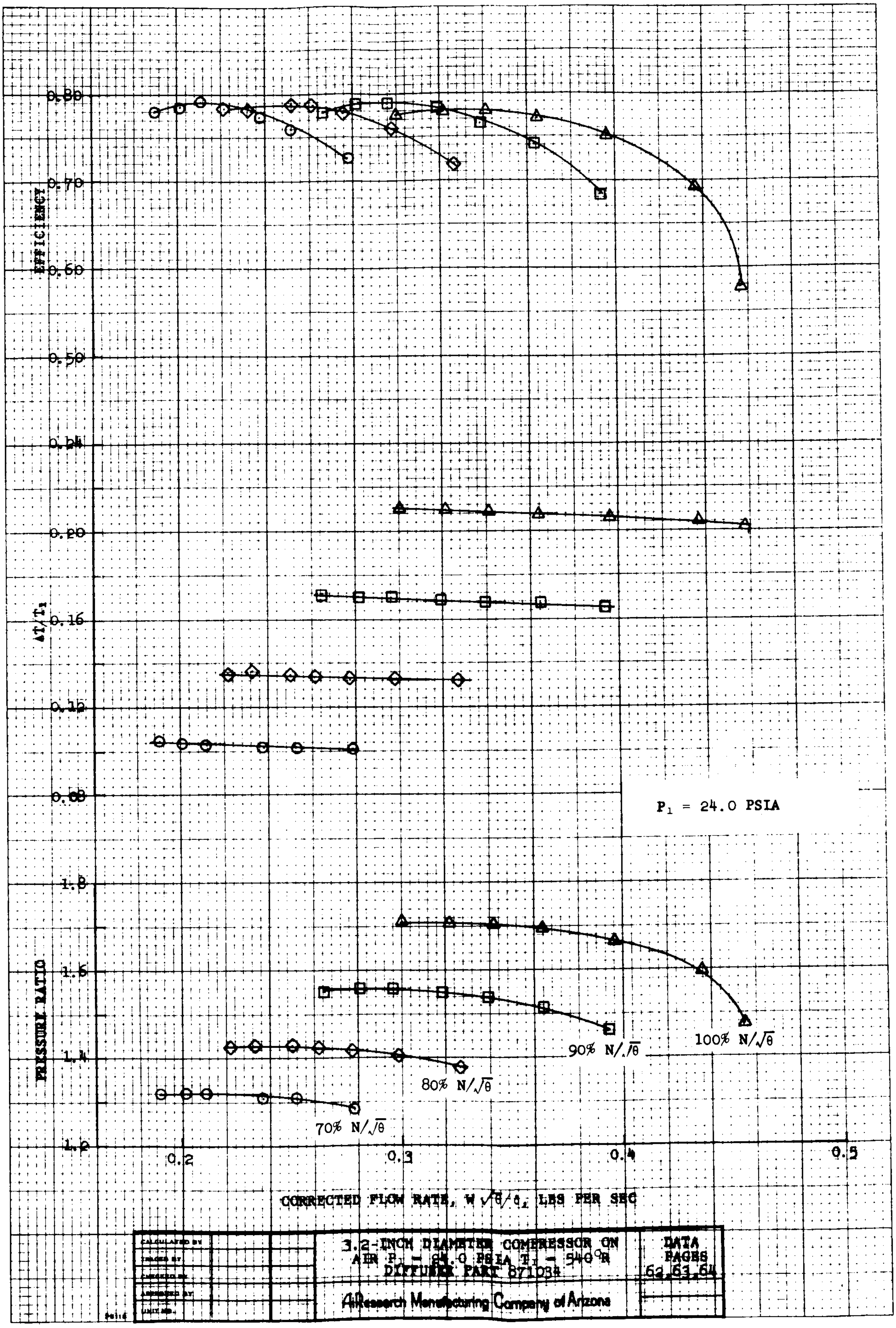

0.80
0.70
EFFICIENCY
0.60
0.50
0.24
0.20
$\Delta T/T_1$
0.16
0.12
0.08
1.8
1.6
PRESSURE RATIO
1.4
1.2
0.2
0.3
0.4
0.5
CORRECTED FLOW RATE, $W\sqrt{\theta}/\delta_1$, LBS PER SEC
P_1 = 24.0 PSIA
100% $N/\sqrt{\theta}$
90% $N/\sqrt{\theta}$
80% $N/\sqrt{\theta}$
70% $N/\sqrt{\theta}$
3.2-INCH DIAMETER COMPRESSOR ON AIR P_1 = 24.0 PSIA T_1 = 540°R DIFFUSER PART 871034
DATA PAGES 62,63,64
AiResearch Manufacturing Company of Arizona

FIGURE 23

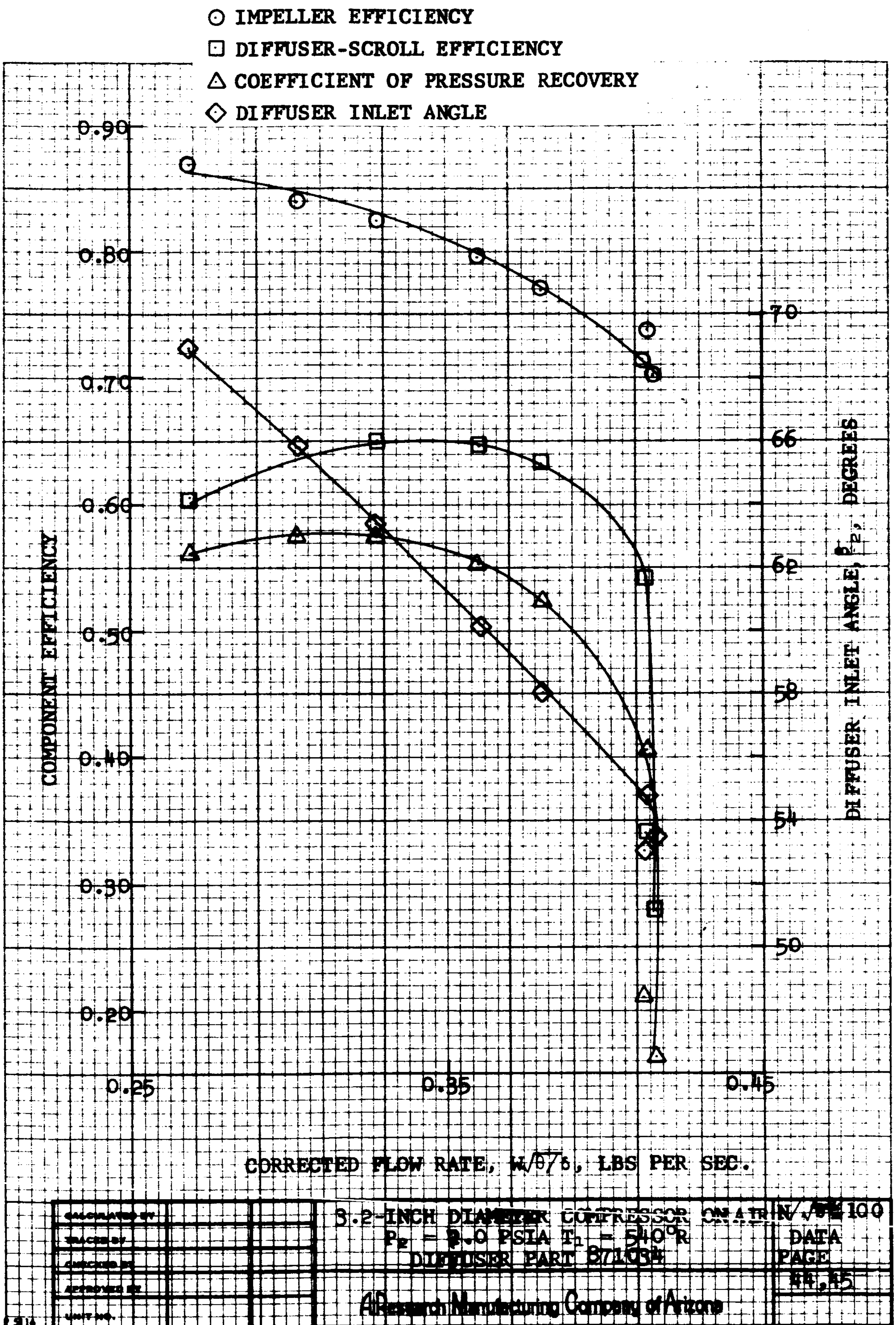

FIGURE 24
APS-5211-R
Page 41

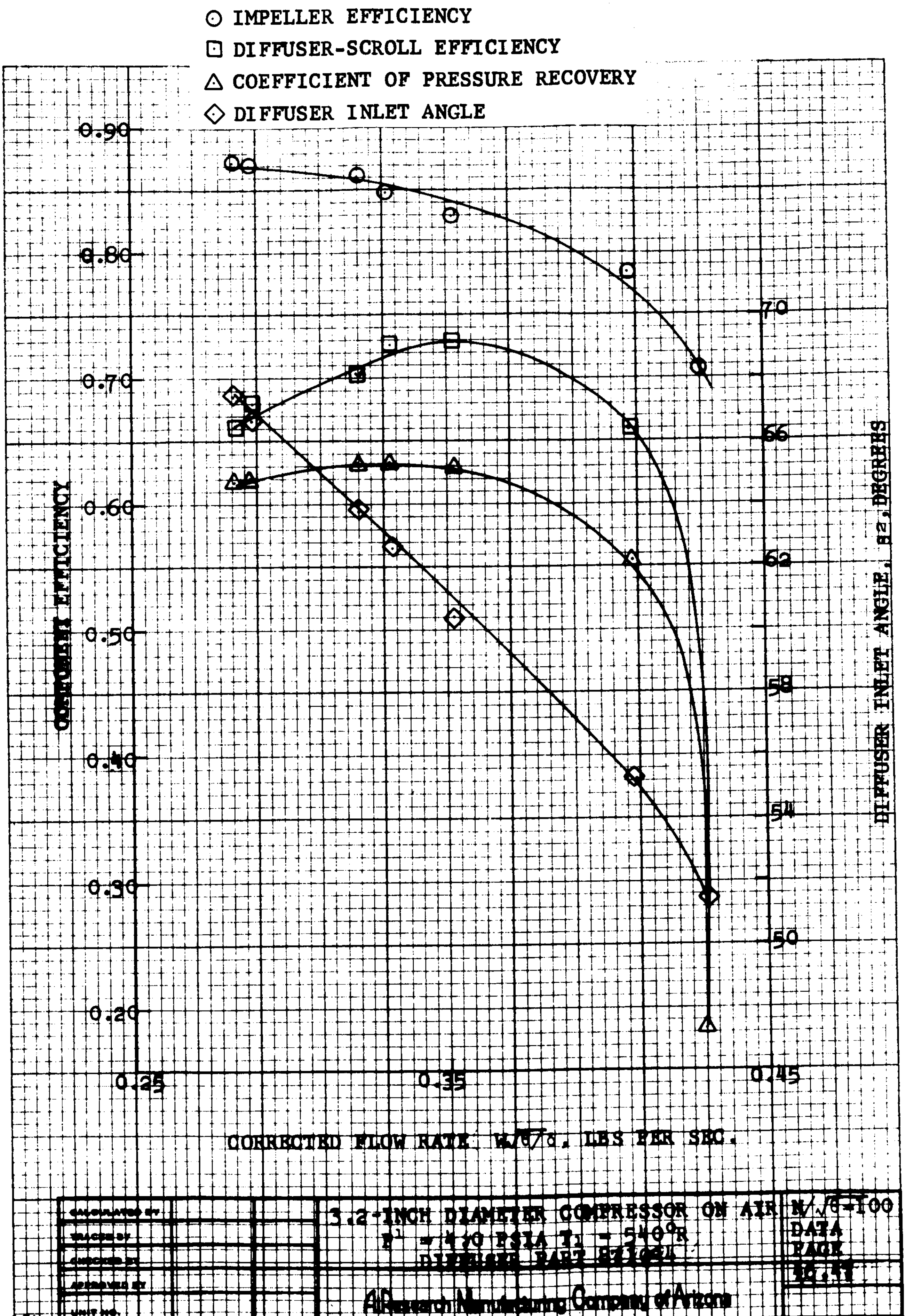

IMPELLER EFFICIENCY
DIFFUSER-SCROLL EFFICIENCY
COEFFICIENT OF PRESSURE RECOVERY
DIFFUSER INLET ANGLE
0.90
0.80
0.70
0.60
0.50
0.40
0.30
0.20
70
66
62
58
54
50
0.25
0.35
0.45
DIFFUSER INLET ANGLE, β2, DEGREES
CORRECTED FLOW RATE W√θ/δ, LBS PER SEC.
3.2-INCH DIAMETER COMPRESSOR ON AIR
DATA
PAGE
AiResearch Manufacturing Company of Arizona

FIGURE 25

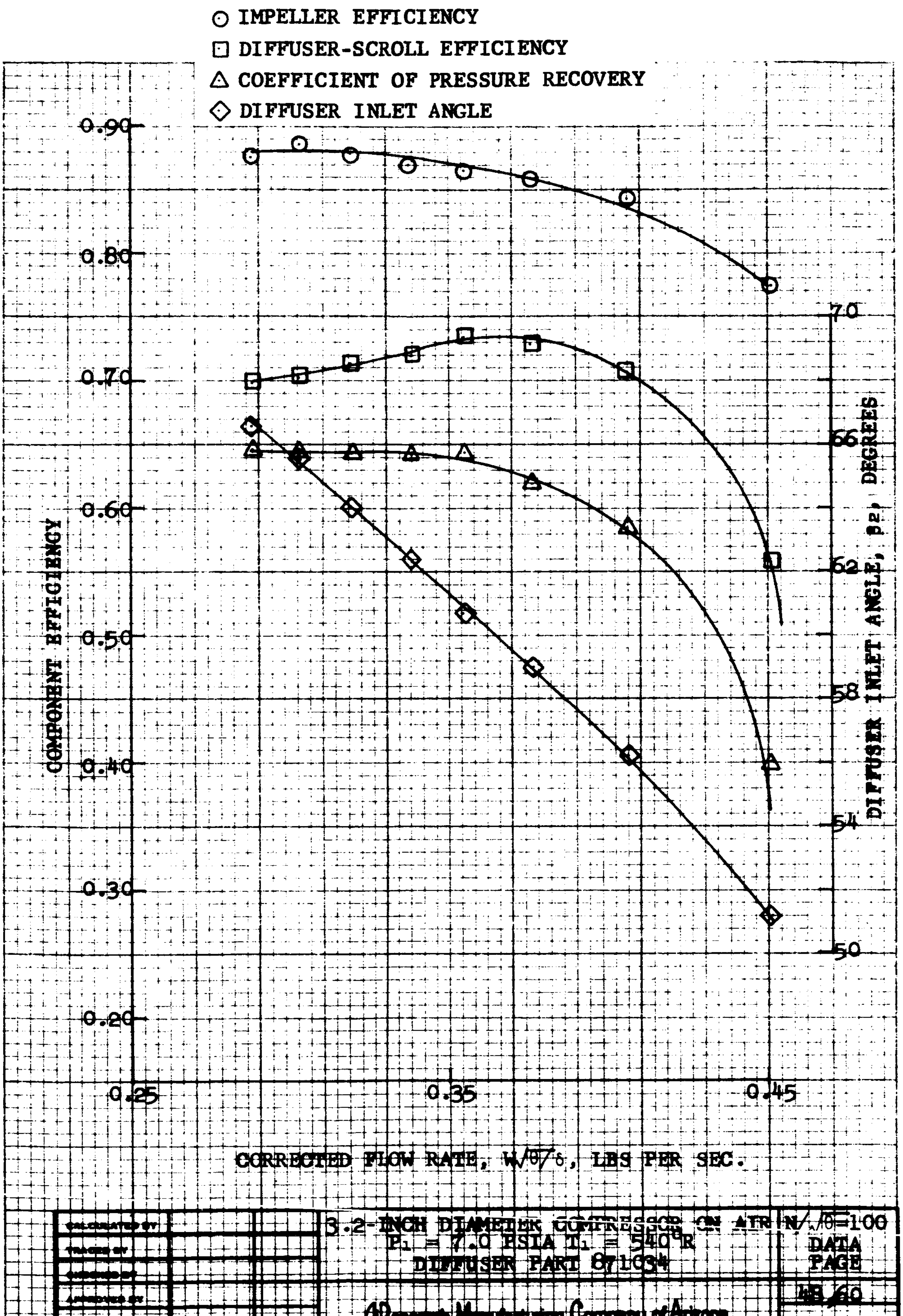
IMPELLER EFFICIENCY
DIFFUSER-SCROLL EFFICIENCY
COEFFICIENT OF PRESSURE RECOVERY
DIFFUSER INLET ANGLE
COMPONENT EFFICIENCY
0.90
0.80
0.70
0.60
0.50
0.40
0.30
0.20
DIFFUSER INLET ANGLE, β_2, DEGREES
70
66
62
58
54
50
0.25
0.35
0.45
CORRECTED FLOW RATE, $W\sqrt{\theta}/\delta$, LBS PER SEC.
3.2-INCH DIAMETER COMPRESSOR ON AIR
P_1 = 7.0 PSIA T_1 = 540 R
DIFFUSER PART 871634
$N/\sqrt{\theta}$=100
DATA PAGE
AiResearch Manufacturing Company of Arizona

FIGURE 26

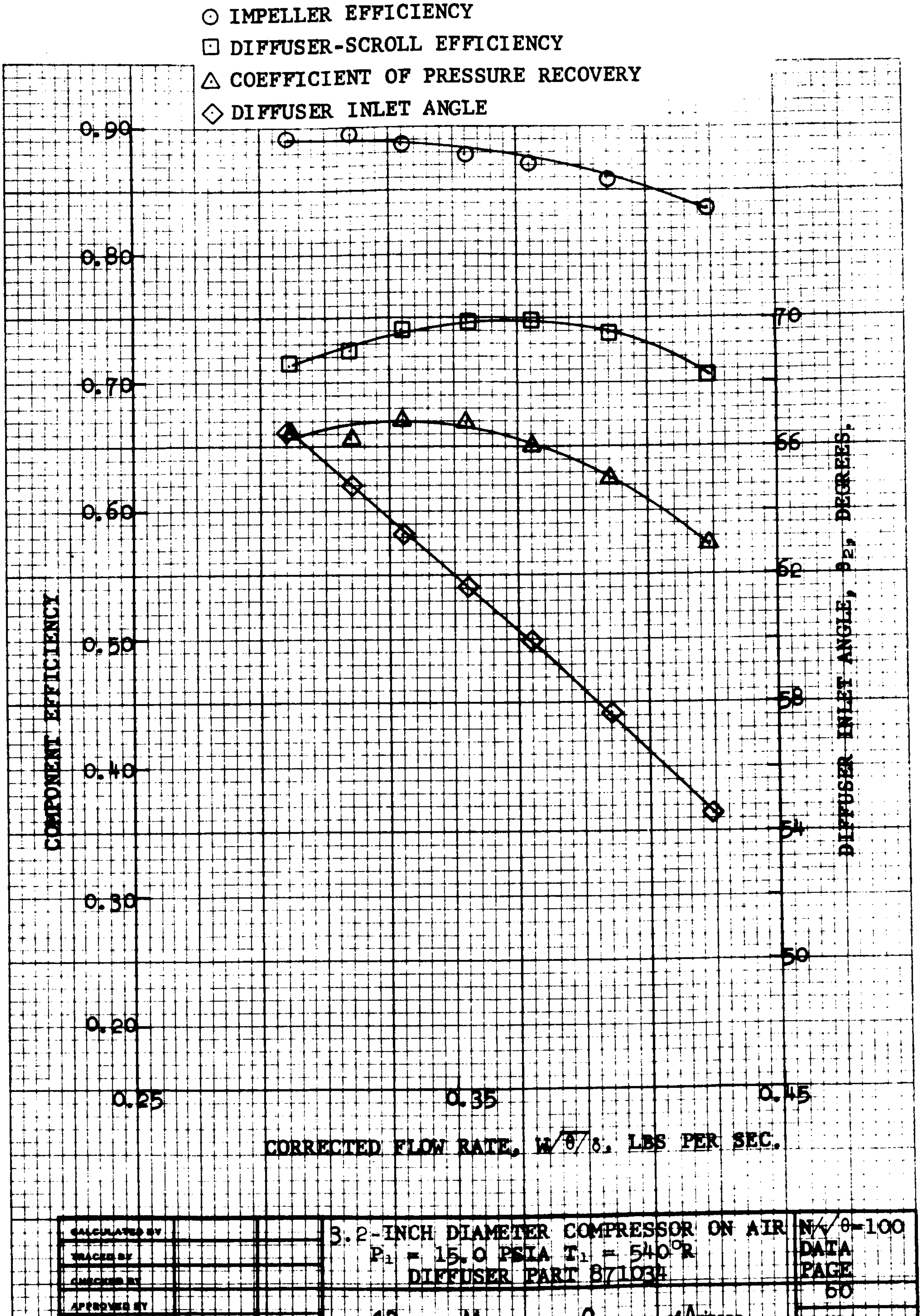

⊙ IMPELLER EFFICIENCY
⊡ DIFFUSER-SCROLL EFFICIENCY
△ COEFFICIENT OF PRESSURE RECOVERY
◇ DIFFUSER INLET ANGLE
0.90
0.80
0.70
0.60
0.50
0.40
0.30
0.20
70
66
62
58
54
50
0.25
0.35
0.45
COMPONENT EFFICIENCY
DIFFUSER INLET ANGLE, β_2, DEGREES.
CORRECTED FLOW RATE, $W\sqrt{\theta}/\delta$, LBS PER SEC.
3.2-INCH DIAMETER COMPRESSOR ON AIR
P_1 = 15.0 PSIA T_1 = 540°R
DIFFUSER PART 871034
$N/\sqrt{\theta}$=100
DATA PAGE 60
AiResearch Manufacturing Company of Arizona

FIGURE 27

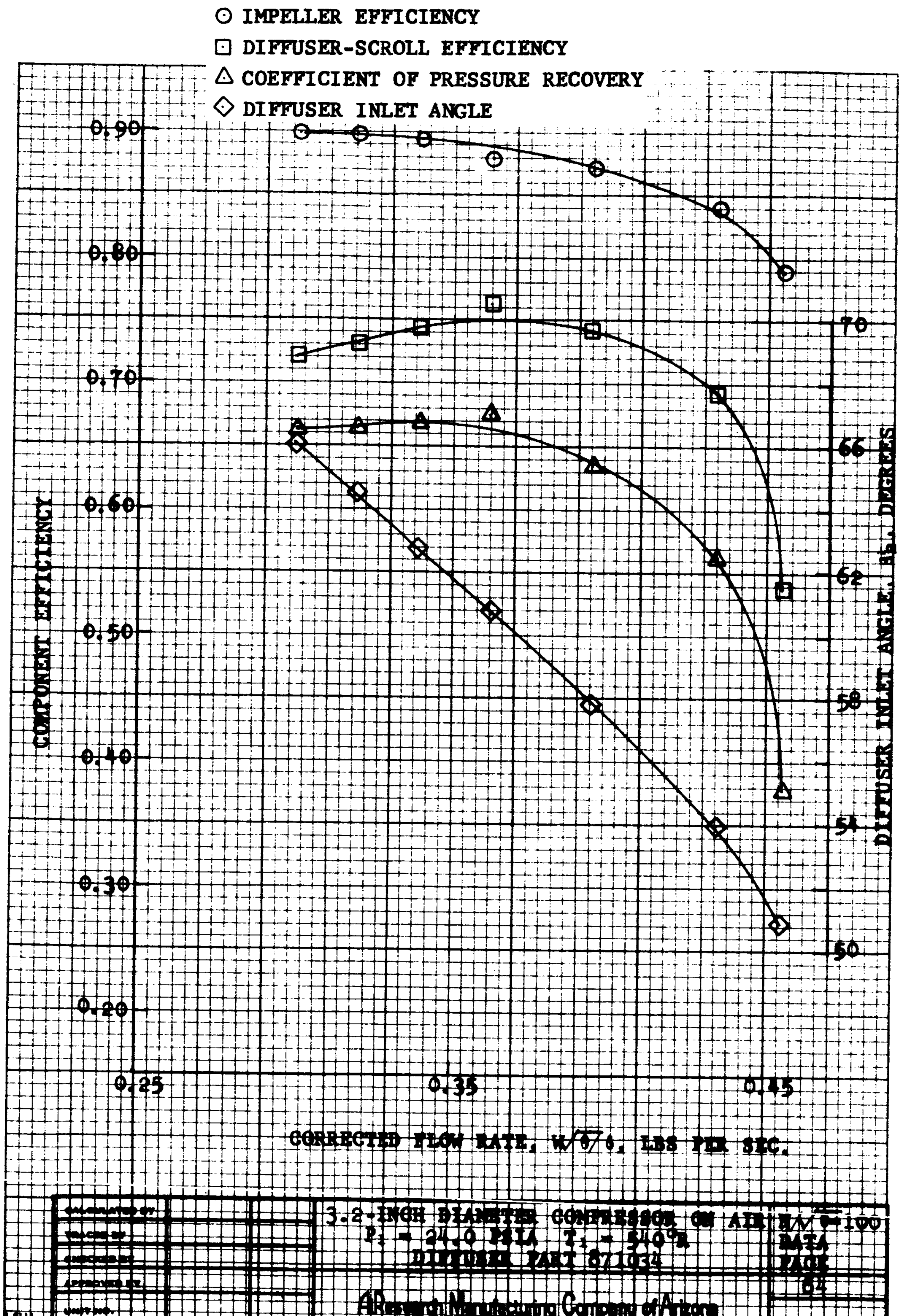
⊙ IMPELLER EFFICIENCY
⊡ DIFFUSER-SCROLL EFFICIENCY
△ COEFFICIENT OF PRESSURE RECOVERY
◇ DIFFUSER INLET ANGLE
COMPONENT EFFICIENCY
0.90
0.80
0.70
0.60
0.50
0.40
0.30
0.20
DIFFUSER INLET ANGLE, DEGREES
70
66
62
58
54
50
0.25
0.35
0.45
CORRECTED FLOW RATE, LBS PER SEC.
3.2-INCH DIAMETER COMPRESSOR ON AIR
DIFFUSER PART 871034
DATA
PAGE
AiResearch Manufacturing Company of Arizona

FIGURE 28

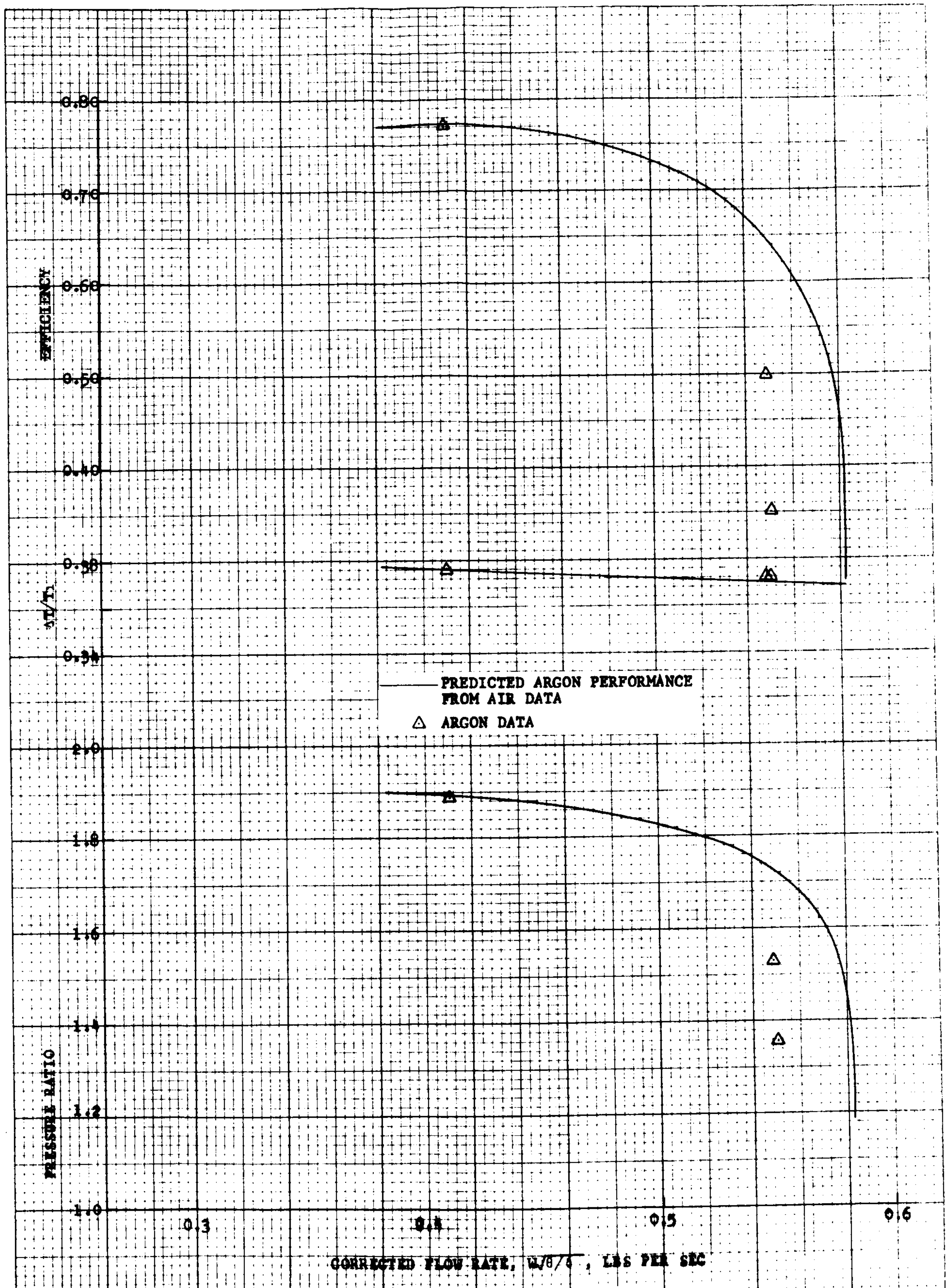

CALCULATED BY TRACED BY CHECKED BY APPROVED BY UNIT NO.	3.2- IN. DIA. COMPRESSOR ARGON PERFORMANCE P_1 = 7.0 PSIA, T_1 = 540°R DIFFUSER PART 369790-20	DATA PAGE 41
	AiResearch Manufacturing Company of Arizona	

FIGURE 29

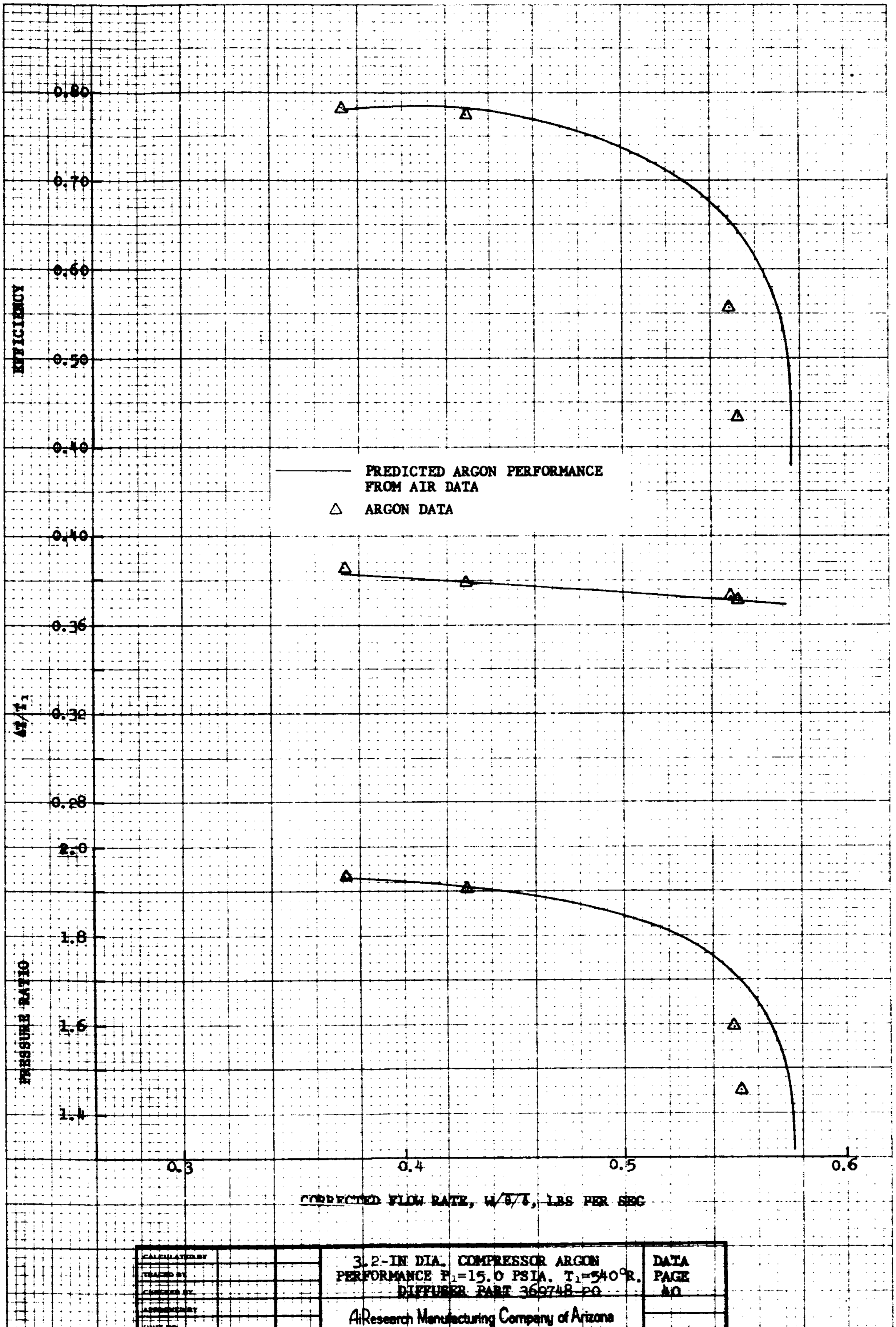

0.80
0.70
0.60
0.50
0.40
EFFICIENCY
PREDICTED ARGON PERFORMANCE FROM AIR DATA
△ ARGON DATA
0.40
0.36
0.32
0.28
ΔT/T1
2.0
1.8
1.6
1.4
PRESSURE RATIO
0.3
0.4
0.5
0.6
CORRECTED FLOW RATE, W√θ/δ, LBS PER SEC
3.2-IN DIA. COMPRESSOR ARGON PERFORMANCE P1=15.0 PSIA. T1=540°R. DIFFUSER PART 369748-90
DATA PAGE 40
AiResearch Manufacturing Company of Arizona

FIGURE 30

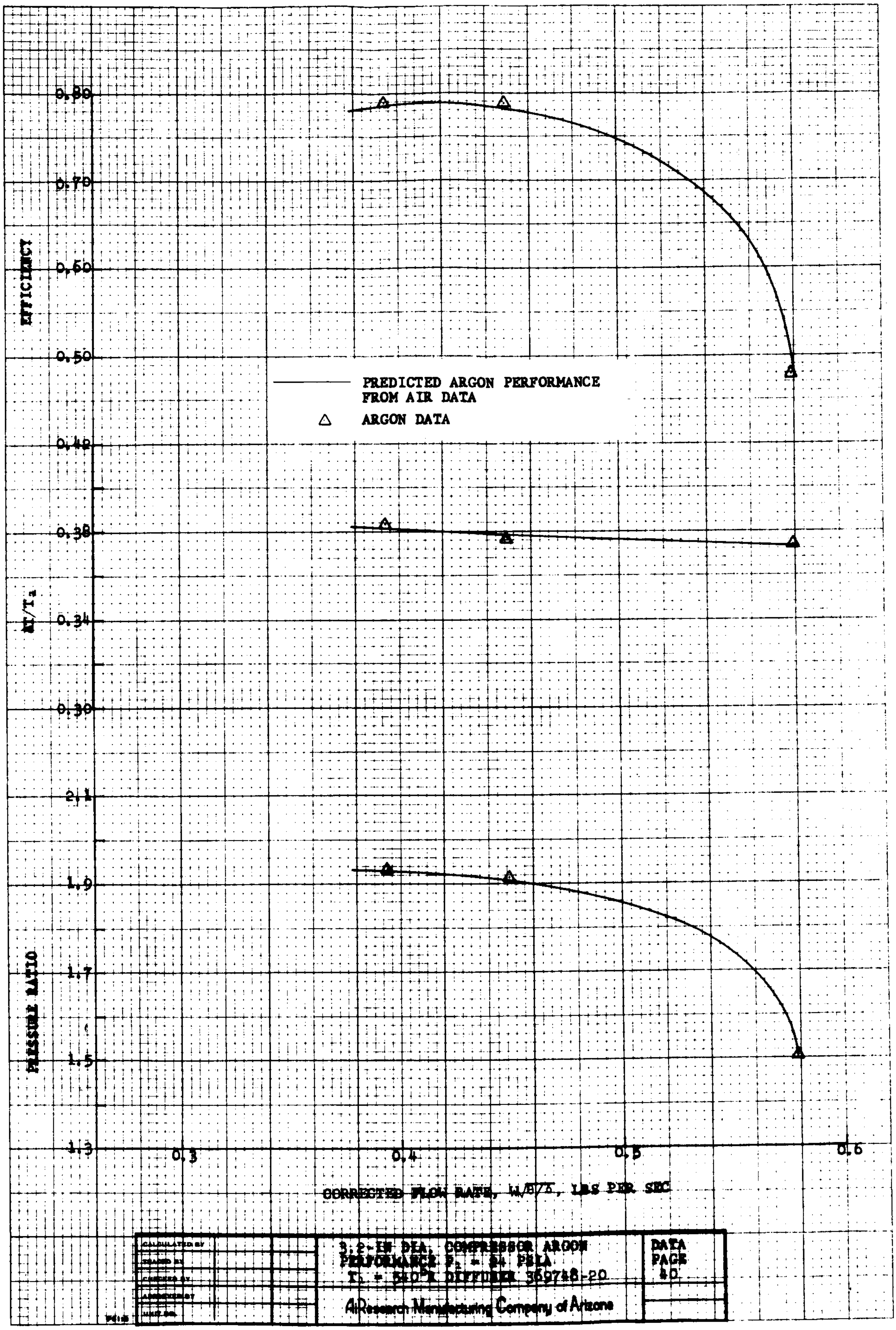

EFFICIENCY
0.80
0.70
0.60
0.50
0.42
0.38
0.34
0.30
2.1
1.9
1.7
1.5
1.3
PRESSURE RATIO
PREDICTED ARGON PERFORMANCE FROM AIR DATA
ARGON DATA
0.3
0.4
0.5
0.6
CORRECTED FLOW RATE, W√θ/δ, LBS PER SEC
3.2-IN DIA. COMPRESSOR ARGON
DATA PAGE 40
AiResearch Manufacturing Company of Arizona

FIGURE 31

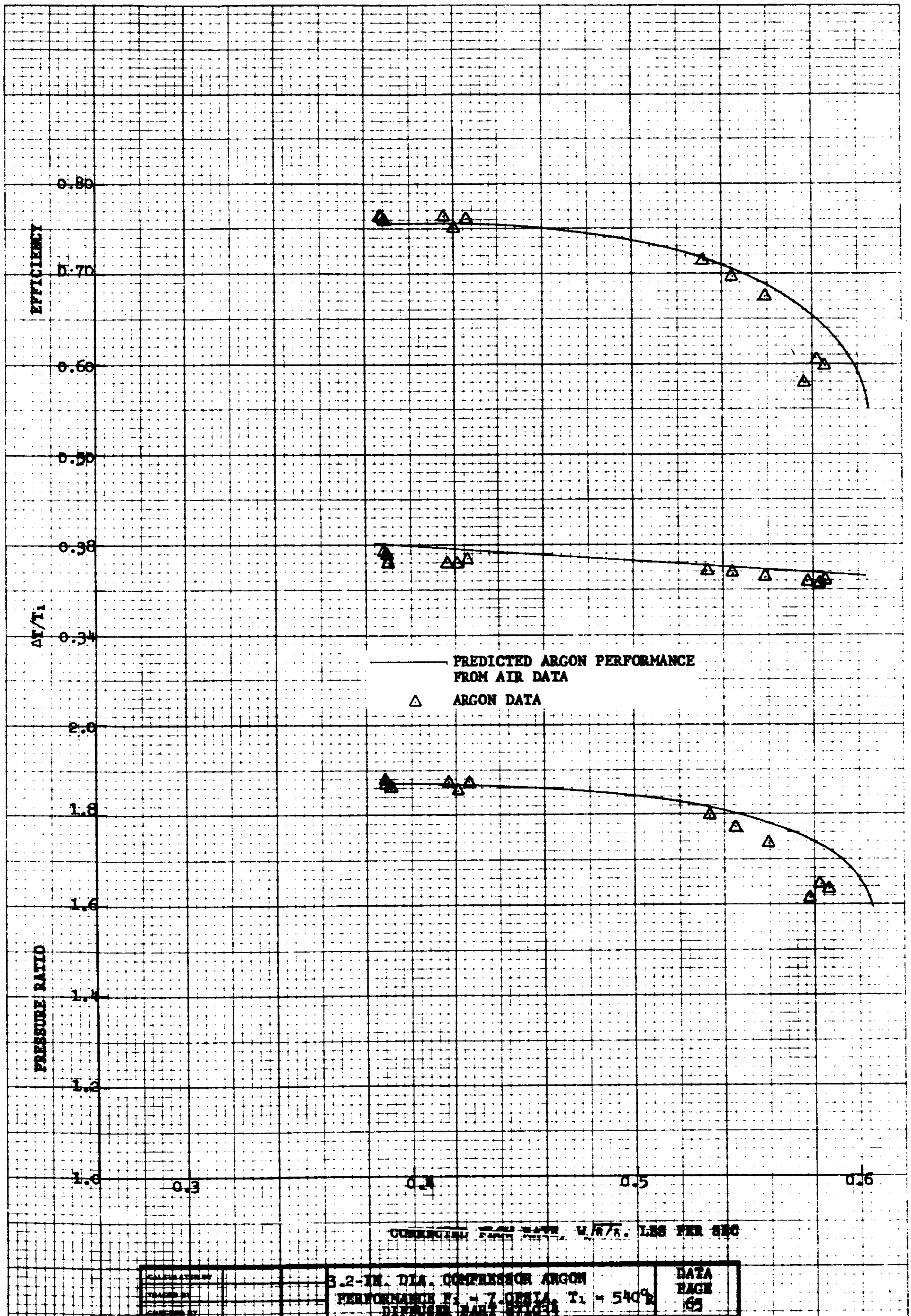
EFFICIENCY
0.80
0.70
0.60
0.50
0.38
ΔT/T₁
0.34
PREDICTED ARGON PERFORMANCE
FROM AIR DATA
ARGON DATA
2.0
1.8
1.6
PRESSURE RATIO
1.4
1.2
1.0
0.3
0.4
0.5
0.6
LBS PER SEC
AiResearch Manufacturing Company of Arizona
DATA
PAGE

FIGURE 32

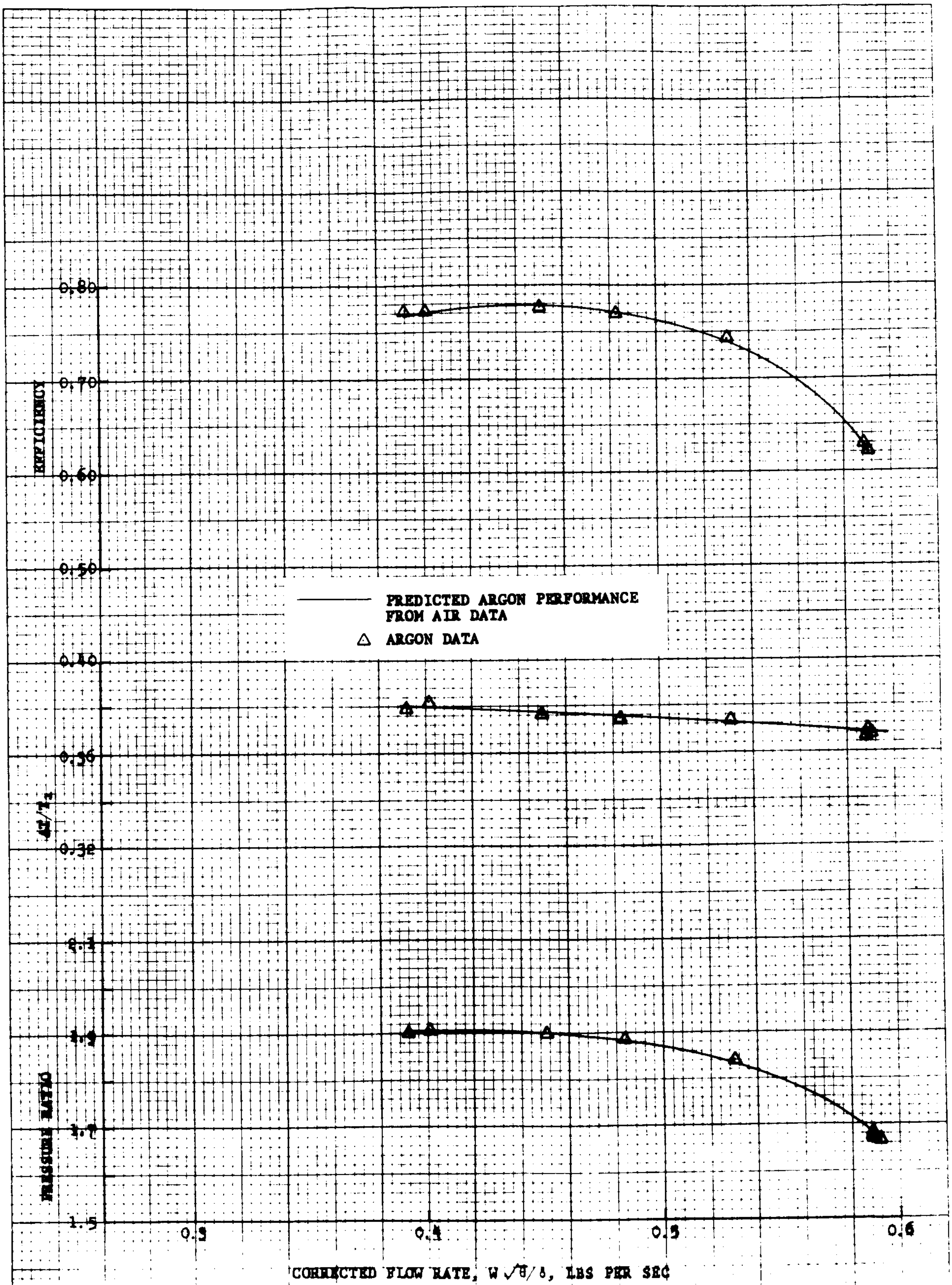

CALCULATED BY		3.2-INCH DIAMETER COMPRESSOR ARGON PERFORMANCE P_1 = 15.0 PSIA T_1 = 540°R DIFFUSER 871034	DATA PAGE 65
TRACED BY			
CHECKED BY			
APPROVED BY		AiResearch Manufacturing Company of Arizona	
UNIT NO.			

FIGURE 33

readout and the standard manometer was apparent. A plot of the percent error as a function of pressure level is shown in Figure 34. Note that very large errors occur at the lower pressures.

All overall data and diffuser-impeller performance breakdowns for both Phase I and Phase II test results have been corrected in accordance with this calibration.

Because of the number of pressures recorded in the diffuser mean line static pressure distributions shown in Appendix I,it was deemed impractical to correct these data. As a result, the level of the static pressure distributions for the lower inlet pressure levels is slightly high. The error is significant only for the 2 psia data, and, if necessary, corrections can be made for specific data points by use of Figure 34.

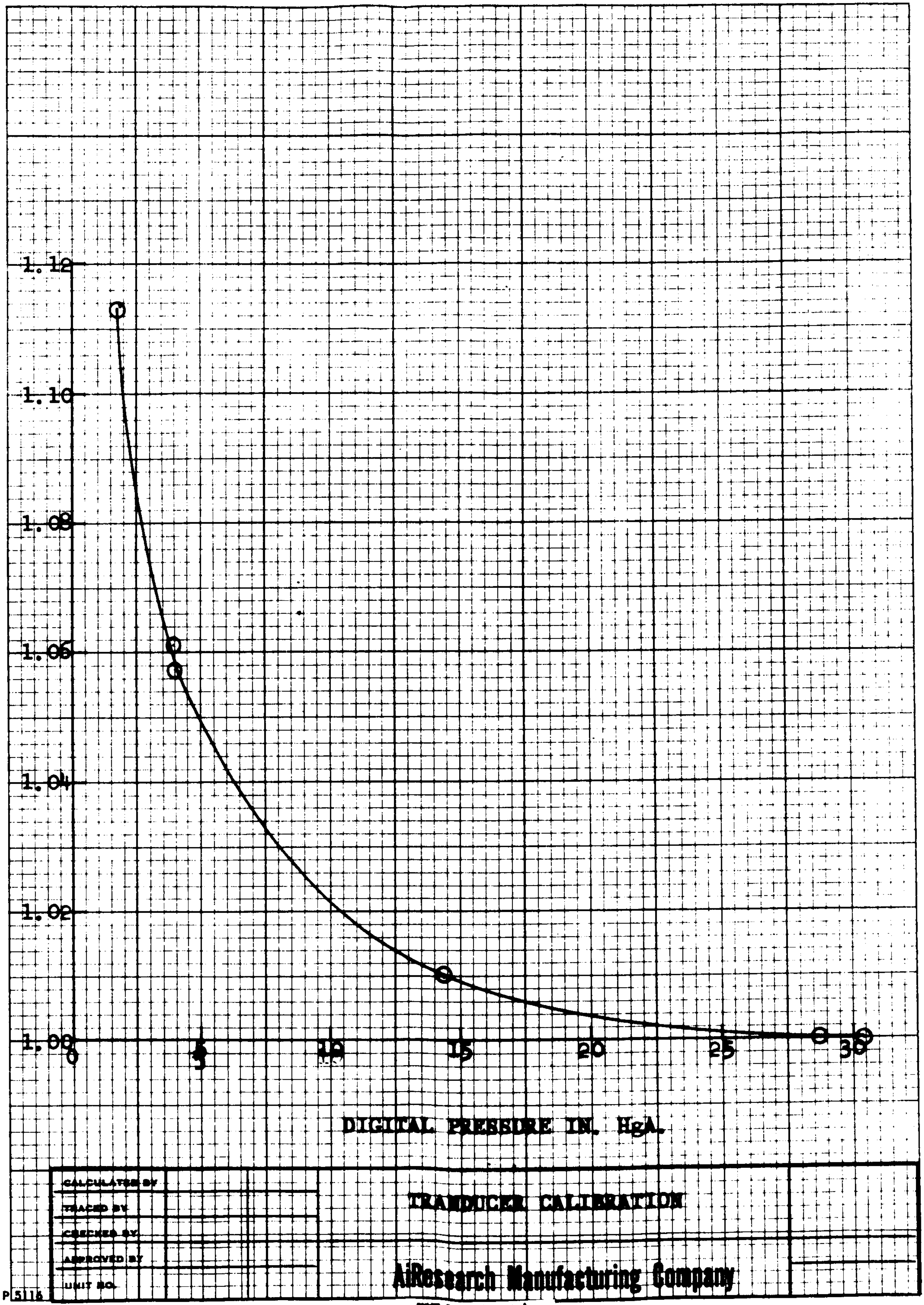

1.12
1.10
1.08
1.06
1.04
1.02
1.00
$P_{TRUE}/P_{DIGITAL}$
0
5
10
15
20
25
30
DIGITAL PRESSURE IN. HgA.
CALCULATED BY
TRACED BY
CHECKED BY
APPROVED BY
UNIT NO.
TRANDUCER CALIBRATION
AiResearch Manufacturing Company
P 5116

FIGURE 34

ANALYSIS OF TEST RESULTS

Overall Performance

An initial perusal of the overall data for both the original and redesigned diffusers indicated unexpected trends, particularly at the low pressure levels, 2 and 4 psia. Instead of the anticipated depreciation in overall efficiency with decreasing inlet pressure (i.e., Reynolds number), the efficiency of the configuration utilizing the original diffuser actually appeared to increase according to the 2-psia inlet pressure data. The peak efficiencies observed with the redesigned diffuser also seemed to vary irregularly for the 2-psia case.

A survey of the individual thermocouple and pressure probe readings revealed that the values were remarkably consistent, i.e., the inconsistent data was not due to isolated bad thermocouples or pressure probes.

Because of past difficulty in measuring temperatures at extremely low pressure levels, a general error in thermocouple readings due to the extremely small mass flow per unit area resulting in a relatively poor heat-transfer condition was next suspected. In order to check this theory the observed values of $\frac{\Delta T}{T_1}$ for fixed corrected flows (one near surge and one near choke for each speed) were plotted as a function of inlet pressure. The results are shown in Figure 35 for the original diffuser and in Figure 36 for the redesigned diffuser. These plots indicate that for the higher pressure levels (7 psia and greater) the values of $\frac{\Delta T}{T_1}$ are essentially constant; while at 4 psia and lower, $\frac{\Delta T}{T_1}$ appears to go up, down, or remain constant, depending on speed or which

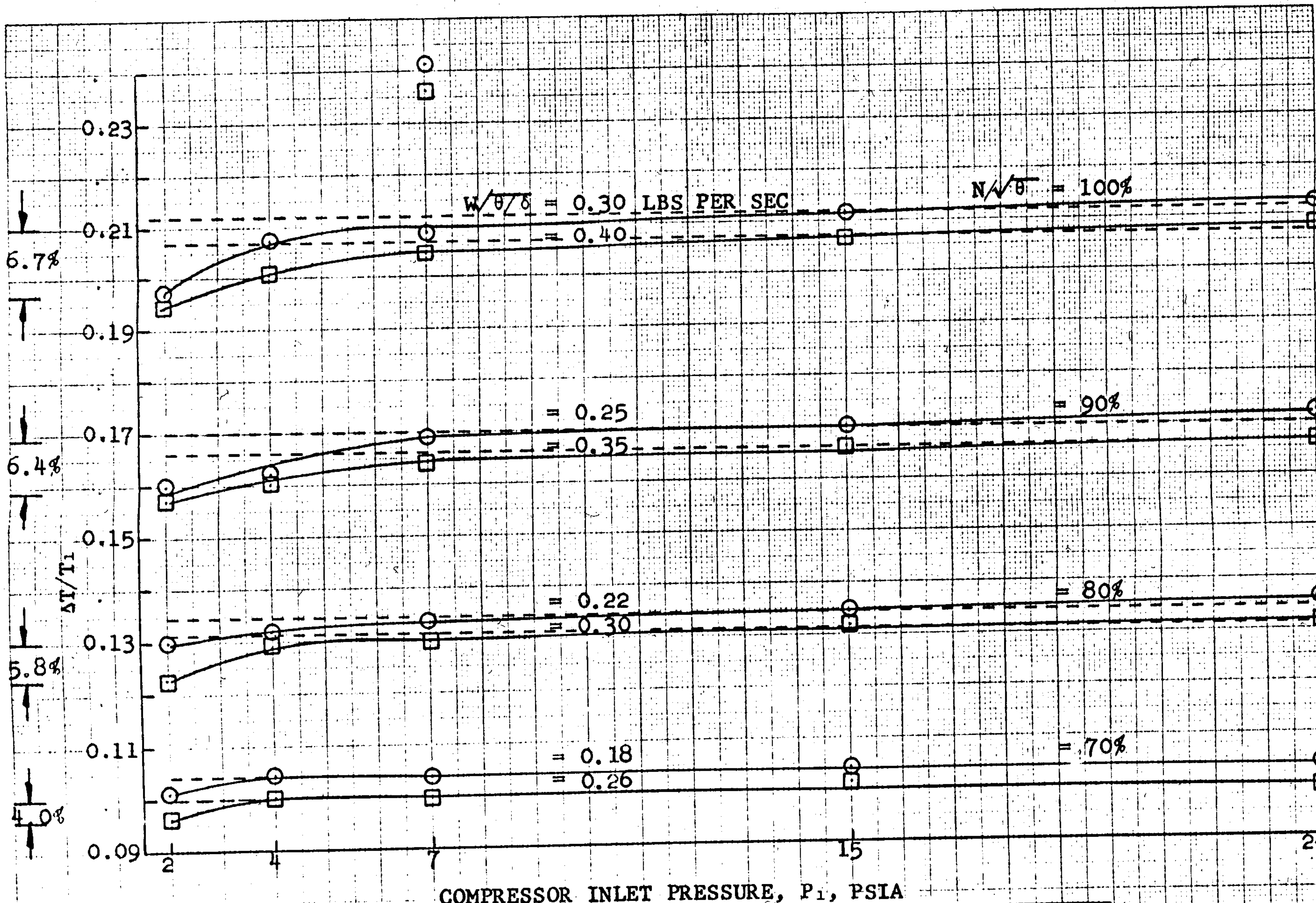

CALCULATED BY	
TRACED BY	
CHECKED BY	
APPROVED BY	
UNIT NO.	

3.2-INCH DIAMETER COMPRESSOR ON AIR
T_1 = 540°R DIFFUSER PART 369748-20
$\Delta T/T_1$ VERSUS INLET PRESSURE

AiResearch Manufacturing Company of Arizona

FIGURE 35

P5105

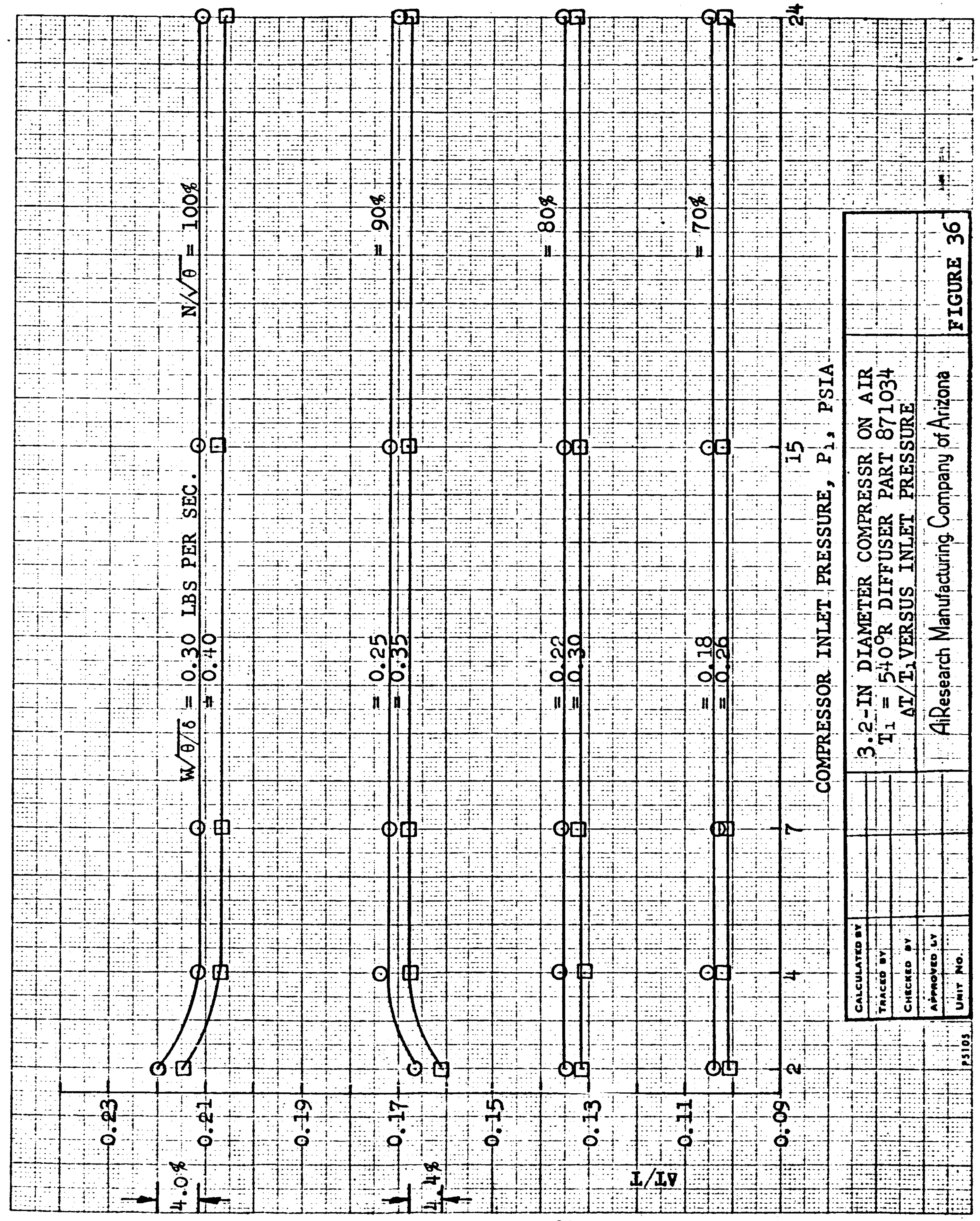

3.2-IN DIAMETER COMPRESSR ON AIR
T_1 = 540°R DIFFUSER PART 871034
$\Delta T/T_1$ VERSUS INLET PRESSURE

FIGURE 36

diffuser is installed. It is extremely unlikely that the observed $\frac{\Delta T}{T_1}$ are representative of the actual values, particularly in view of data (Ref. 1 - 4) indicating a high degree of thermocouple error when small mass flows per unit area are encountered. Since no more suitable instrumentation was avilable, retesting did not appear to be warranted.

In light of the significant effect of $\frac{\Delta T}{T_1}$ on efficiency, the following assumptions were made in an attempt to obtain meaningful results from the observed data.

(1) The pressure ratio was assumed to be accurate.

(2) $\frac{\Delta T}{T_1}$ was assumed to be constant for all pressure levels. The level chosen was that displayed at the 15 psia condition, as shown in Figure 35.

Assumption (1) is substantiated by the general quality of the pressure data. Assumption (2) is purely arbitrary but is based on the fact that, for about 75 percent of the data taken, $\frac{\Delta T}{T_1}$ was essentially constant as a function of pressure for a fixed speed. This is not a rigorous argument. In fact, it may be argued on the one hand that as the pressure level (Reynolds number) is reduced, an increasingly large quantity of low energy boundary layer is produced. This boundary layer, in combination with the strong secondary flows normally existing in a centrifugal impeller, could cause an increased quantity of recirculating fluid, manifesting itself as an <u>increase</u> in $\frac{\Delta T}{T_1}$. However, on the other hand, it may also be argued that a heat leak from the assembly could reduce $\frac{\Delta T}{T_1}$, if the heat leak is not correctly measured or insulated against.

The values of overall efficiency were, therefore, "corrected" by using these assumptions for that portion of the data when required, mainly 2 and 4 psia data. The "corrected" efficiencies and $\frac{\Delta T}{T_1}$ values are shown as dashed lines on Figures 8, 9, 10, and 19. The resulting efficiencies seem to be more realistic and also generally follow the trend established by the data taken at the higher pressure levels.

With the "corrected" values used, the effect of inlet pressure on overall performance is presented for the original diffuser in Figure 37 and for the redesigned diffuser in Figure 38.

Generally, on an <u>overall</u> efficiency basis, the original diffuser appears to yield superior performance at 4 psia. The effect of pressure level on overall efficiency also appears to be significant, particularly at inlet pressures less than 4 psia.

The solid curves on Figures 37 and 38 represent an attempt to establish a general trend of efficiency vs pressure level for all the data taken with the two diffuser configurations. By use of these curves and Reynolds numbers based on average tip speed, a plot of $1 - \eta_{max}$ as a function of average Reynolds number is shown for both diffusers in Figure 39.

For comparison, a line is also shown along which $1 - \eta_{max}$ varies inversely as the Reynolds number raised to the 0.2 power, i.e., $\frac{1 - \eta}{1 - \eta_{ref}} = \left(\frac{Re_{ref}}{Re}\right)^{0.2}$. The reference Reynolds number was taken so as to correspond to approximately standard sea level conditions for the subject compressor, and the reference efficiency was taken as the average of the observed efficiencies for the compressor with the original and redesigned diffusers.

It appears that the 0.2 "law" is valid when Reynolds numbers lower than those occurring at standard conditions with this particular compressor are encountered, but does not necessarily hold for higher Reynolds numbers. Stated another way, it appears that, when a fixed geometrical configuration is operated at low Reynolds numberes, an efficiency decrement compared with performance at standard conditions can be predicted with reasonable accuracy by using the 0.2 "law." At Reynolds numbers higher than standard, however, it appears that little or no gain in efficiency should be expected.

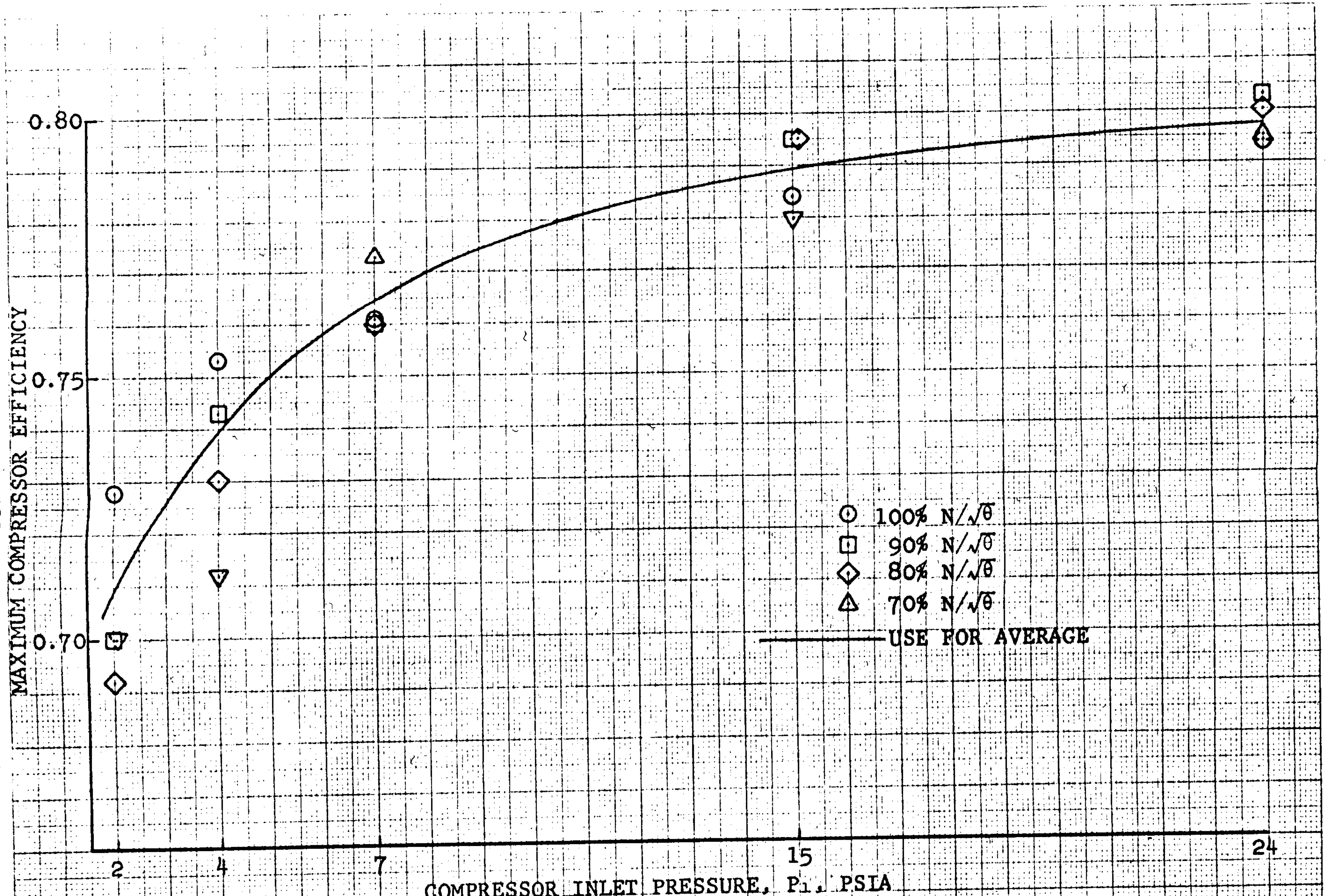

CALCULATED BY		3.2-IN. DIAMETER COMPRESSOR ON AIR T_1 = 540°R. AVERAGE PERFORMANCE DIFFUSER 369748-20
TRACED BY		
CHECKED BY		
APPROVED BY		AiResearch Manufacturing Company of Arizona
UNIT NO.		FIGURE 37

P5105

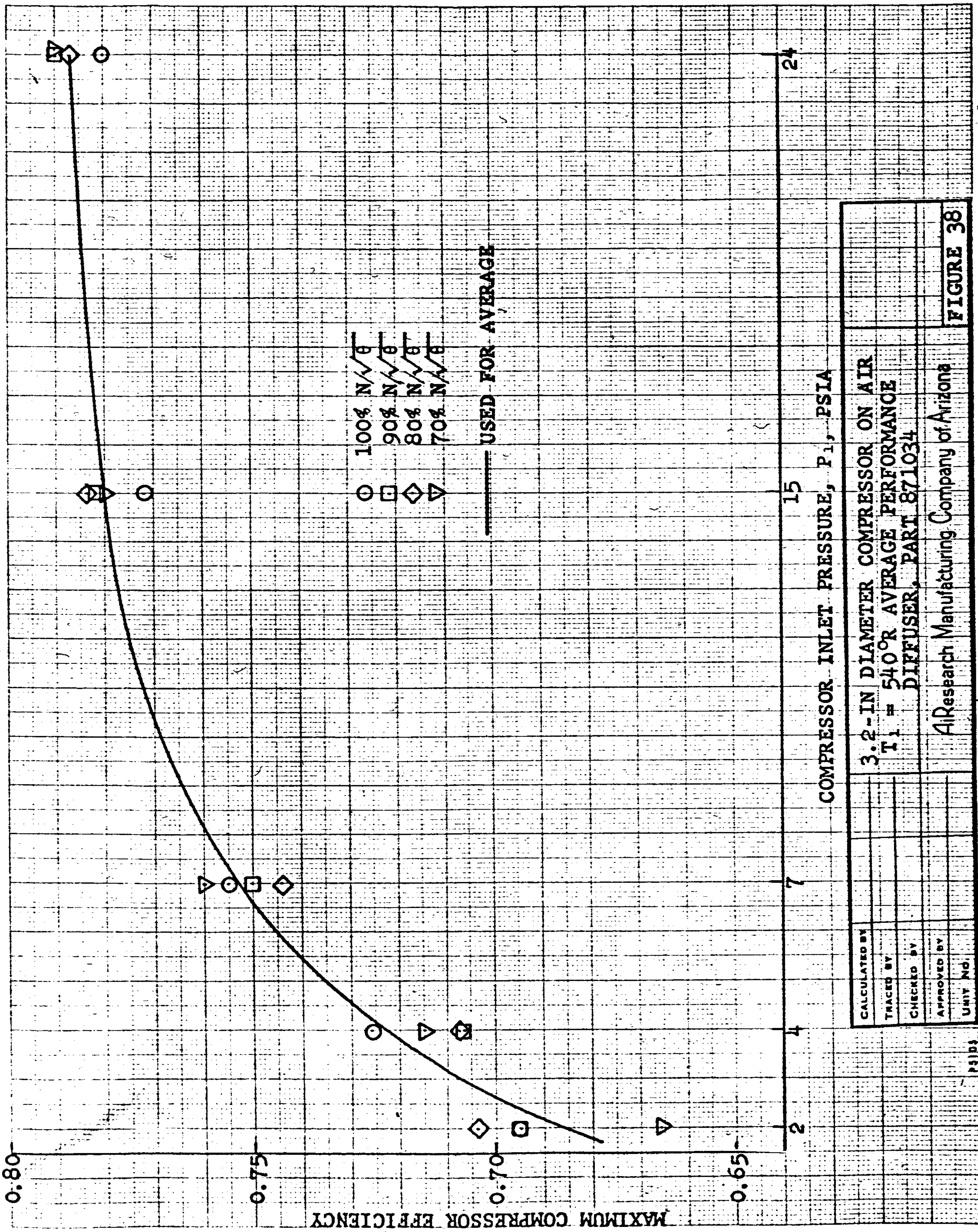
MAXIMUM COMPRESSOR EFFICIENCY
0.80
0.75
0.70
0.65
2
4
7
15
24
COMPRESSOR INLET PRESSURE, P_1, PSIA
○ 100% $N/\sqrt{\theta}$
□ 90% $N/\sqrt{\theta}$
◇ 80% $N/\sqrt{\theta}$
▽ 70% $N/\sqrt{\theta}$
USED FOR AVERAGE
CALCULATED BY
TRACED BY
CHECKED BY
APPROVED BY
UNIT NO.
3.2-IN DIAMETER COMPRESSOR ON AIR
T_1 = 540°R AVERAGE PERFORMANCE
DIFFUSER, PART 871034
AiResearch Manufacturing Company of Arizona
FIGURE 38

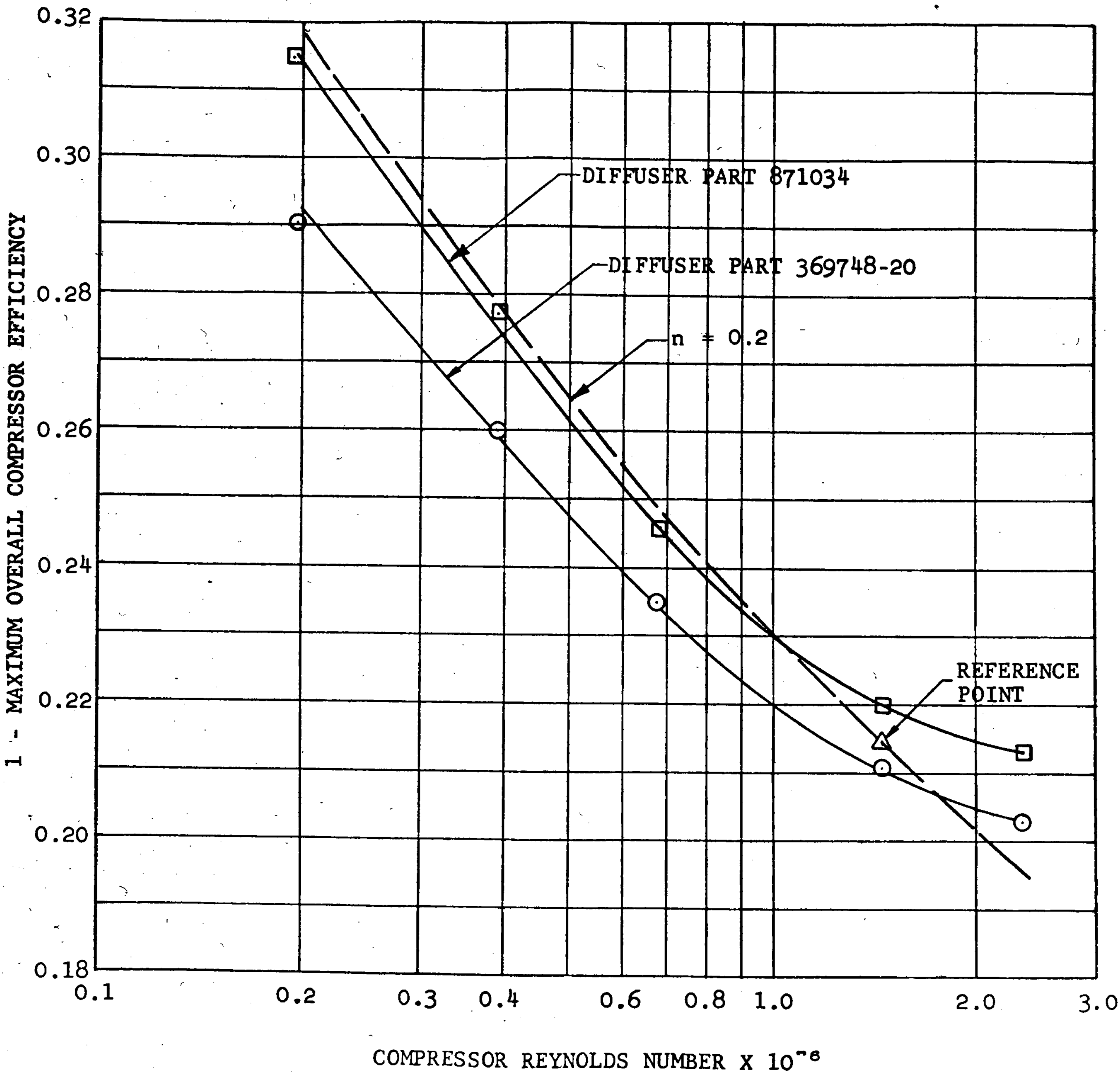

EFFECT OF REYNOLDS NUMBER ON
COMPRESSOR PERFORMANCE

FIGURE 39

It must be reiterated that the above conclusions hold only if the assumption that the $\frac{\Delta T}{T_1}$ remains constant with pressure level is valid.

Diffuser Performance

As previously mentioned, the breakdown between impeller and diffuser (plus scroll) performance for 100 percent speed and all inlet pressures is shown in Figures 13 through 17 and 24 through 28. Because of the difficulty encountered in measuring temperatures accurately at the lower pressure levels, as discussed in the preceding section, it is doubtful whether the efficiency breakdowns shown for the 2 psia and 4 psia inlet conditions represents a true comparison of old and new diffuser performance. It should be noted that this data can be recalculated to correspond to the overall performance data obtained by using the adjusted $\frac{\Delta T}{T_1}$ distributions shown as dashed lines on Figures 8, 9, 10, and 19. However, due to the arbitrary nature of that adjustment, a similar correction to the impeller and diffuser performance data is not deemed to be justified at this time.

At an impeller inlet pressure of 7 psia and 100 percent speed, the following observations can be made. (Figures 15 and 26.)

1. The impeller characteristic is about the same for both the original and redesigned diffuser. This is as expected, since the effect of the diffuser on the impeller should be negligible. Confidence is thus justified in the diffuser performance comparison.

2. The peak efficiency for the redesigned diffuser plus scroll is identical to that of the original diffuser (about 0.735). The redesigned diffuser characteristic appears to have been shifted so that its peak efficiency does not occur at the same corrected flow as the impeller peak efficiency. This results in a reduced peak stage efficiency and explains the decrease in peak overall efficiency observed in Figures 10 and 20 between the performance with the original and redesigned diffusers. Apparently the redesign did not improve the peak performance of the diffuser-scroll combination.

The preceding statements made concerning the 7-psia data are equally applicable to the 15- and 24-psia data. This leads to the conclusion that the peak efficiency performance of the diffuser-scroll combination at high Reynolds numbers was not affected by the redesign.

The static pressure distributions along the diffuser mean line and at the scroll exit, presented in Appendix I, must now be evaluated. When the distributions on pages 14 and 37 of Appendix I are compared (for 7-psia air data at design speed for the original and redesigned diffusers respectively), an interesting factor becomes apparent. When considering only the pressure distributions at a flow point near surge (the upper curves), both diffusers have the same inlet static pressure (about 19.6 in. Hg abs). At the exit of the redesigned diffuser, the static pressure is 23.95 in. Hg abs, as compared with 23,60 in. Hg abs at the exit of the original diffuser. At the scroll exit the static pressure with the original diffuser is 24.20 compared to 24.00 for the redesigned diffuser. Since the inlet conditions are identical, it seems that the redesigned diffuser has better recovery than the original diffuser. Due to a mismatch with the scroll, the efficiency of the diffuser-scroll combination appears to be lower with the redesigned diffuser. Note that the contract did not allow for modification of the scroll from its original design to account for the re-designed diffuser.

A similar trend is observed in the data for 100 percent speed and 15 psia, pages 18 and 41, and for the 100 percent speed, 24 psia data pages 22 and 45 of Appendix I. It thus appears that, in general, a small improvement has been obtained in diffuser efficiency at all pressure levels. It is of further interest to note that the trend observed in air is duplicated in the 100 percent speed data for the argon check points for both 7 and 15 psia inlet pressures.

A further check of all diffuser static pressure data at all speeds and pressures indicates that invariably the scroll recovery is considerably higher when it is preceded by the original diffuser for which it was designed.

CONCLUSIONS

The results of the tests indicate that:

1. Considerable difficulty is present in accurately measuring temperatures at very low pressure levels.

2. If the assumption is made that the impeller work input does not change over the range of Reynolds numbers tested, a reasonable correlation can be obtained of stage efficiency versus Reynolds number. For the compressor tested, this correlation indicates that for Reynolds numbers higher than those corresponding to its standard conditions, the efficiency increase is small but at lower Reynolds numbers, the efficiency drops approximately in accordance with the following relationship:

$$\left(\frac{1-\eta}{1-\eta_{ref}}\right) = \left(\frac{Re_{ref}}{Re}\right)^{0.2}$$

3. The argon check points confirmed the fact that it is possible to predict the performance of a given compressor geometry in one fluid from data taken in another fluid or different gas constant and ratio of specific heats. Exceptional accuracy was obtained in predicting peak efficiencies and surge flows, but predicted choke flows tended to be high.

4. The overall performance of the configuration using the original diffuser tended to be higher than that obtained with the new diffuser. A breakdown of diffuser-scroll and impeller performance indicates that the lower overall performance observed with the redesigned diffuser results from a shifting of the peak diffuser-scroll efficiency point away from the impeller peak efficiency point. The peak efficiencies of both diffuser-scroll combinations are identical for all pressure levels.

5. Diffuser static pressure distributions indicate that the pressure recovery in the scroll is considerably lower when it follows the redesigned diffuser. This apparently results from an aerodynamic mismatch of the scroll with the new diffuser and also indicates that the new diffuser is slightly superior to the original at all pressure levels with respect to pressure recovery.

RECOMMENDATIONS

Results of the compressor test program indicate that:

1. Temperature-sensing instrumentation at low pressure and low-flow conditions needs further development to achieve the accuracy required for compressor evaluation.

2. Further effort in improving the match between the impeller scroll, and diffuser would provide only a slight increase in overall efficiency. Experience to date would indicate that a greater increase in overall efficiency can be obtained from further impeller development.

REFERENCES

1. Carson, A. B., "A Study of the Effect of a Vortex Sheet on the Temperature Distribution in a Fluid Stream Initially Containing Temperature Stratification," ASU Report (15 Sept. 1959).

2. Haig, Laurence B, "A Design Procedure for Thermocouple Probes," SAE 158C-60 (1960).

3. Freeze, Paul D. and Caldwell, Frank R., "Performance Tests of Jet-Engine Thermocouples," WADC Technical Report 56-476 (ASTIA AD-120 863)(1956).

4. Wormser, Alex F., "Experimental Determination of Thermocouple Time Constants with Use of a Variable Turbulence, Variable Density Wind Tunnel and the Analytic Evaluation of Conduction, Radiation and Other Secondary Effects," SAE 158 D-60 (1960).

APPENDIX I

STATIC PRESSURE DISTRIBUTION

The following curves show the static pressure distribution along the centerline of the two diffusers, Parts 369748-20 and 871034. It should be noted that the pressures as presented must be corrected for the transducer calibration shown in Figure 34 of the main text. The following is a summary of the curves, by page number, presented in the appendix.

DIFFUSER PART 369748-20
(31 PSIA INLET DESIGN)

	Inlet Pressure, psia				
	2	4	7	15	24
AIR					
Speed line, $\%N/\sqrt{\theta}$ = 70	3	7	11	15	19
= 80	4	8	12	16	20
= 90	5	9	13	17	21
=100	6	10	14	18	22
ARGON					
Speed line, $\%N/\sqrt{\theta}$= 100			23	24	25

DIFFUSER, PART 871034
(4 PSIA INLET DESIGN)

	Inlet Pressure, psia				
	2	4	7	15	24
AIR					
Speed lin, % $N/\sqrt{\theta}$ = 70	26	30	34	38	42
= 80	27	31	35	39	43
= 90	28	32	36	40	44
= 100	29	33	37	41	45
ARGON					
Speed line, % $N/\sqrt{\theta}$ = 100			46	47	

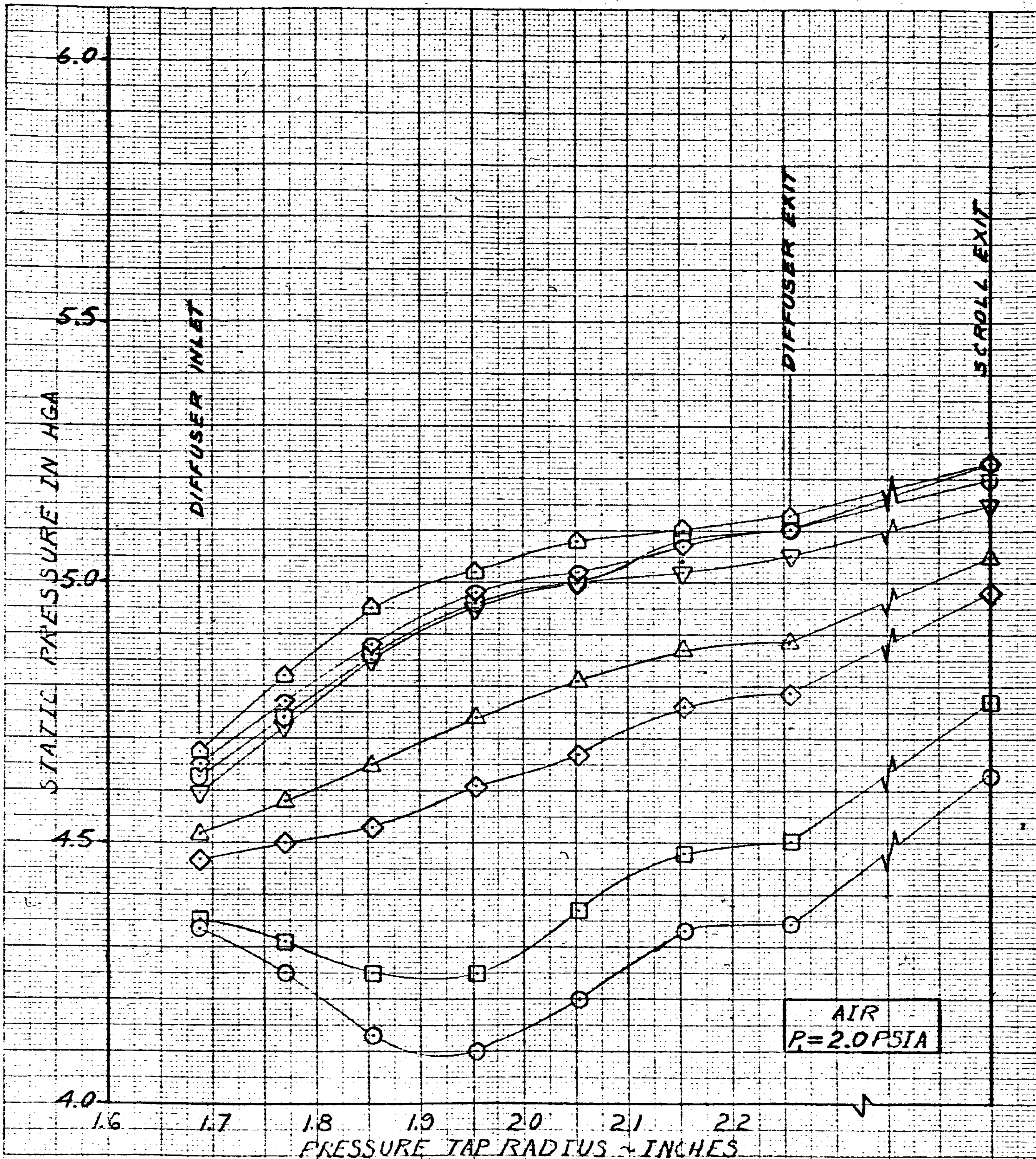

CALCULATED BY		
TRACED BY	Indwic	3-25-64
CHECKED BY	Y...	
APPROVED BY		
UNIT NO.		

P 5106

STATIC PRESSURE DISTRIBUTION ALONG DIFFUSER PART 369748-20

$\% \frac{N}{\sqrt{\theta}} = 70$

DATA PAGE 50

AIRESEARCH MANUFACTURING COMPANY

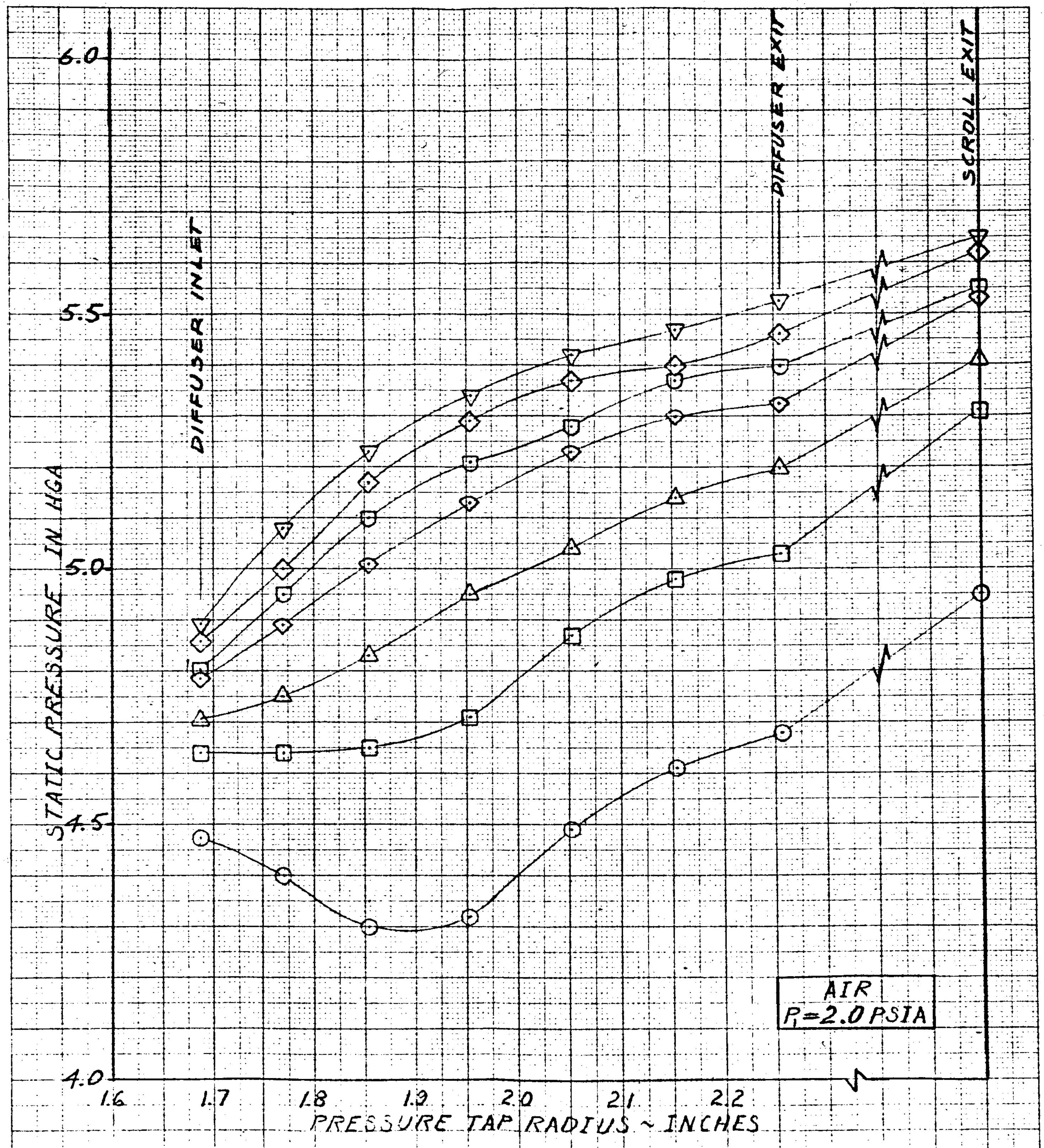

CALCULATED BY			STATIC PRESSURE DISTRIBUTION ALONG DIFFUSER PART 369748-20	$\% \frac{N}{\sqrt{\theta}} = 80$
TRACED BY	Ludwig	5-25-46		
CHECKED BY				
APPROVED BY			AIRESEARCH MANUFACTURING COMPANY	DATA PAGE 50
UNIT NO.				

P 5106

CALCULATED BY		
TRACED BY	Lindung	3-26-66
CHECKED BY		
APPROVED BY		
UNIT NO.		

STATIC PRESSURE DISTRIBUTION ALONG DIFFUSER PART 369748-20

$\% \frac{N}{\sqrt{\theta}} = 90$

AIRESEARCH MANUFACTURING COMPANY

DATA PAGE 51

P 5106

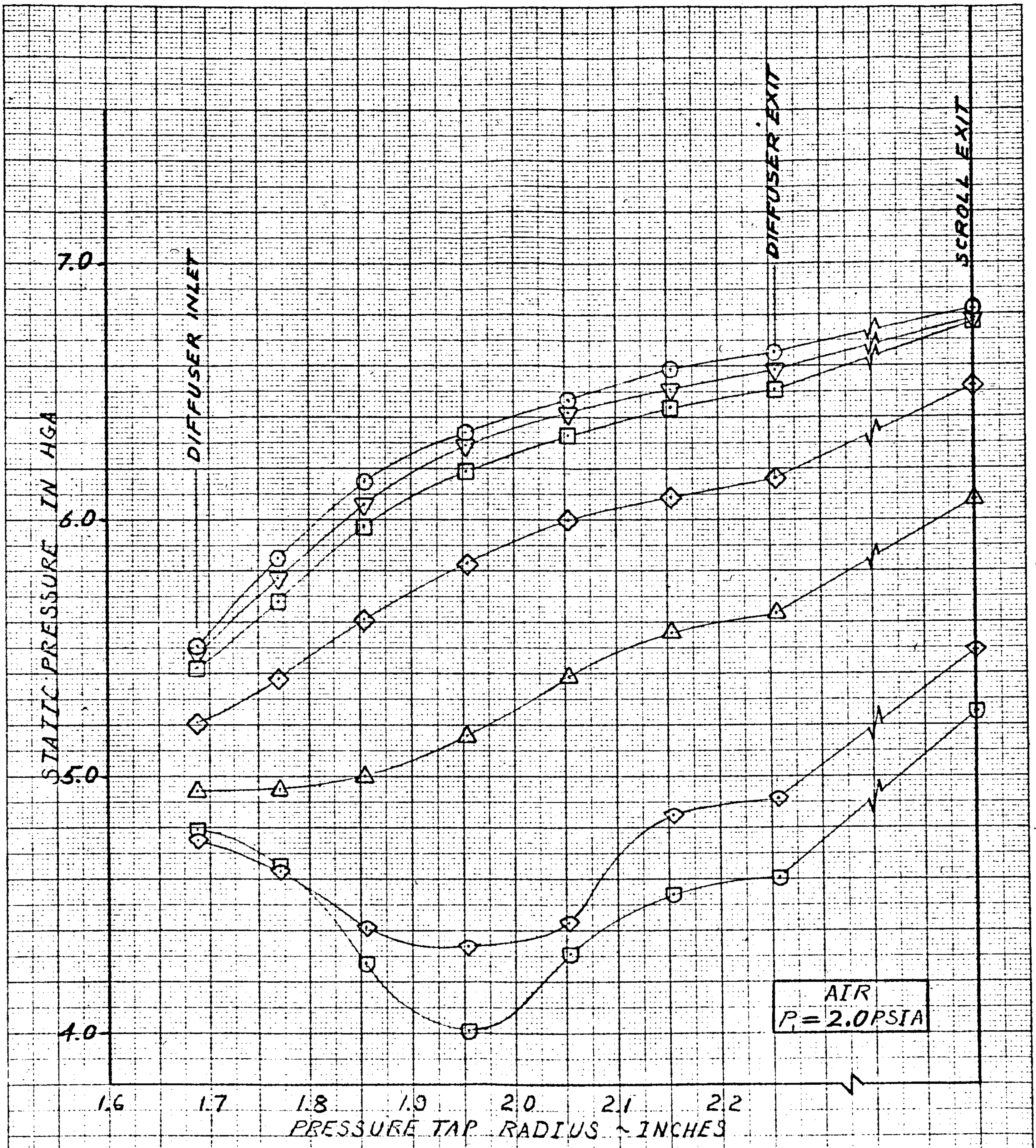

CALCULATED BY		
TRACED BY	[illegible]	3-26-64
CHECKED BY	[illegible]	
APPROVED BY		
UNIT NO.		

STATIC PRESSURE DISTRIBUTION ALONG DIFFUSER PART 369748-20

% $\frac{N}{\sqrt{\theta}}$ = 100

DATA PAGE 59

AIRESEARCH MANUFACTURING COMPANY

P 5106

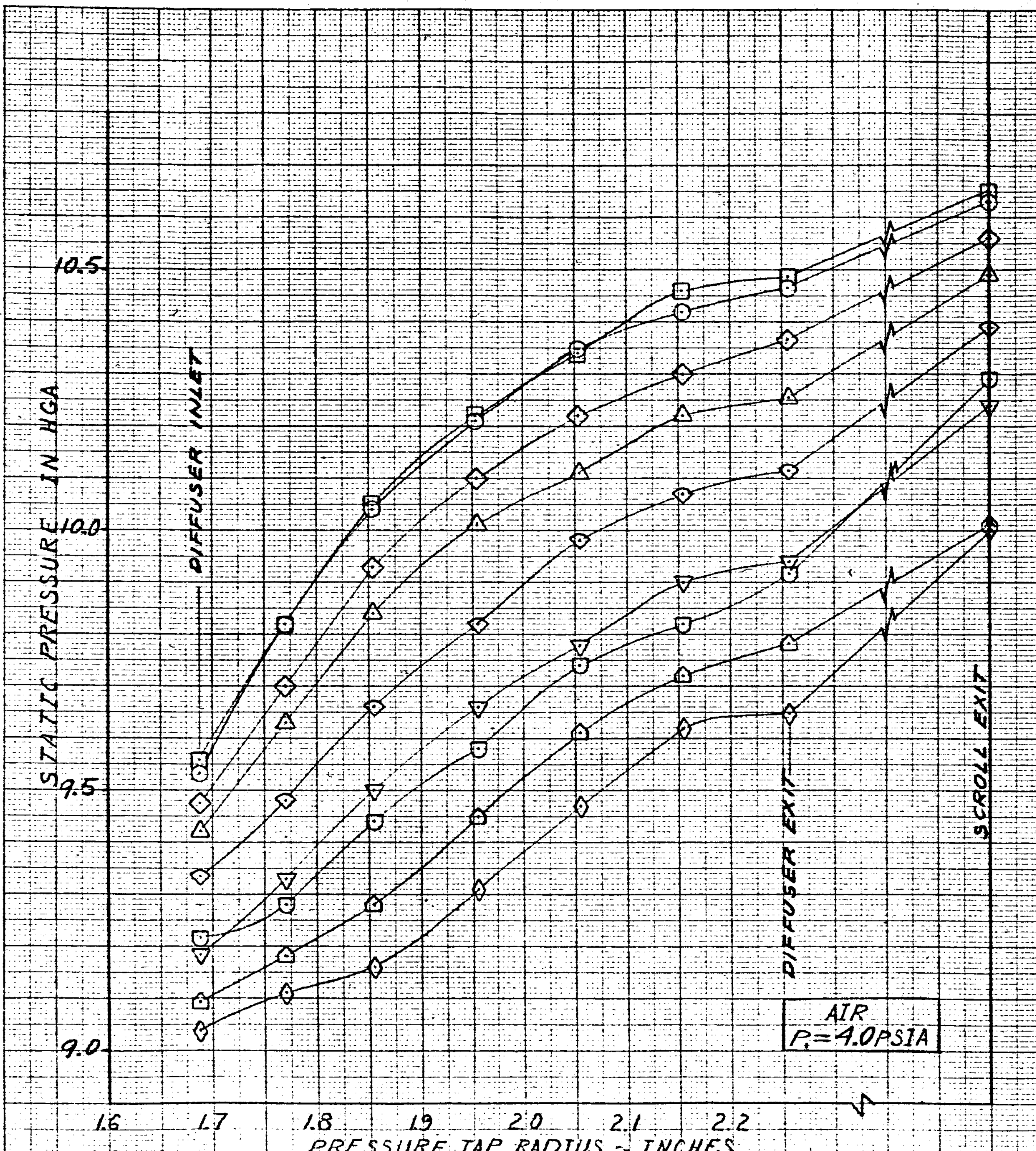

CALCULATED BY			STATIC PRESSURE DISTRIBUTION ALONG DIFFUSER PART 369748-20	$\frac{N}{\sqrt{\theta}}$ = 70
TRACED BY	Zuchwiz	3-26-66		
CHECKED BY				
APPROVED BY			AIRESEARCH MANUFACTURING COMPANY	DATA PAGE
UNIT NO.				51

P 5106

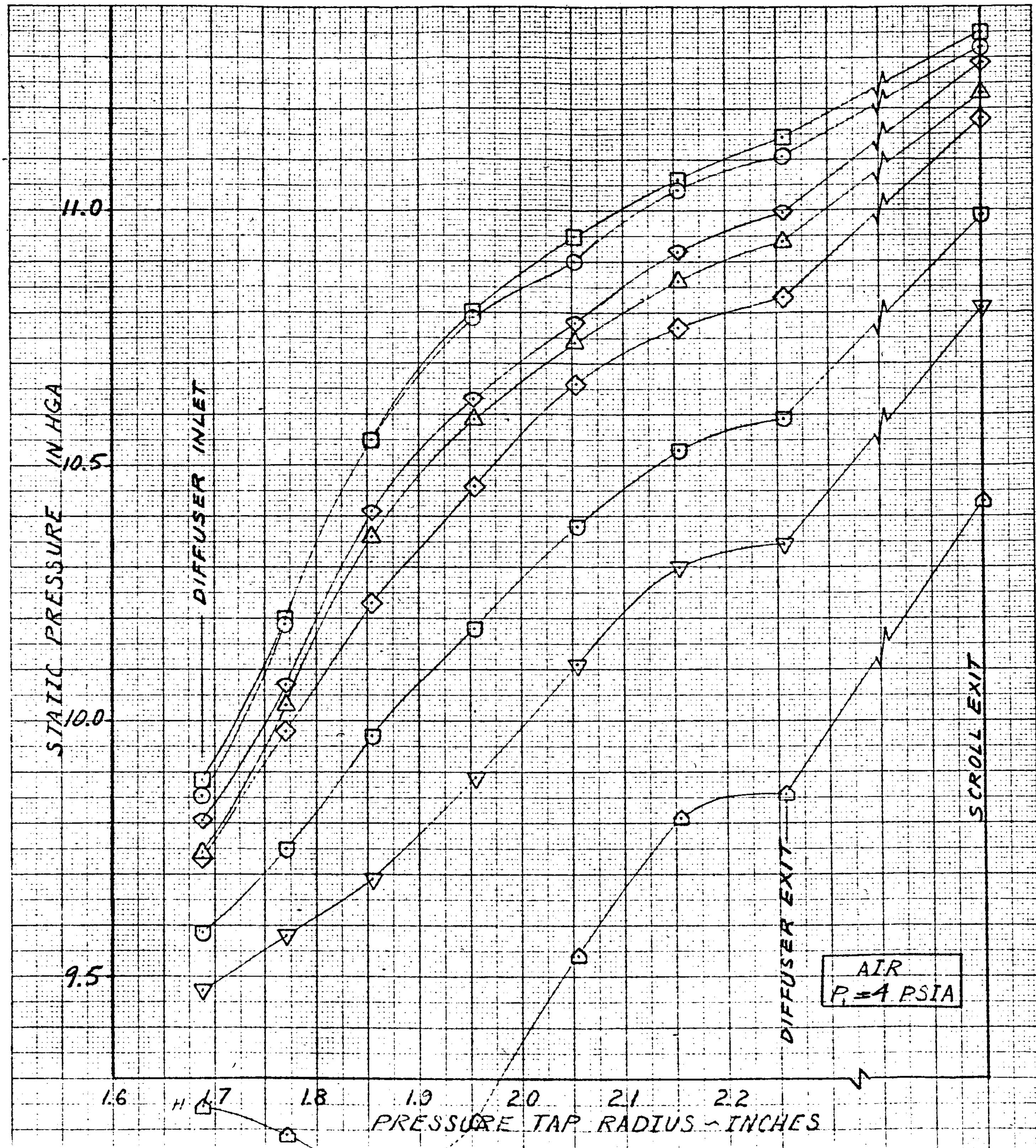

CALCULATED BY			STATIC PRESSURE DISTRIBUTION ALONG DIFFUSER PART 369748-20	% $\frac{N}{\sqrt{\theta}}$ = 80
TRACED BY				
CHECKED BY				
APPROVED BY			AIRESEARCH MANUFACTURING COMPANY	DATA PAGE
UNIT NO.				52

P 5106

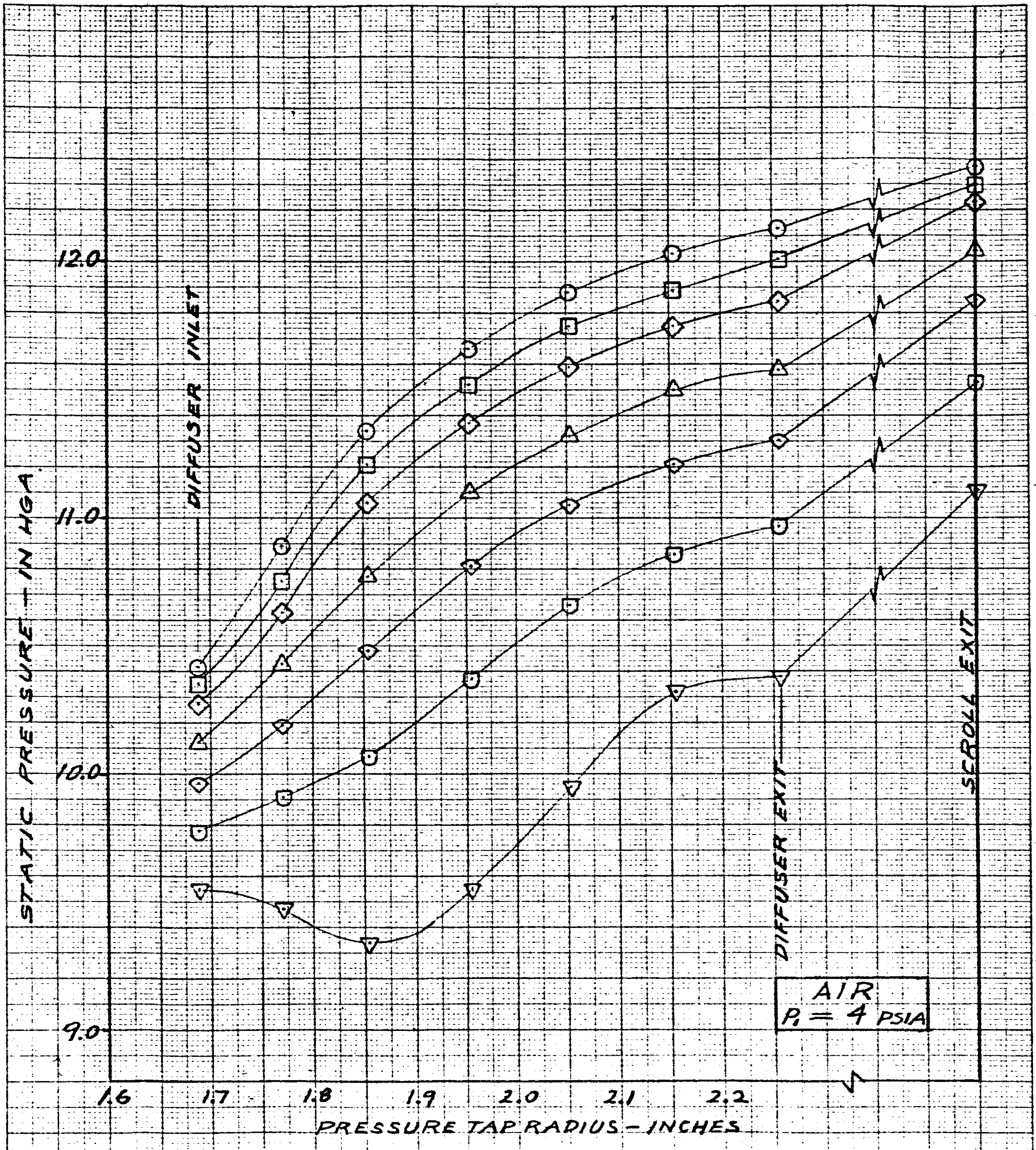

CALCULATED BY			STATIC PRESSURE DISTRIBUTION ALONG DIFFUSER PART 369748-20	$\% \frac{N}{\sqrt{\theta}} = 90$
TRACED BY		3-26-66		
CHECKED BY				
APPROVED BY			AIRESEARCH MANUFACTURING COMPANY	DATA FASE
UNIT NO.				53

P 5106

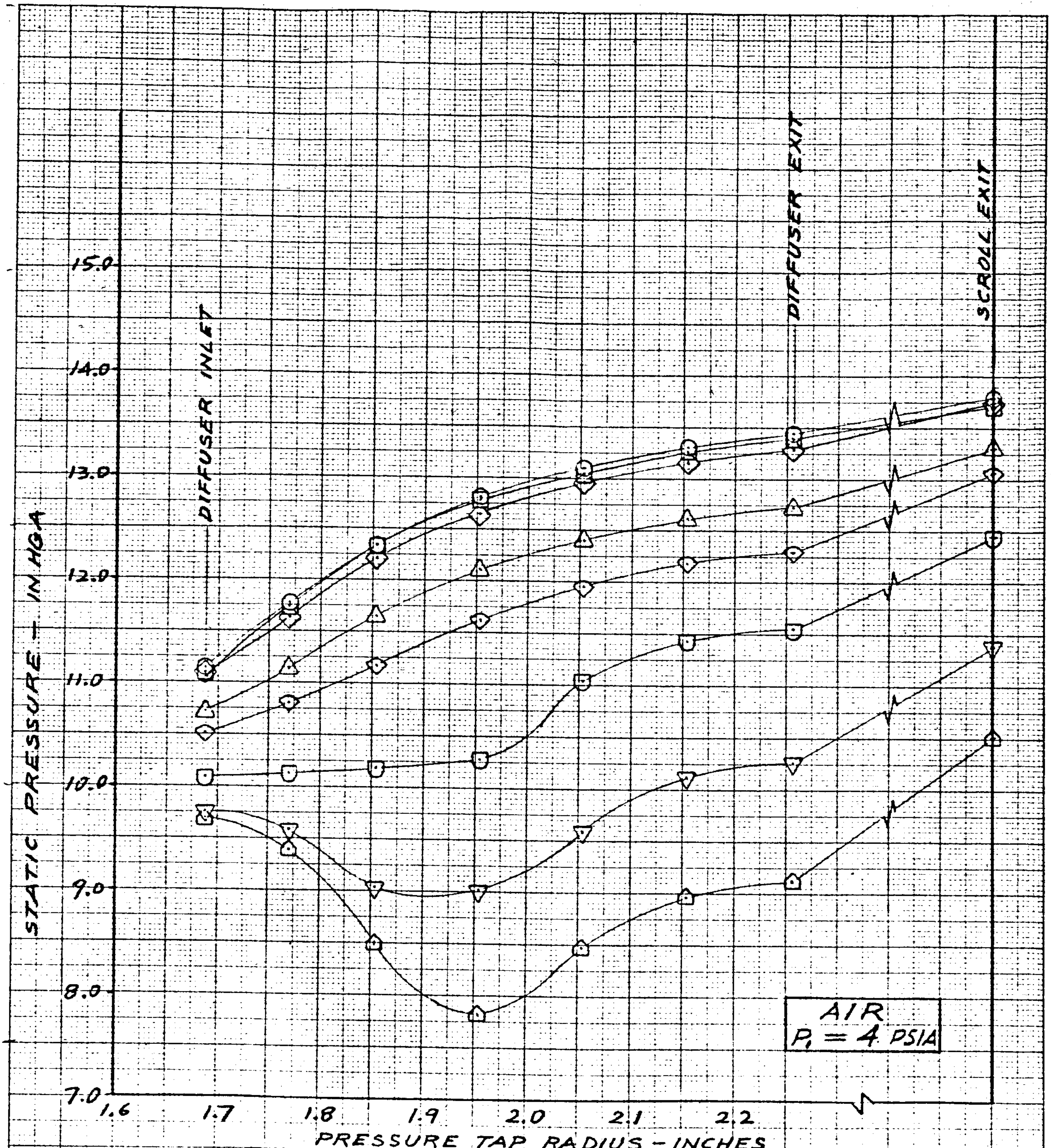

CALCULATED BY		
TRACED BY	Ludwix	3-26-66
CHECKED BY		
APPROVED BY		
UNIT NO.		

P 5106

STATIC PRESSURE DISTRIBUTION
ALONG DIFFUSER PART 369748-20

$\% \frac{N}{\sqrt{\theta}} = 100$

AIRESEARCH MANUFACTURING COMPANY

DATA BASE
58, 59

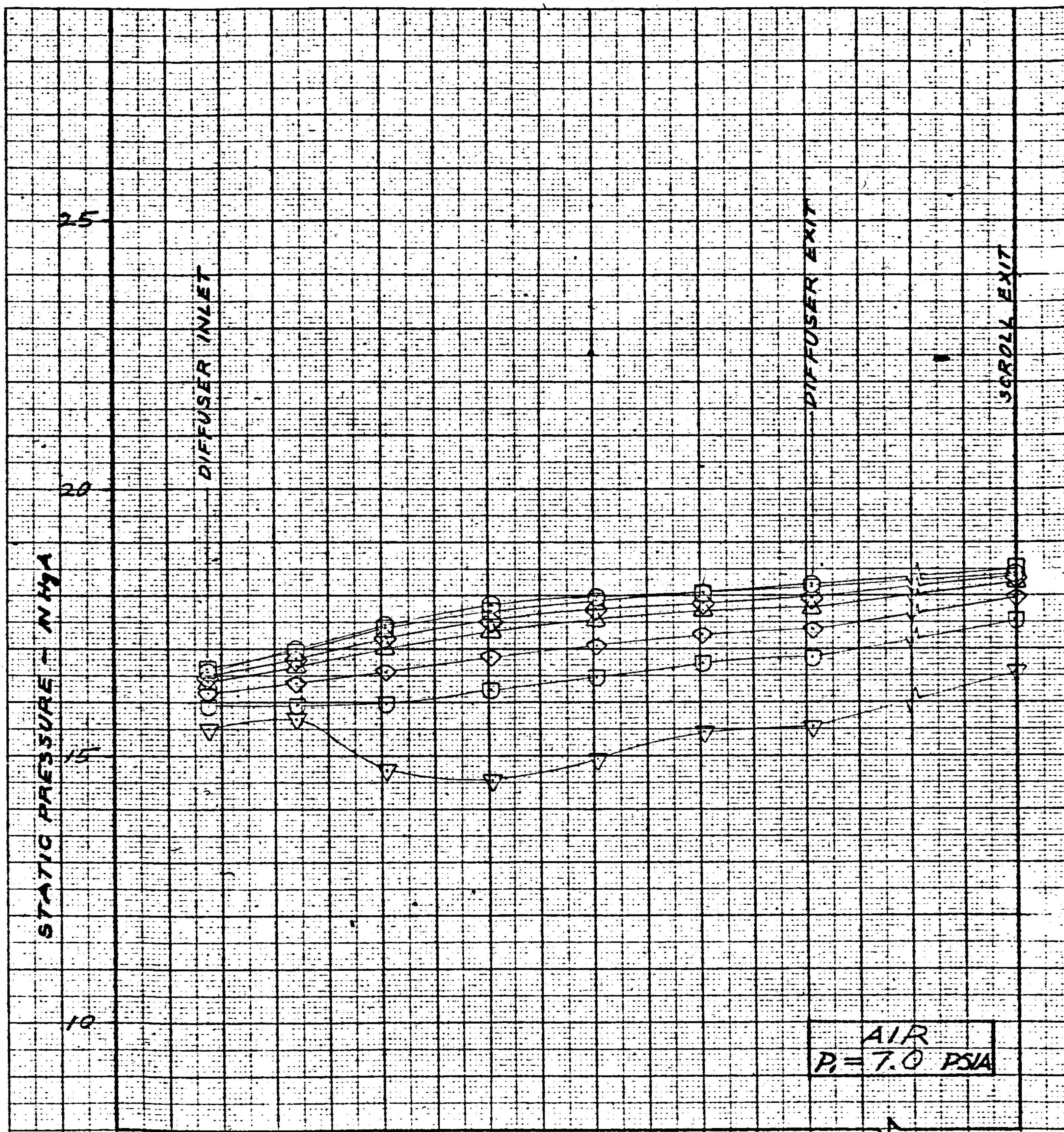

CALCULATED BY		STATIC PRESSURE DISTRIBUTION ALONG DIFFUSER PART 369748-20	$\%N/\sqrt{\theta} = 70$
TRACED BY	3-30-66		
CHECKED BY			
APPROVED BY		AIRESEARCH MANUFACTURING COMPANY	DATA FFE3
UNIT NO.			53

P 5106

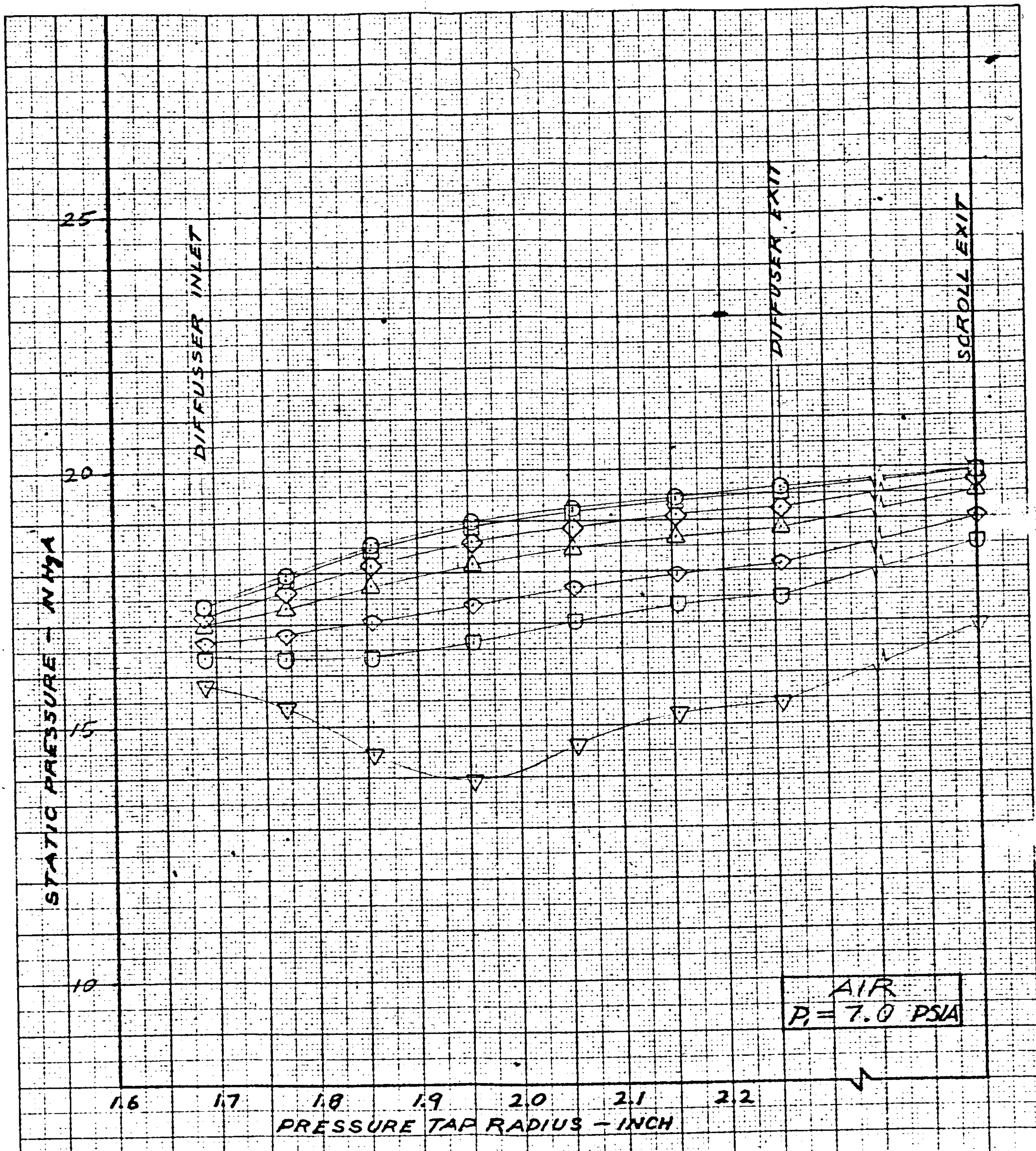

CALCULATED BY		
TRACED BY	[illegible]	5-30-66
CHECKED BY		
APPROVED BY		
UNIT NO.		

STATIC PRESSURE DISTRIBUTION
ALONG DIFFUSER PART 369748-20

$\%\frac{N}{\sqrt{\theta}} = 80$

AIRESEARCH MANUFACTURING COMPANY

53

P 3106

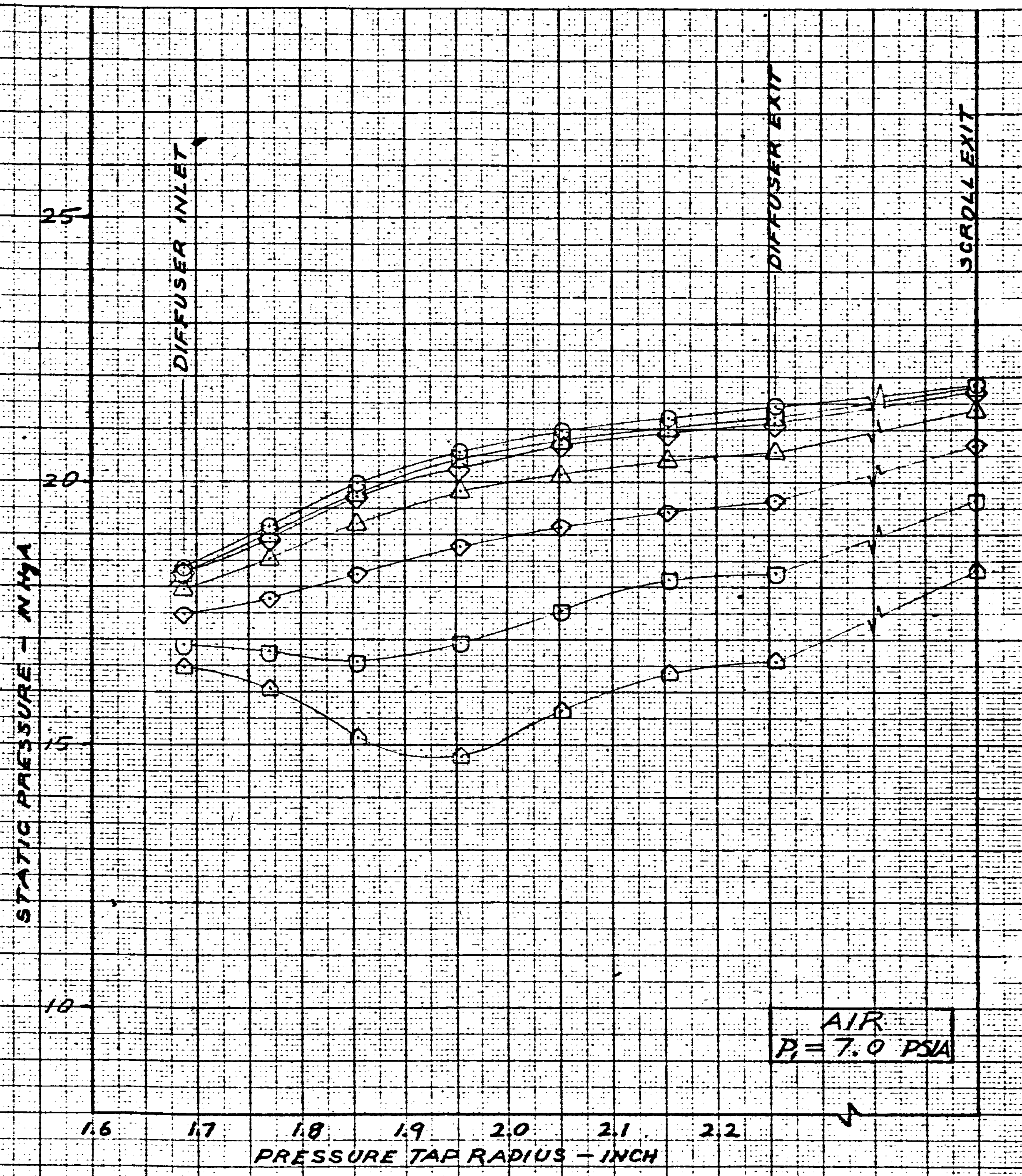

CALCULATED BY		
TRACED BY	Ludwig	3-30-65
CHECKED BY		
APPROVED BY		
UNIT NO.		

STATIC PRESSURE DISTRIBUTION
ALONG DIFFUSER PART 369748-20

$\%N/\sqrt{\theta} = 90$

DATA PAGE 54

AIRESEARCH MANUFACTURING COMPANY

P 5106

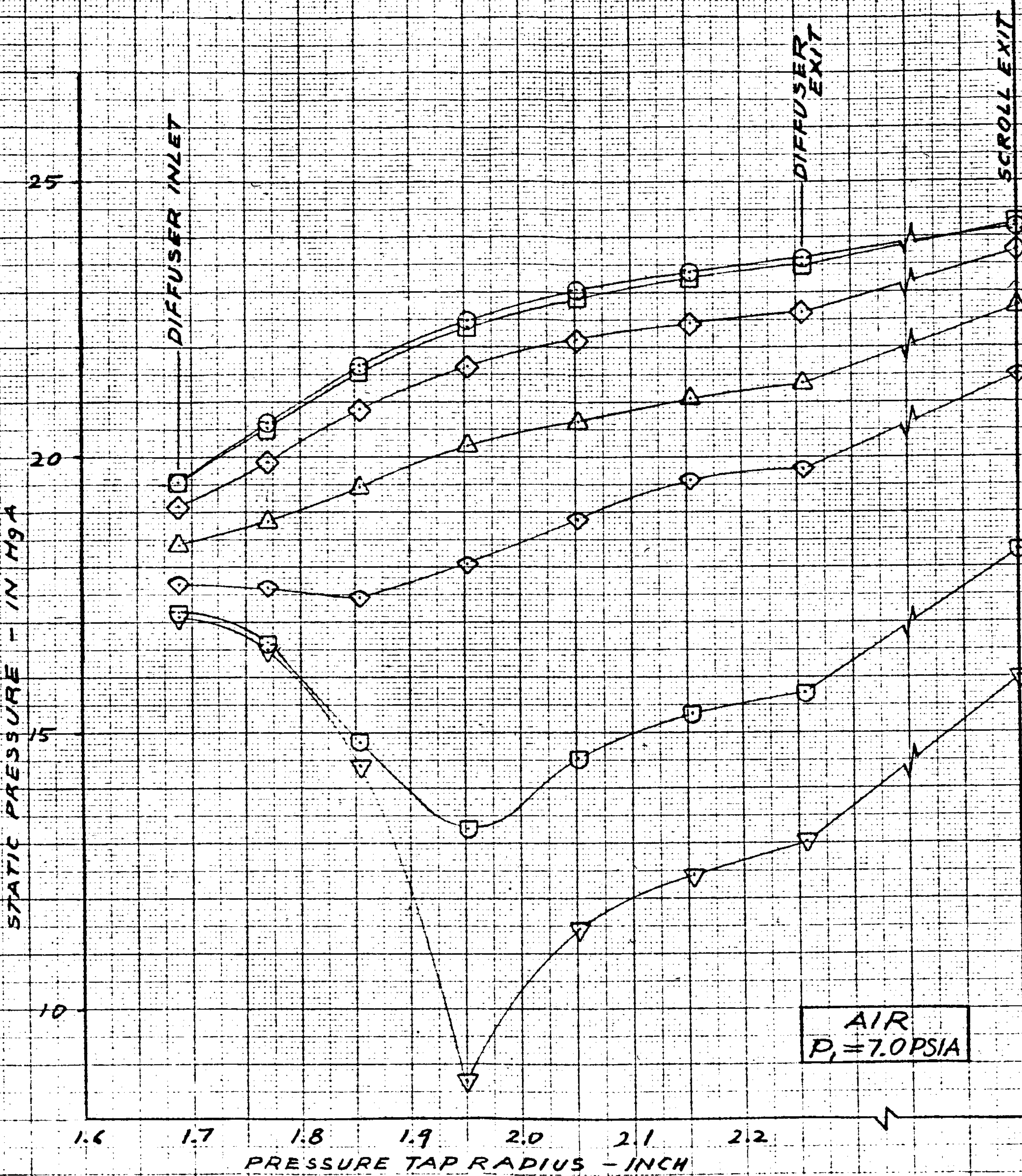

CALCULATED BY		
TRACED BY	[illegible]	3-28-66
CHECKED BY		
APPROVED BY		
UNIT NO.		

STATIC PRESSURE DISTRIBUTION ALONG DIFFUSER PART 369748-20

$\% \frac{N}{\sqrt{\theta}} = 100$

DATA FSEC 59

AIRESEARCH MANUFACTURING COMPANY

P 5106

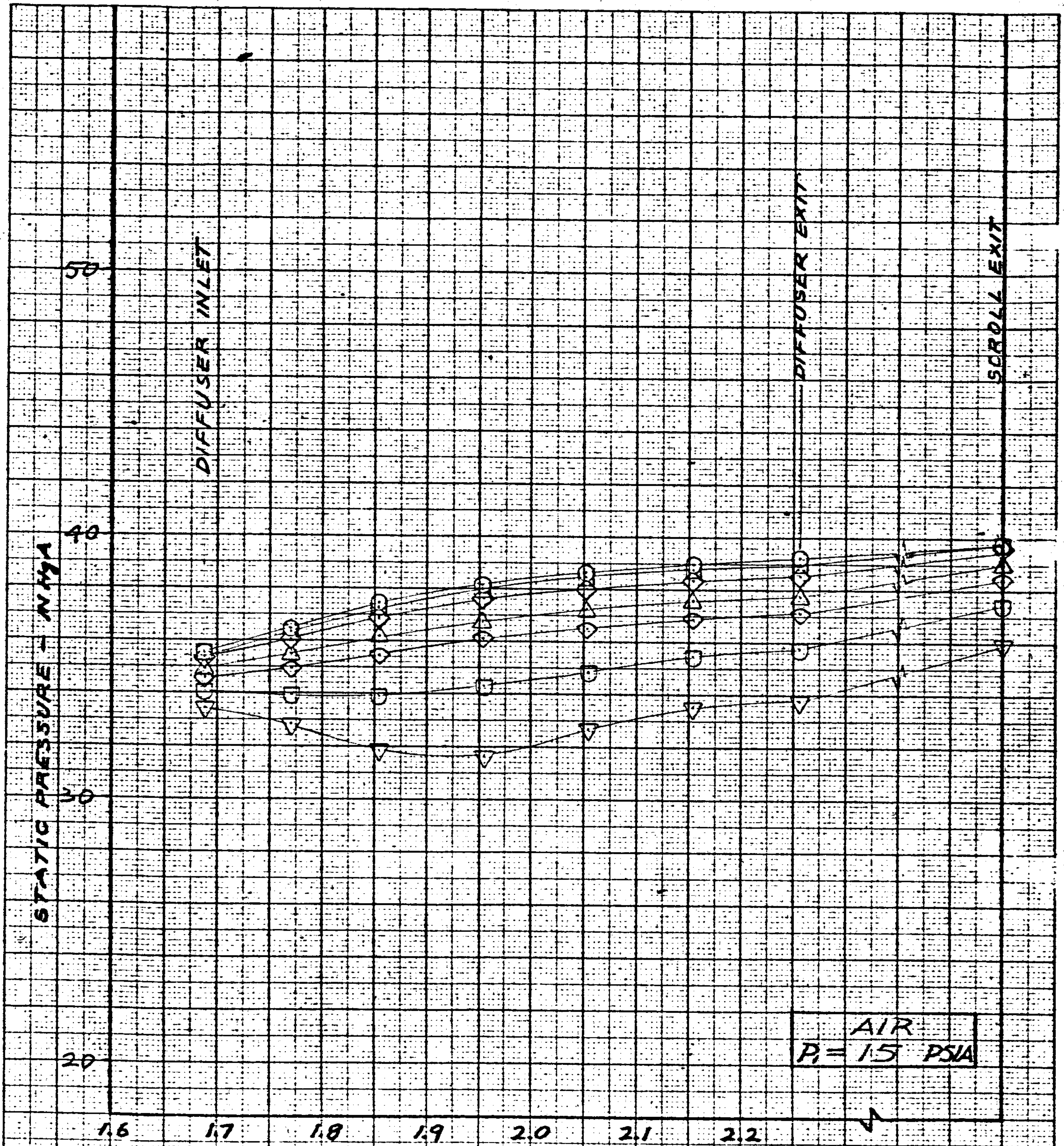

CALCULATED BY		STATIC PRESSURE DISTRIBUTION ALONG DIFFUSER PART 369748-20	$\frac{\% N}{\sqrt{\theta}} = 79$
TRACED BY			
CHECKED BY			
APPROVED BY		AIRESEARCH MANUFACTURING COMPANY	DATA PAGE
UNIT NO.			

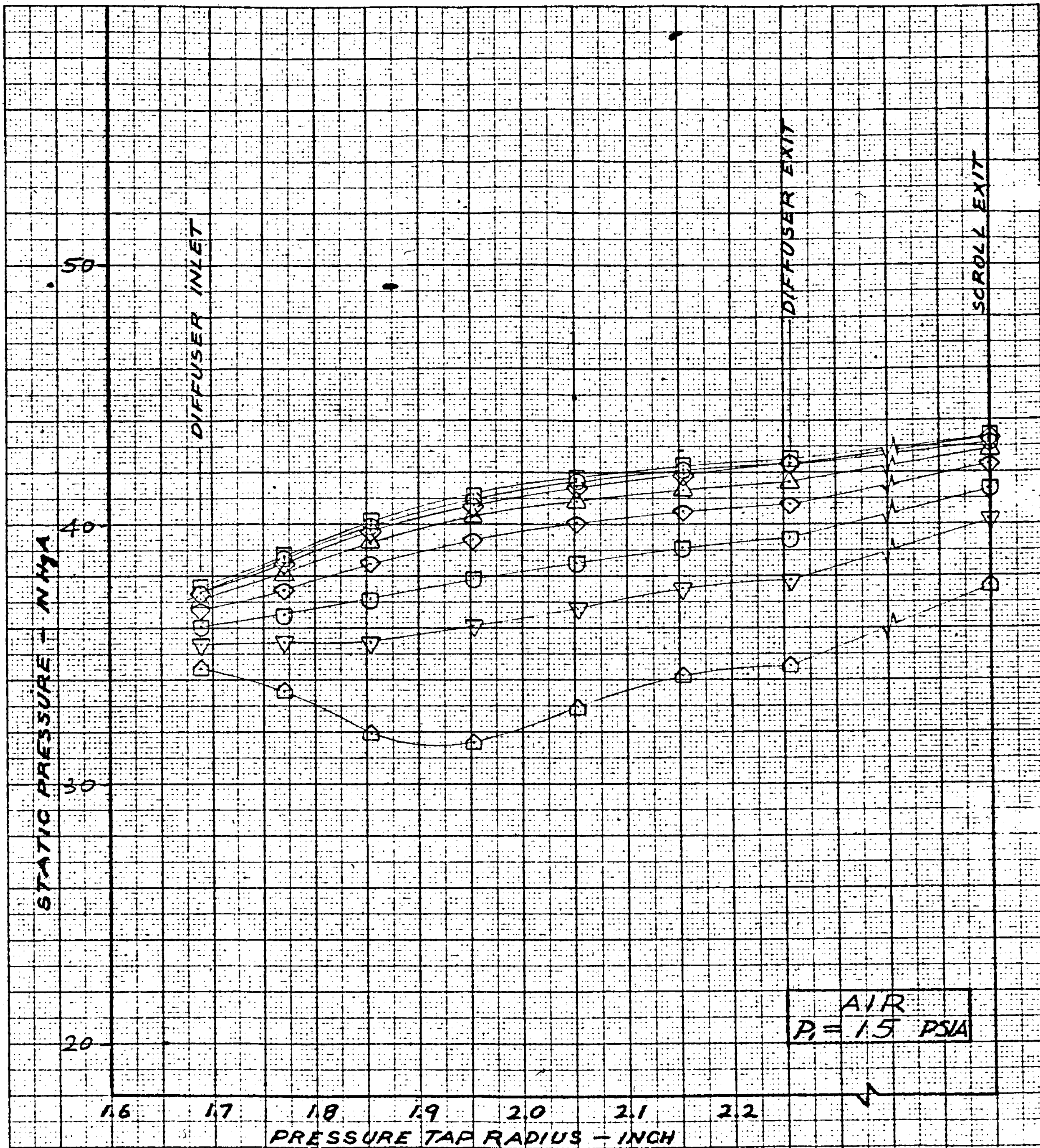

CALCULATED BY		
TRACED BY	[illegible]	2-20-65
CHECKED BY		
APPROVED BY		
UNIT NO.		

STATIC PRESSURE DISTRIBUTION ALONG DIFFUSER PART 369748-20

$\%N/\sqrt{\theta} = 80$

AIRESEARCH MANUFACTURING COMPANY

55

F 5106

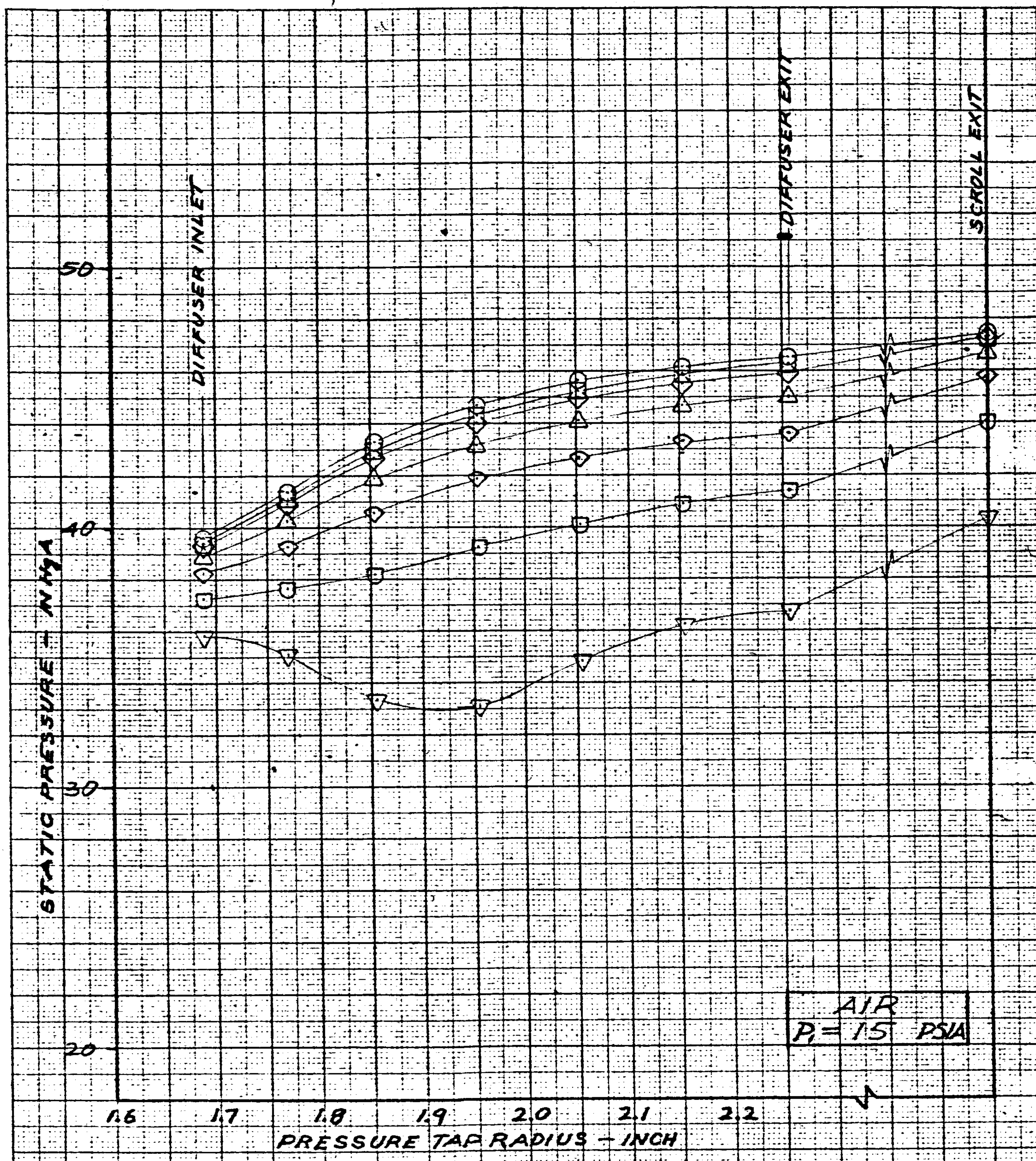

			STATIC PRESSURE DISTRIBUTION ALONG DIFFUSER PART 369748-20	%N/%√θ = 90
CALCULATED BY				
TRACED BY	Indrix	3-31-65		
CHECKED BY				DATA REF.
APPROVED BY			AIRESEARCH MANUFACTURING COMPANY	
UNIT NO.				

P 55C6

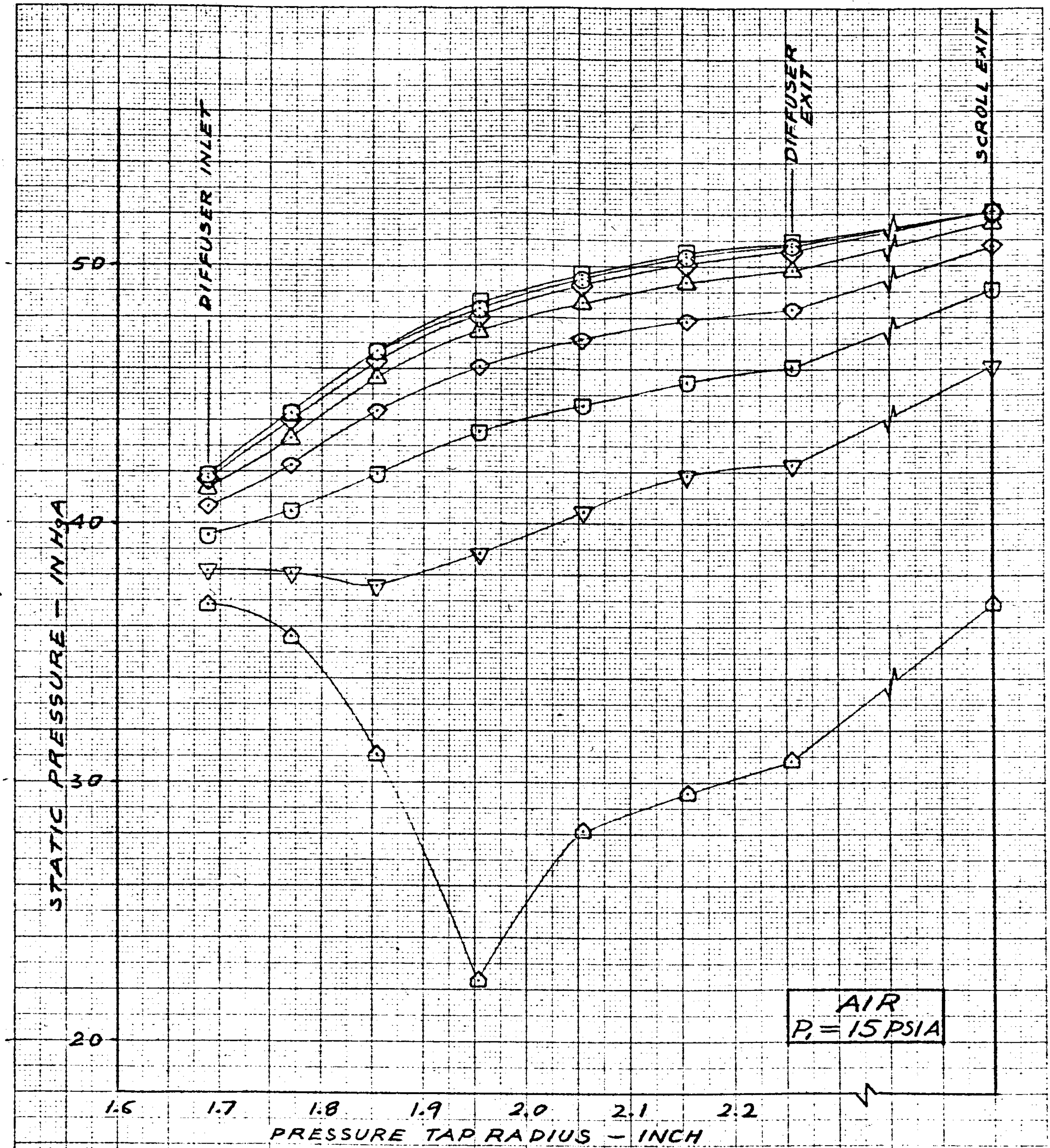

CALCULATED BY		
TRACED BY	[illegible]	[illegible]
CHECKED BY	[illegible]	[illegible]
APPROVED BY		
UNIT NO.		

STATIC PRESSURE DISTRIBUTION ALONG DIFFUSER PART 369748-20

$\% \frac{N}{\sqrt{\theta}} = 100$

DATA PAGE 57, 59

AIRESEARCH MANUFACTURING COMPANY

P 5106

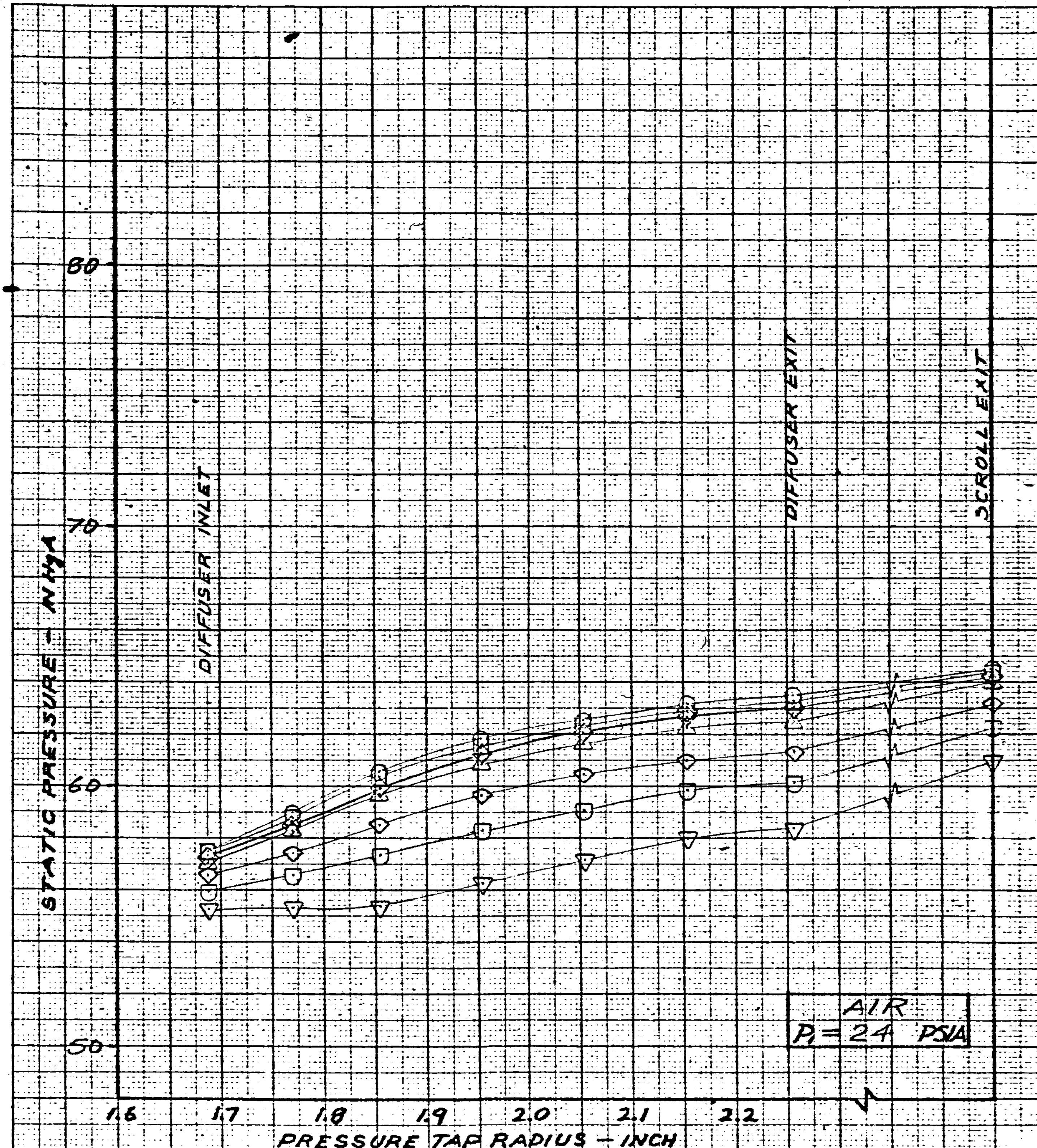

CALCULATED BY			STATIC PRESSURE DISTRIBUTION ALONG DIFFUSER PART 369748-20	$\% \frac{N}{\sqrt{\theta}}$ = 70
TRACED BY		3-3-66		
CHECKED BY				
APPROVED BY			AIRESEARCH MANUFACTURING COMPANY	DATA FIGURE 56
UNIT NO.				

P 5105

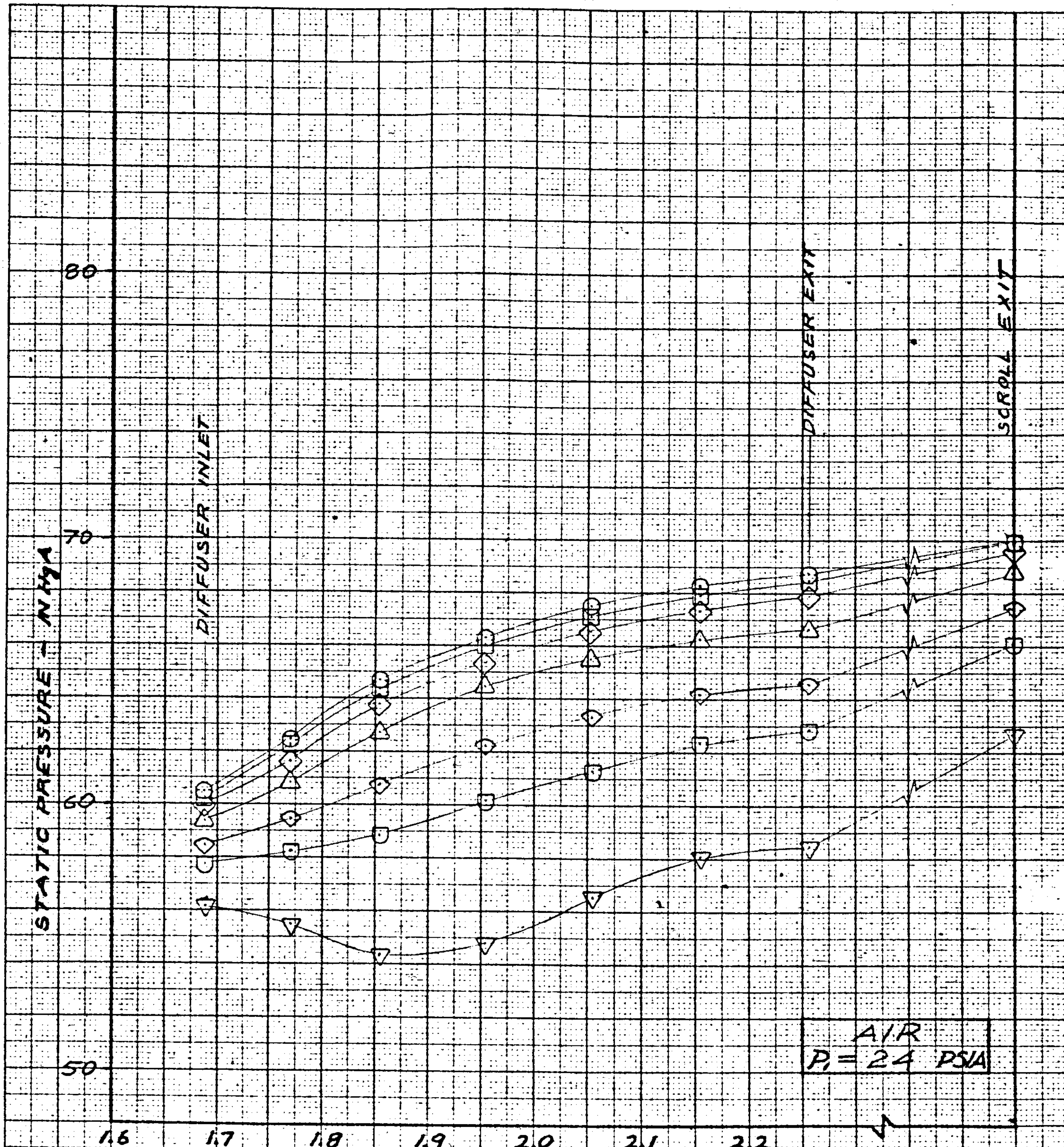

CALCULATED BY		
TRACED BY	Indwitz	3-31-65
CHECKED BY		
APPROVED BY		
UNIT NO.		

STATIC PRESSURE DISTRIBUTION ALONG DIFFUSER PART 369748-20

$\%N/\sqrt{\theta} = 80$

DATA PAGE
F3

AIRESEARCH MANUFACTURING COMPANY

P 5106

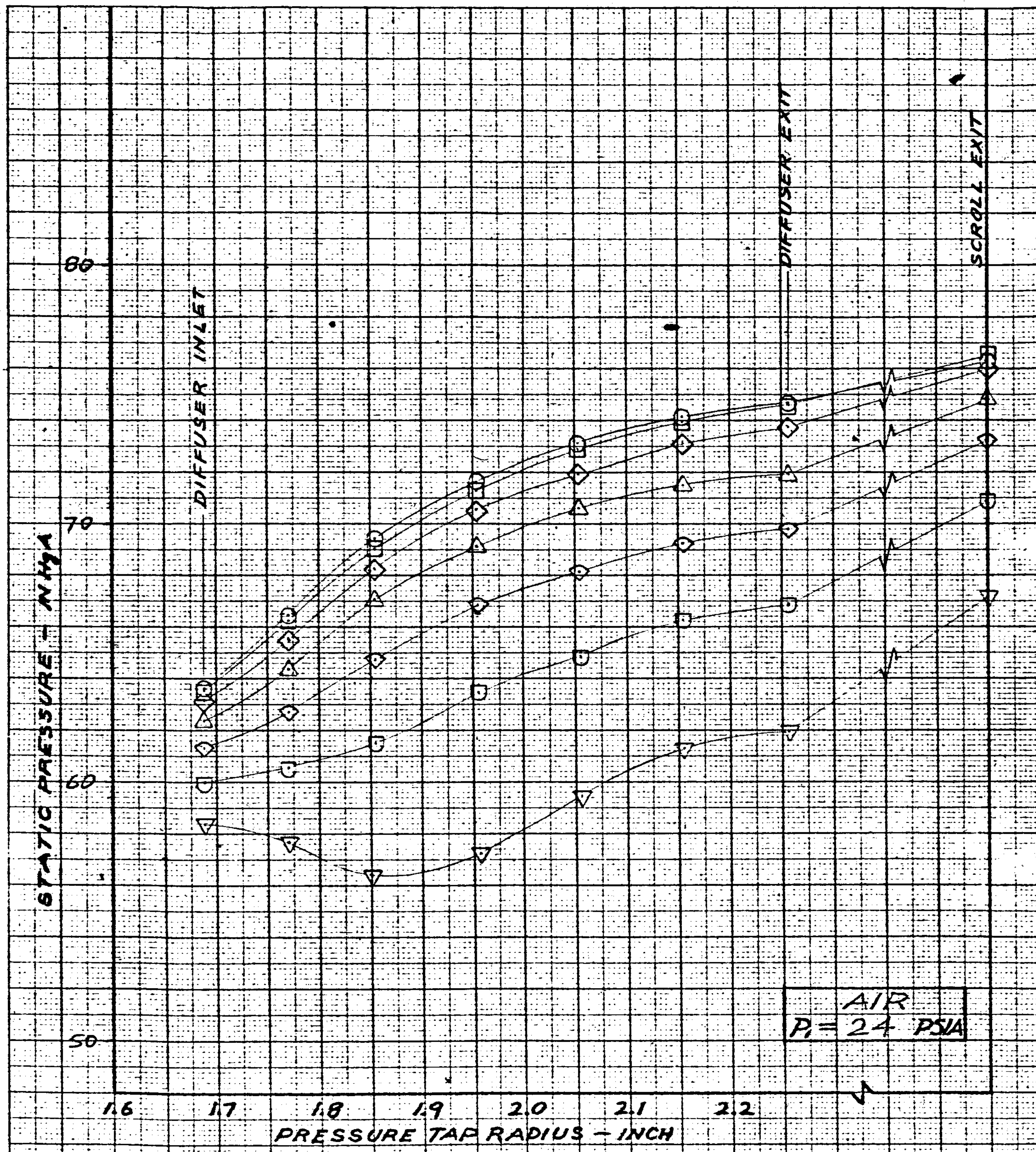

CALCULATED BY			STATIC PRESSURE DISTRIBUTION ALONG DIFFUSER PART 369748-20		$\%N/\sqrt{\theta}$ = 90
TRACED BY	Ludwig	3-31-66			
CHECKED BY					
APPROVED BY			AIRESEARCH MANUFACTURING COMPANY		DATA PAGE
UNIT NO.					53,57

P 5106

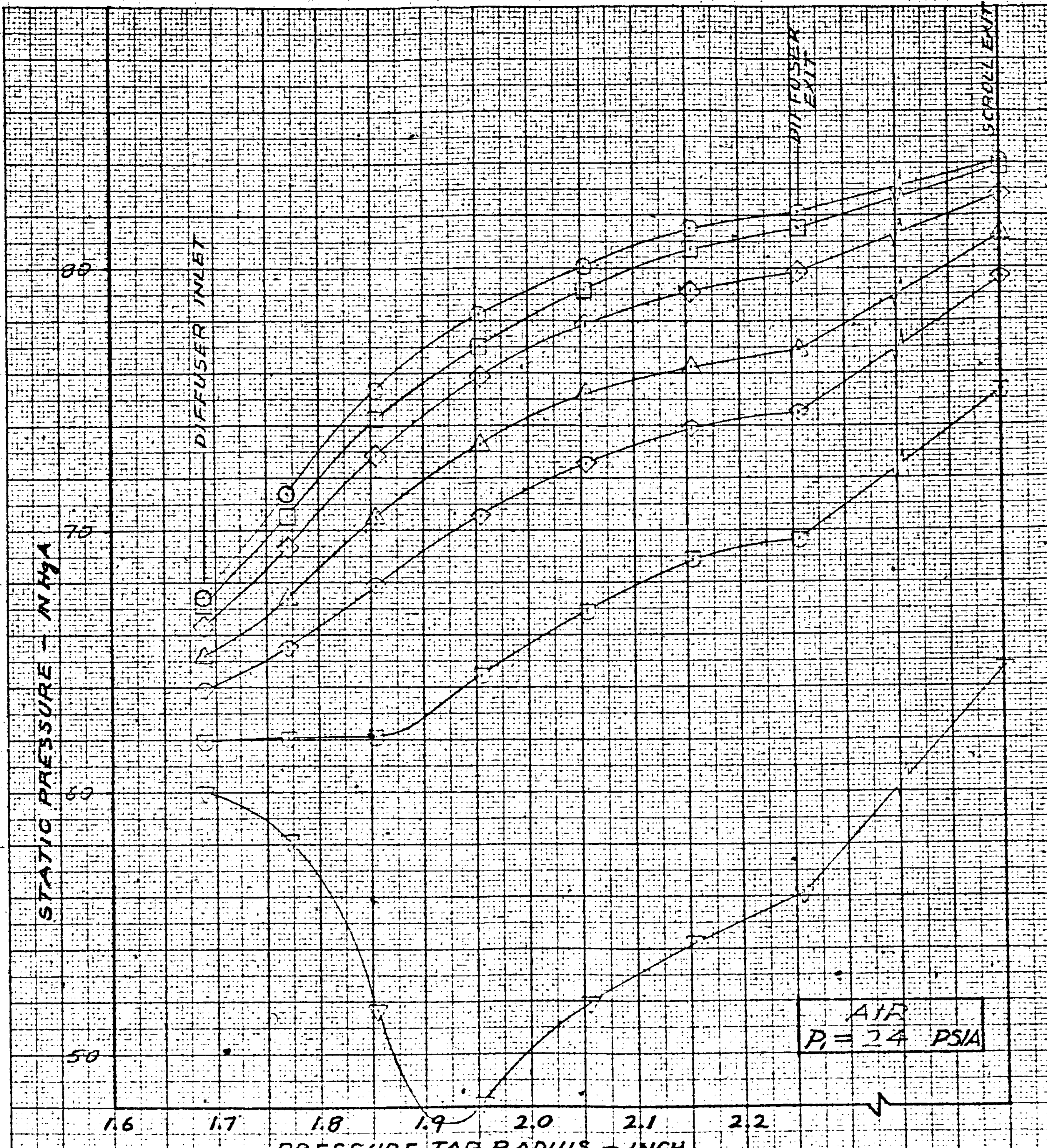

CALCULATED BY	
TRACED BY	
CHECKED BY	
APPROVED BY	
UNIT NO.	

STATIC PRESSURE DISTRIBUTION
ALONG DIFFUSER PART 369748-20

AIRESEARCH MANUFACTURING COMPANY

% $N/\sqrt{\theta}$ = 100

57

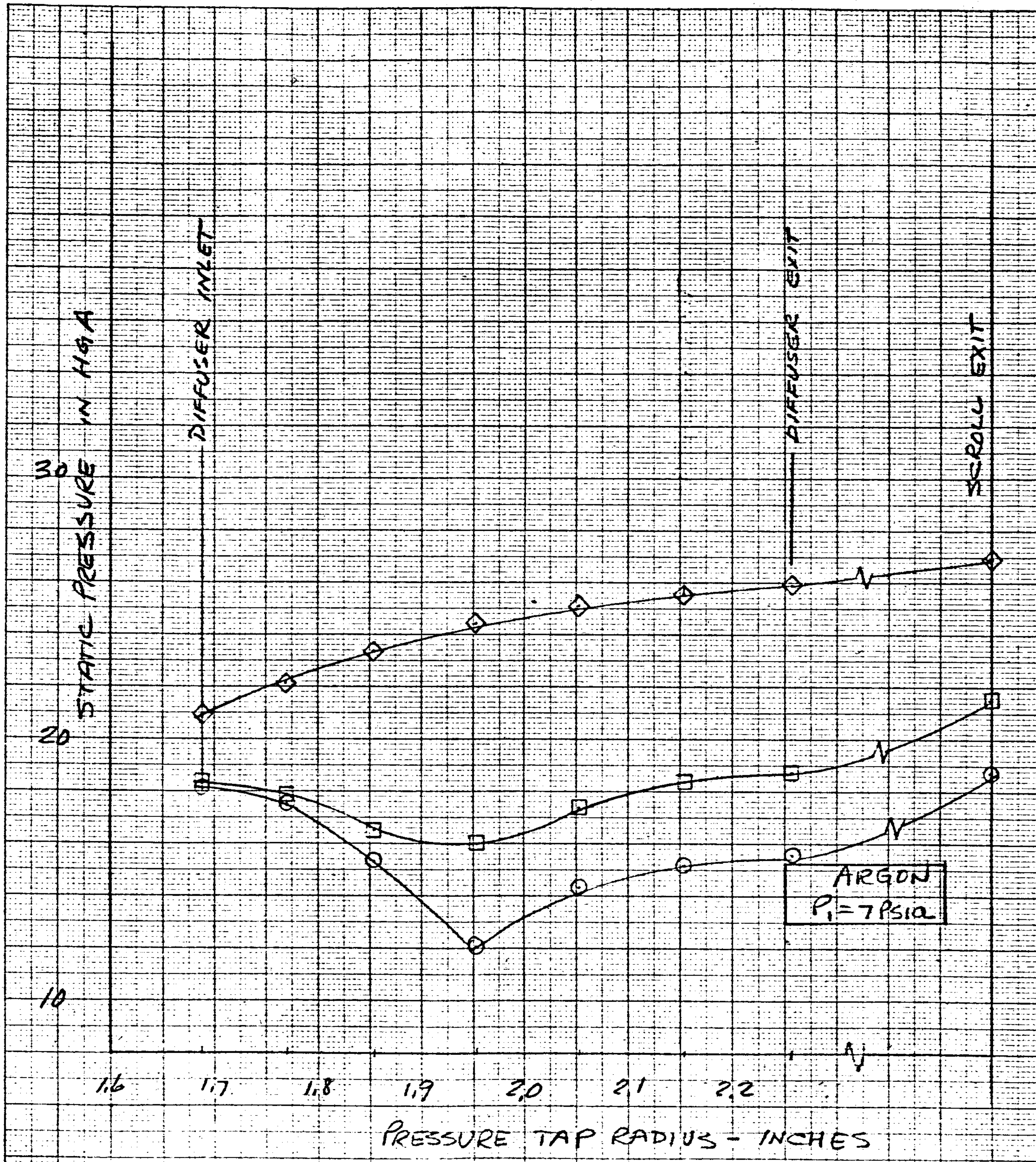

CALCULATED BY			STATIC PRESSURE DISTRIBUTION ALONG DIFFUSER PART 369748-20		$\%\frac{N}{\sqrt{\theta}}=1.0$
TRACED BY					
CHECKED BY					
APPROVED BY			AIRESEARCH MANUFACTURING COMPANY		DATA PAGE
UNIT NO.					41

P 5106

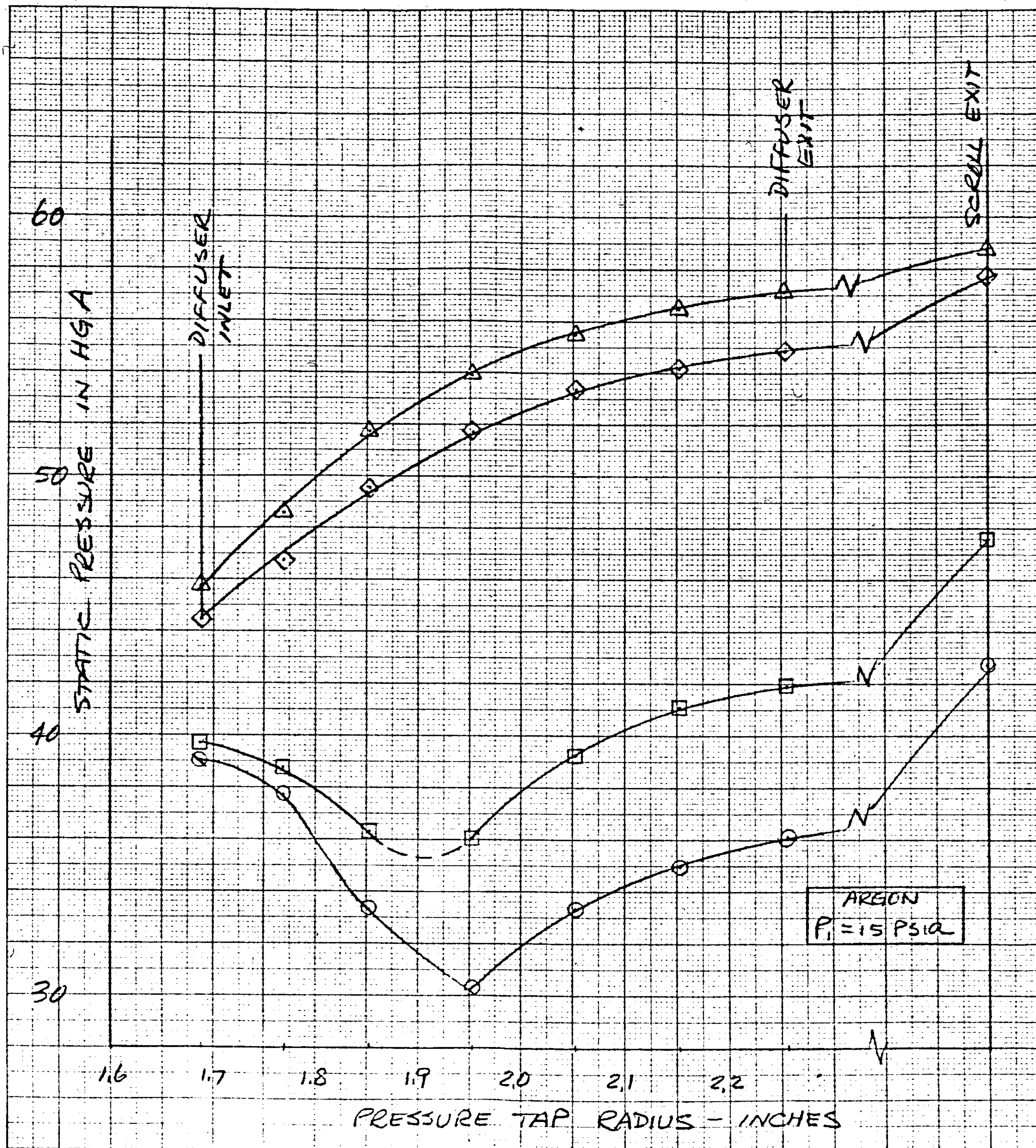

CALCULATED BY			STATIC PRESSURE DISTRIBUTION ALONG DIFFUSER PART 369748-20	$\% \frac{N}{\sqrt{\theta}} = 1.0$
TRACED BY				
CHECKED BY				DATA PAGE
APPROVED BY			AIRESEARCH MANUFACTURING COMPANY	40
UNIT NO.				

P 5106

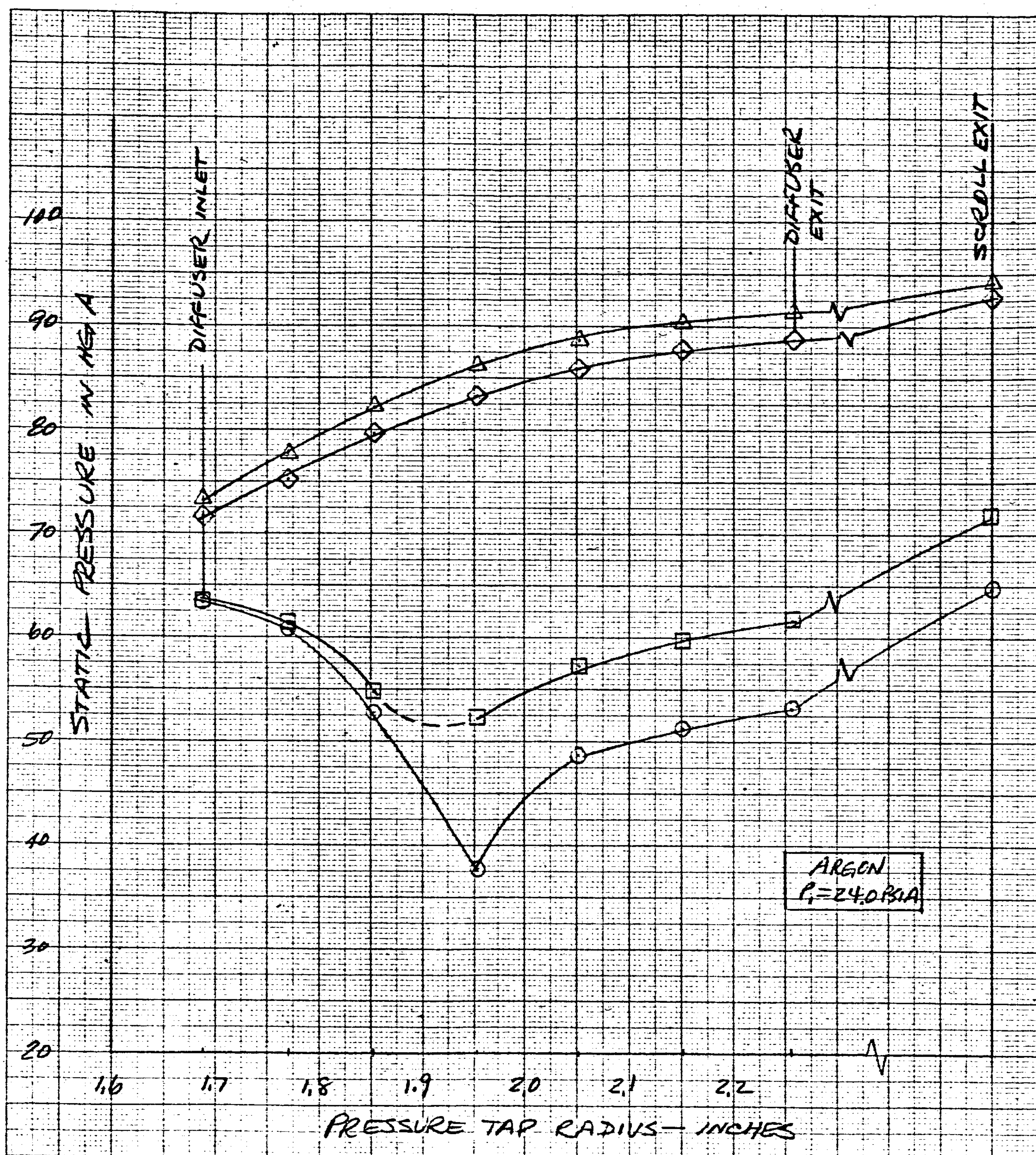

CALCULATED BY			STATIC PRESSURE DISTRIBUTION ALONG DIFFUSER PART 369748-20	$\%\frac{N}{\sqrt{\theta}}=1.0$
TRACED BY	HCL			
CHECKED BY				DATA PAGE
APPROVED BY			AIRESEARCH MANUFACTURING COMPANY	40
UNIT NO.				

P 5106

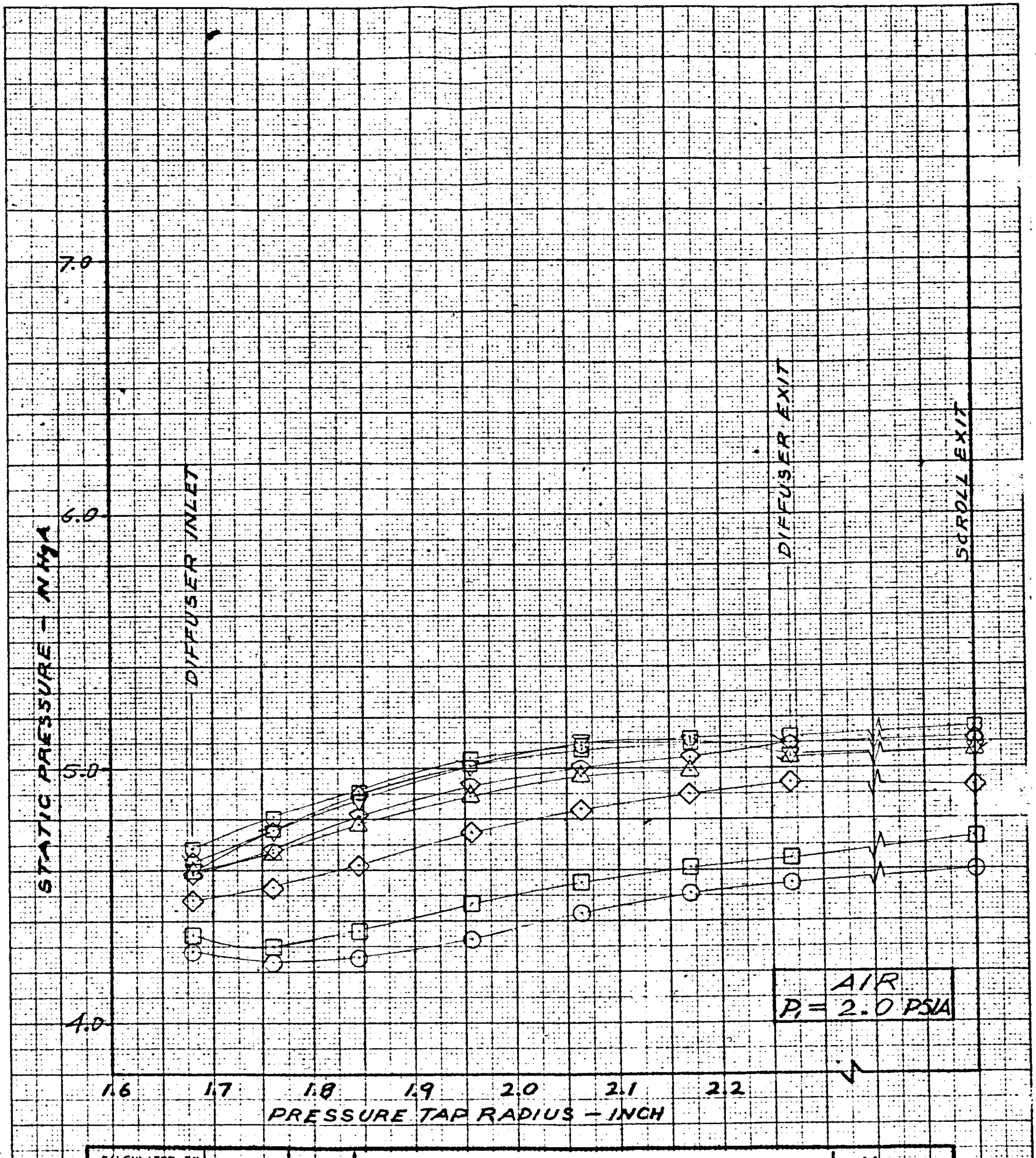

CALCULATED BY			STATIC PRESSURE DISTRIBUTION ALONG DIFFUSER PART 871034	$\%N/\sqrt{\theta} = 70$
TRACED BY	[illegible]	3-31-66		
CHECKED BY				
APPROVED BY			AIRESEARCH MANUFACTURING COMPANY	DATA PAGE 45
UNIT NO.				

P 5106

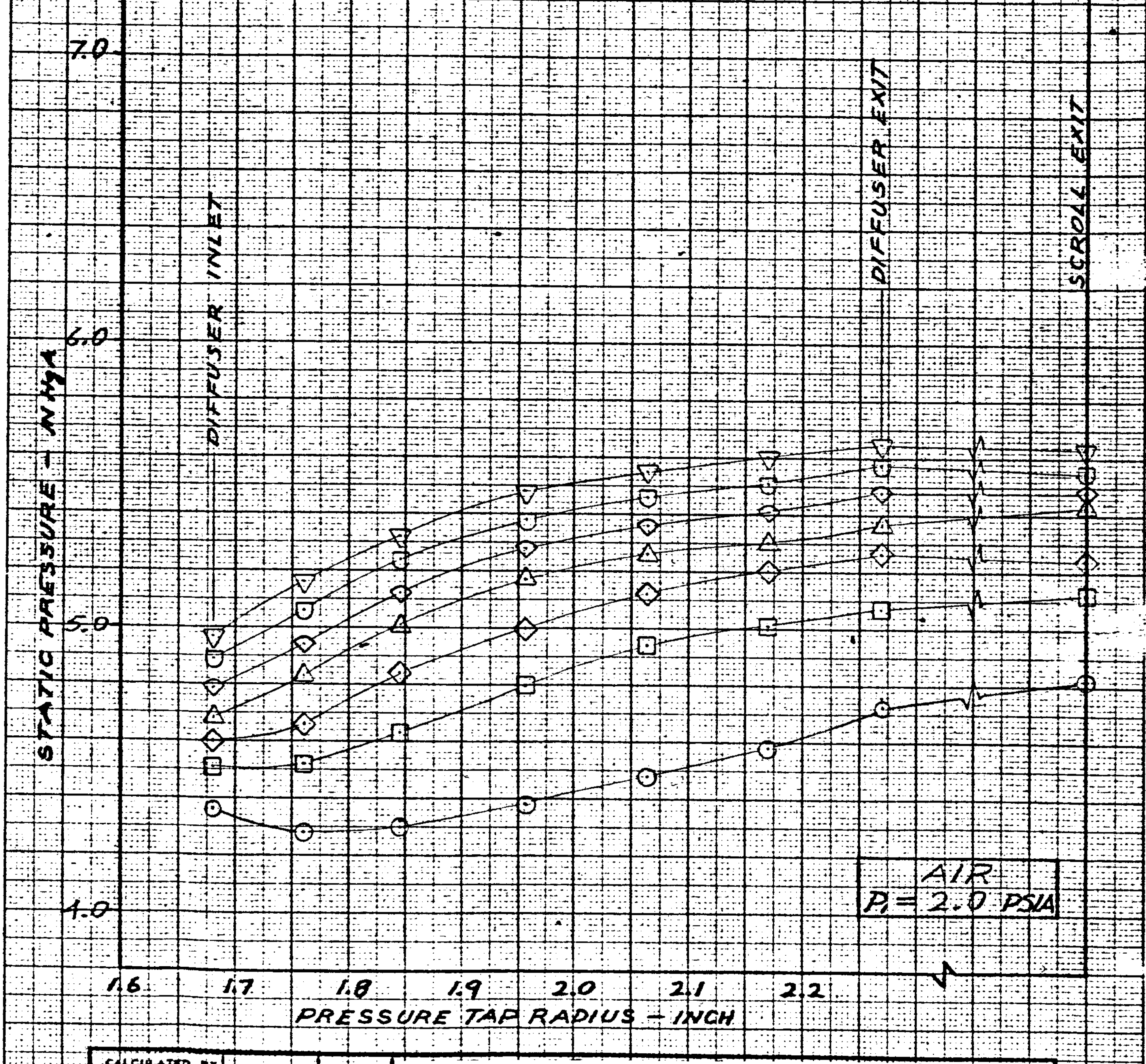

CALCULATED BY			
TRACED BY	Indris	3-31-63	
CHECKED BY			
APPROVED BY			
UNIT NO.			

STATIC PRESSURE DISTRIBUTION ALONG DIFFUSER PART 871034

$\frac{\% N}{\% \sqrt{\theta}} = 80$

DATA PAGE

AIRESEARCH MANUFACTURING COMPANY

P 3506

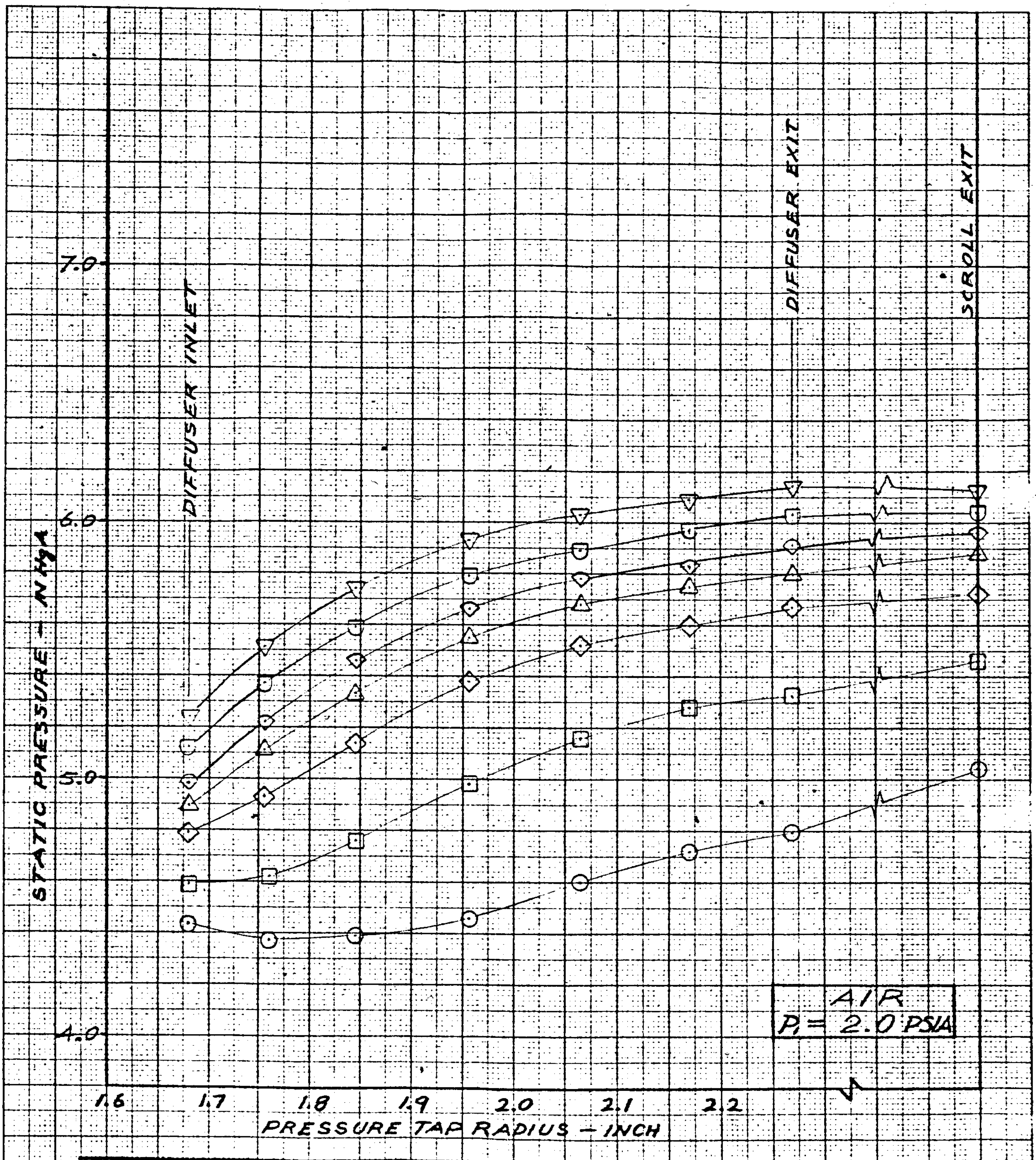

CALCULATED BY			STATIC PRESSURE DISTRIBUTION ALONG DIFFUSER PART 871034	$\% N / \% \sqrt{\theta}$ = 95
TRACED BY				
CHECKED BY				
APPROVED BY			AIRESEARCH MANUFACTURING COMPANY	DATA PAGE
UNIT NO.				41

P 5105

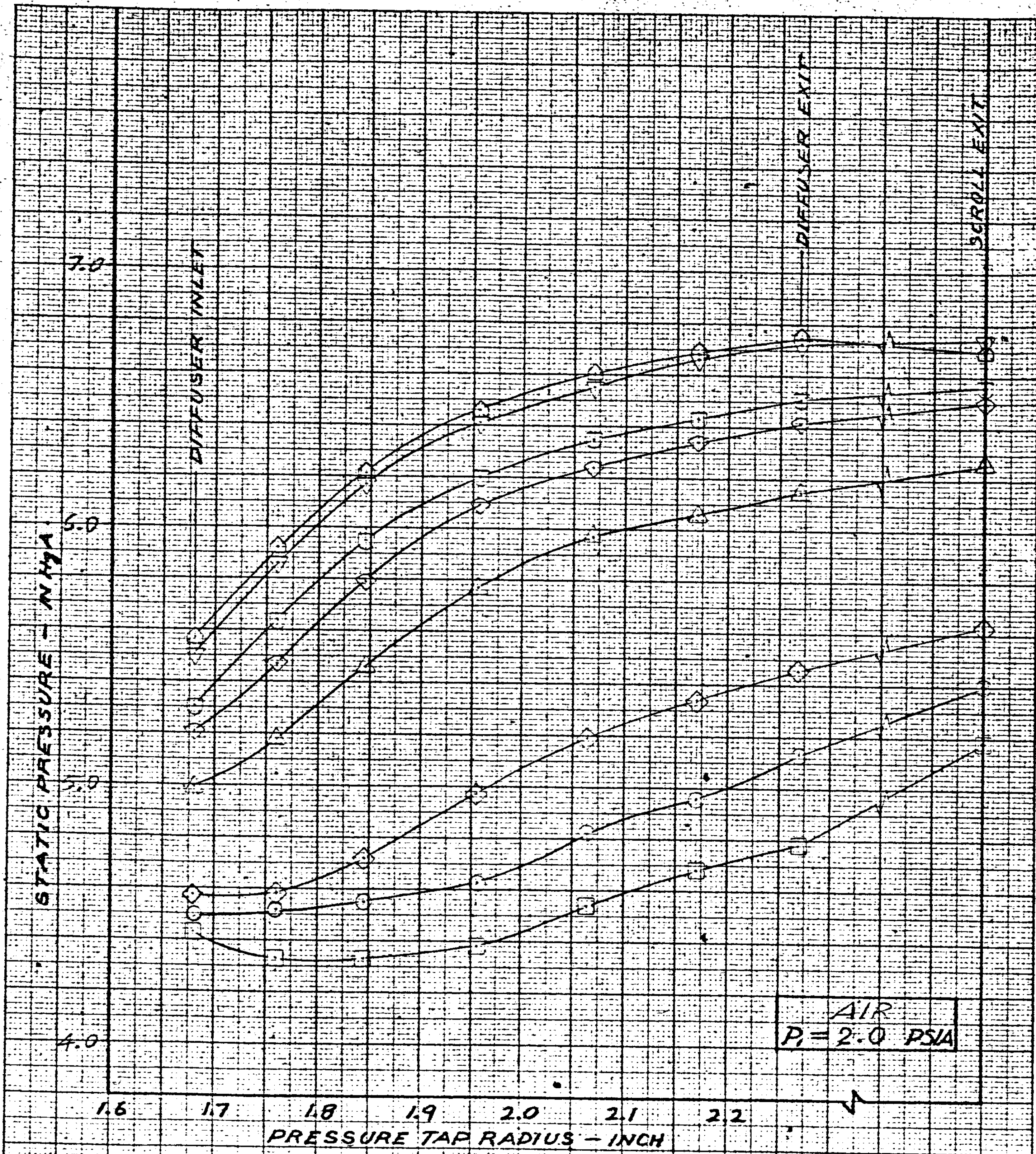

CALCULATED BY		
TRACED BY	Ludwig	3-28-60
CHECKED BY		
APPROVED BY		
UNIT NO.		

STATIC PRESSURE DISTRIBUTION
ALONG DIFFUSER PART 871034

% $\frac{N}{\sqrt{\theta}}$ = 100

DATA PAGE 14,15

AIRESEARCH MANUFACTURING COMPANY

P 5106

CALCULATED BY			STATIC PRESSURE DISTRIBUTION ALONG DIFFUSER PART 871034	$\%\frac{N}{\sqrt{\theta}} = 70$
TRACED BY	Ludwig	4-1-66		
CHECKED BY				
APPROVED BY				DATA PAGE
UNIT NO.			AIRESEARCH MANUFACTURING COMPANY	45

P 8106

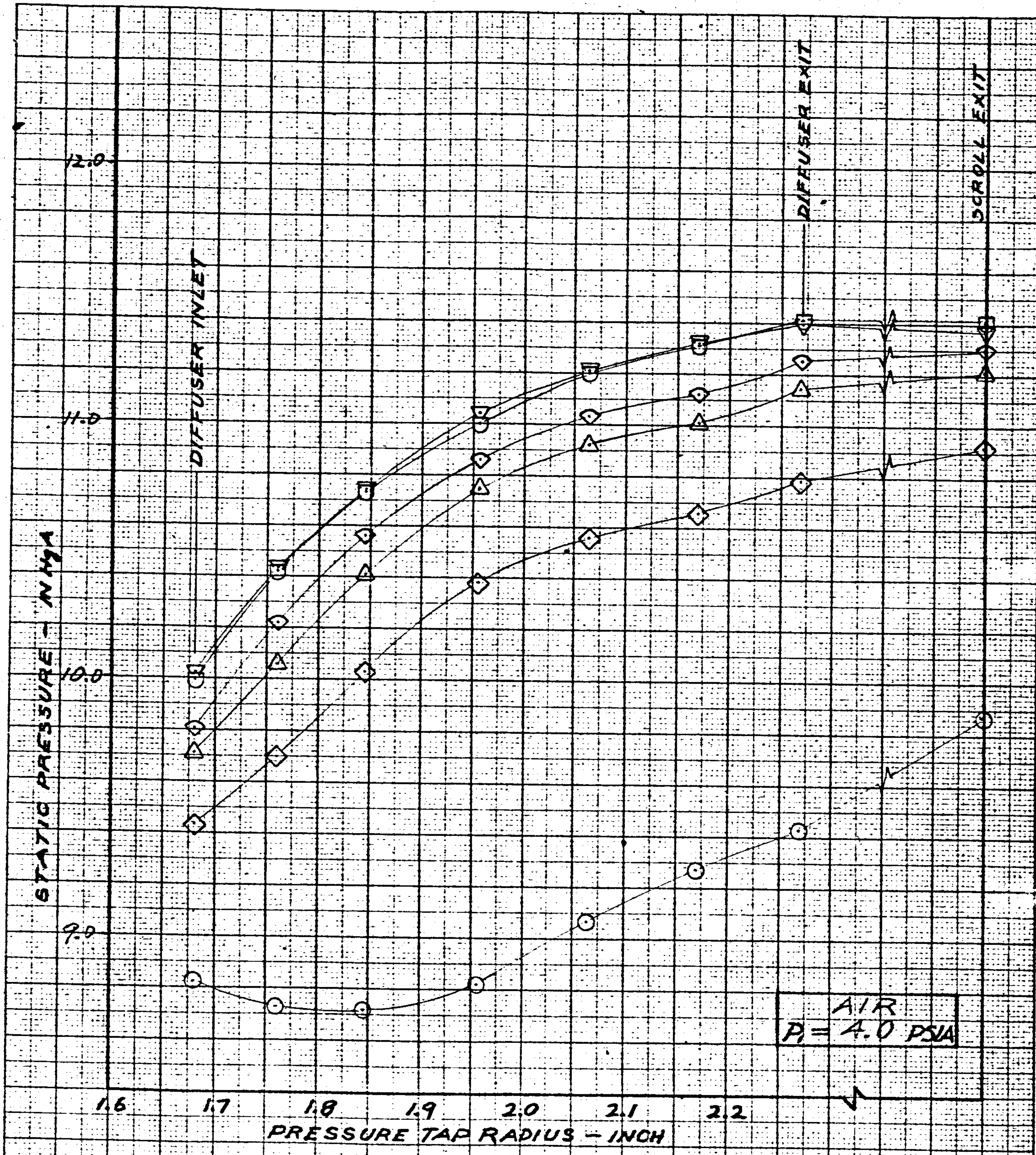

CALCULATED BY		
TRACED BY	Ludwig	4-11-66
CHECKED BY		
APPROVED BY		
UNIT NO.		

STATIC PRESSURE DISTRIBUTION
ALONG DIFFUSER PART 871034

$\%\frac{N}{\sqrt{\theta}}$ = 89

DATA PAGE 45

AIRESEARCH MANUFACTURING COMPANY

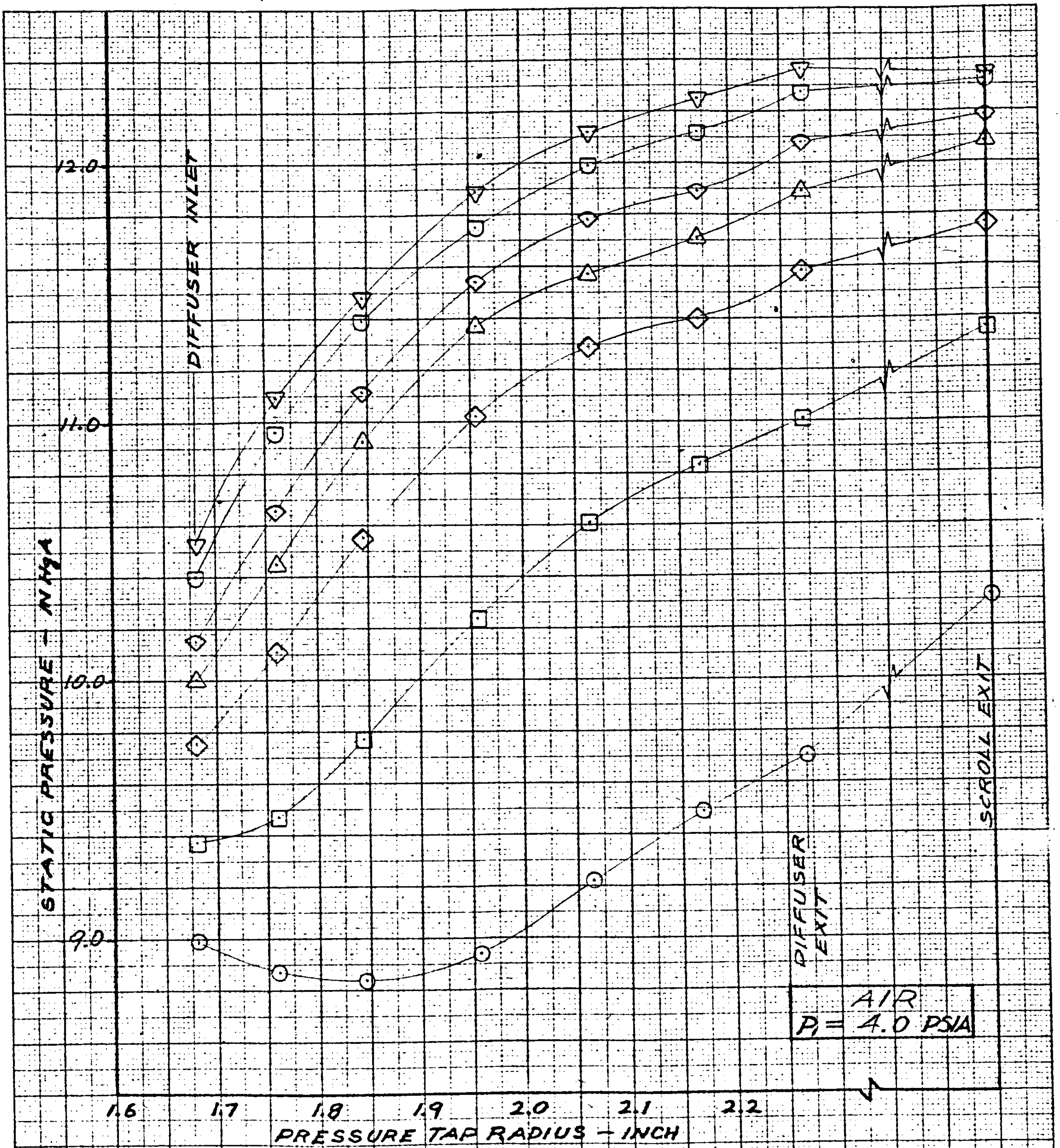

CALCULATED BY		
TRACED BY	Indwig	4-1-65
CHECKED BY		
APPROVED BY		
UNIT NO.		

STATIC PRESSURE DISTRIBUTION
ALONG DIFFUSER PART 871034

$\%\frac{N}{\sqrt{\theta}} = 90$

DATA PAGE
-16

AIRESEARCH MANUFACTURING COMPANY

P 5105

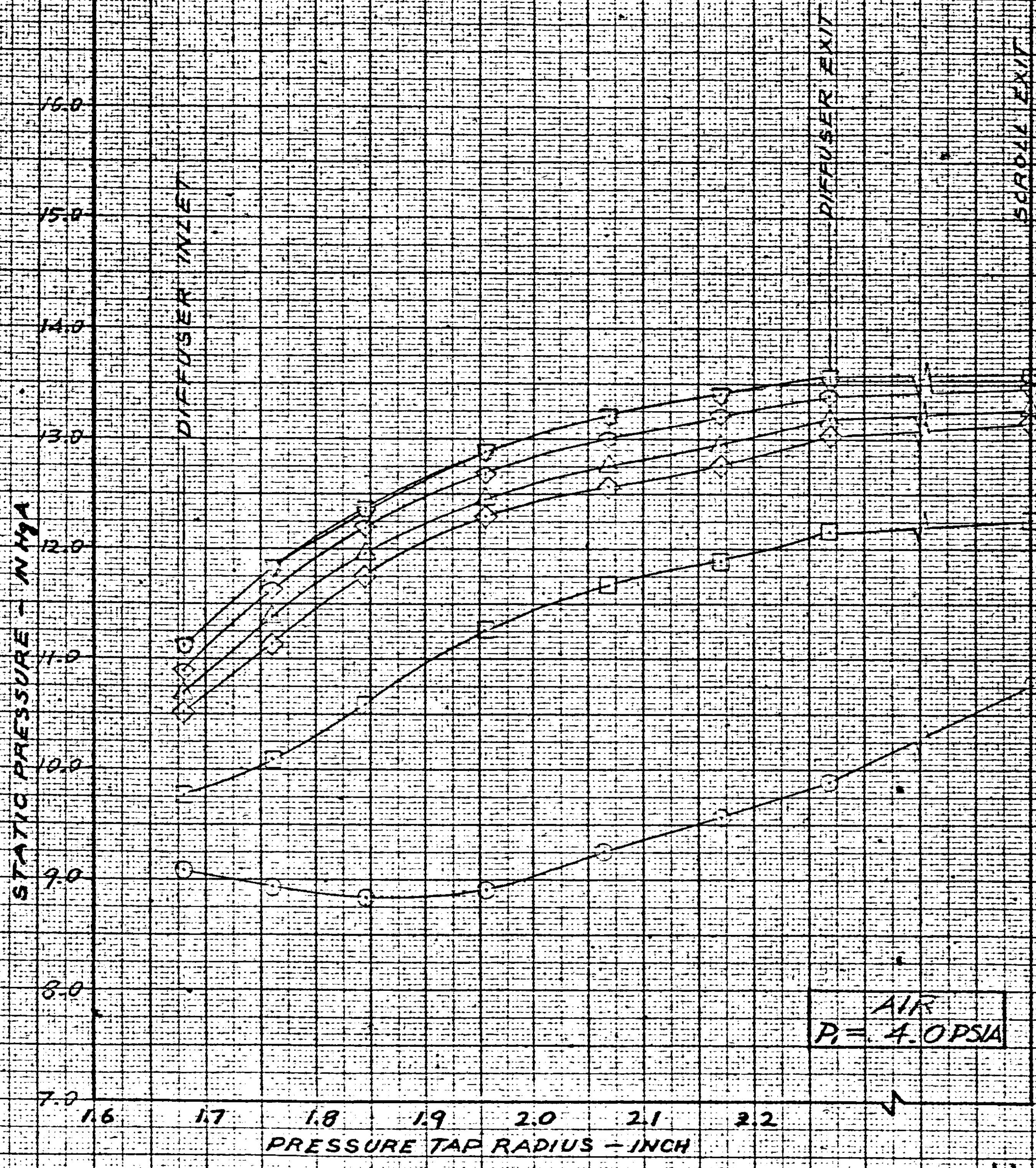

CALCULATED BY		
TRACED BY	[illegible]	5-[illegible]
CHECKED BY	[illegible]	
APPROVED BY		
UNIT NO.		

STATIC PRESSURE DISTRIBUTION
ALONG DIFFUSER PART 871034

$\% \frac{N}{\sqrt{\theta}} = 100$

DATA PAGE 43.4T

AIRESEARCH MANUFACTURING COMPANY

F 5106

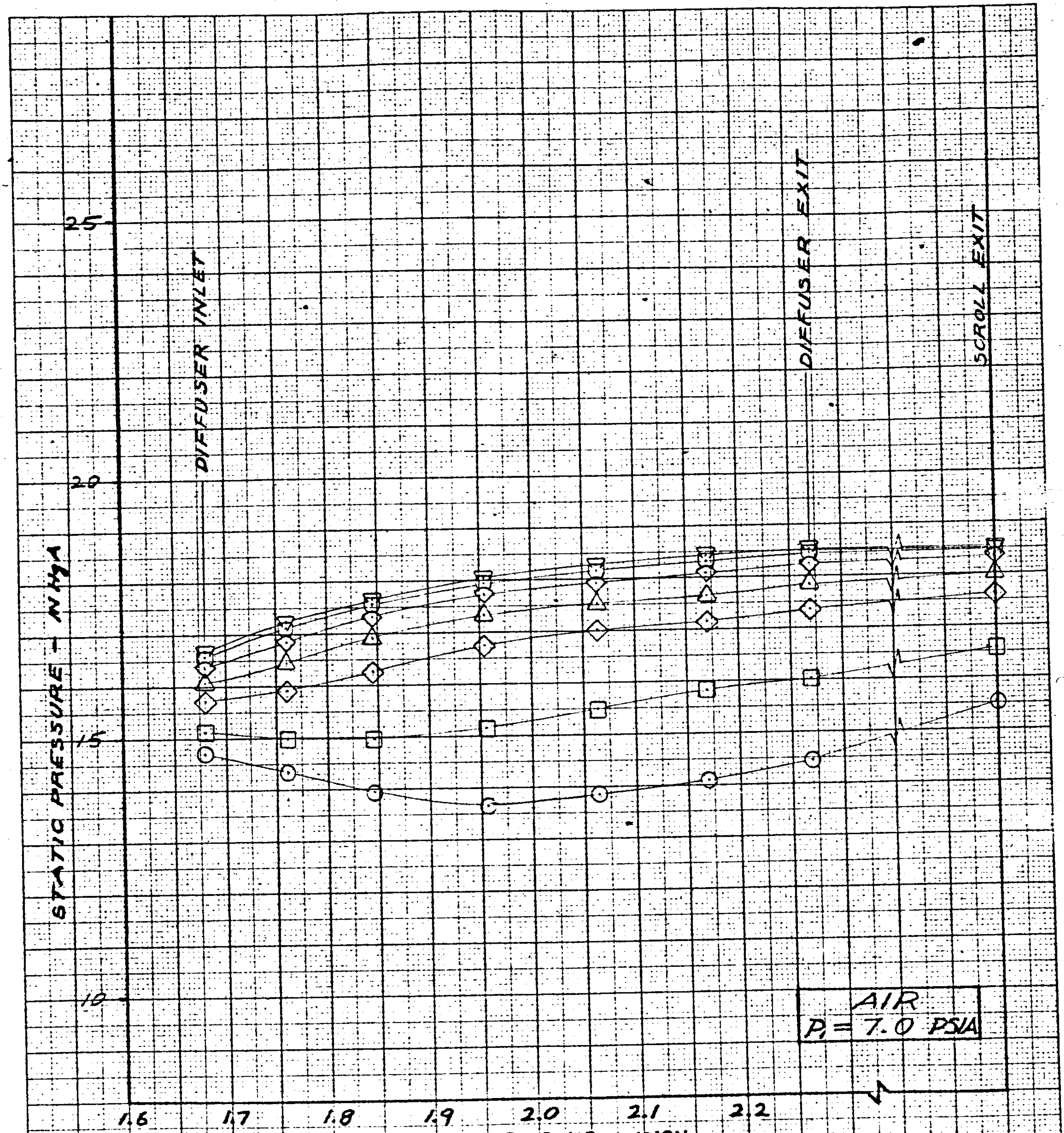

CALCULATED BY		
TRACED BY		
CHECKED BY		
APPROVED BY		
UNIT NO.		

STATIC PRESSURE DISTRIBUTION
ALONG DIFFUSER PART 871034

$\% \frac{N}{\sqrt{\theta}} = 70$

DATA PAGE 47

AIRESEARCH MANUFACTURING COMPANY

P 5106

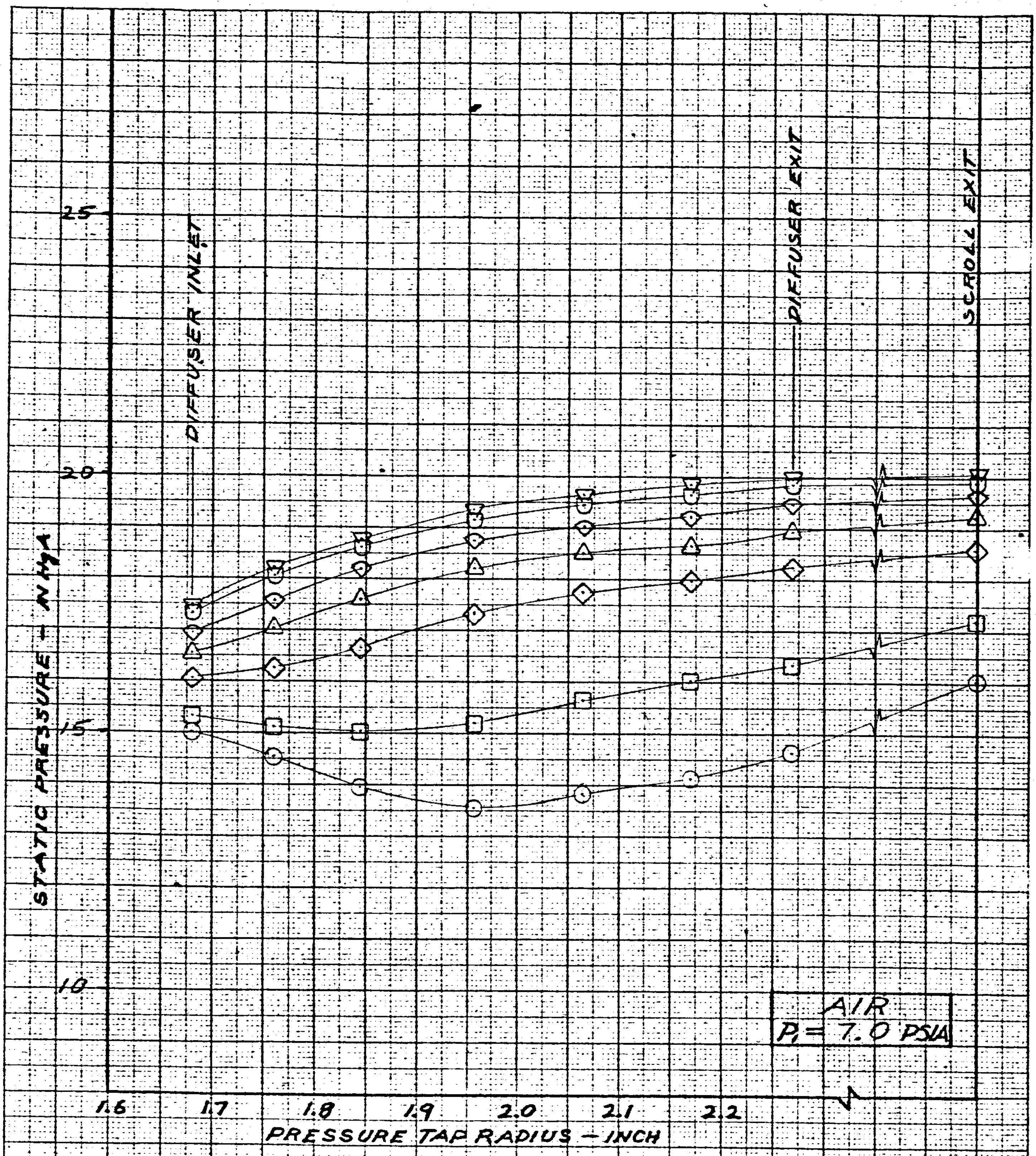

CALCULATED BY		
TRACED BY	[illegible]	11-1-66
CHECKED BY	[illegible]	[illegible]
APPROVED BY		
UNIT NO.		

STATIC PRESSURE DISTRIBUTION ALONG DIFFUSER PART 871034

$\%N/\sqrt{\theta} = 80$

AIRESEARCH MANUFACTURING COMPANY

DATE PAGE 47-48

P 5104

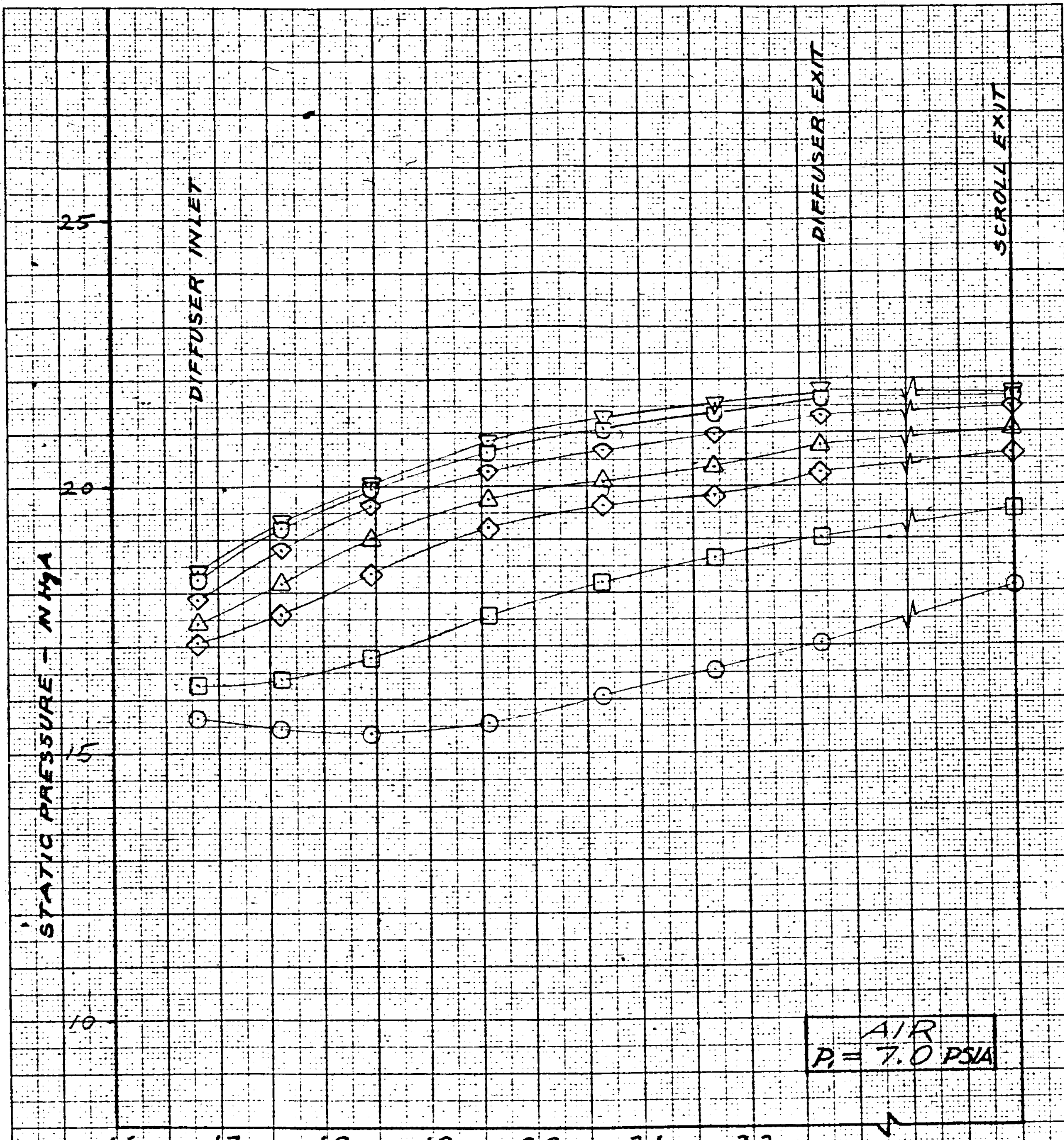

CALCULATED BY		
TRACED BY	Ludwig	4-1-66
CHECKED BY		
APPROVED BY		
UNIT NO.		

STATIC PRESSURE DISTRIBUTION ALONG DIFFUSER PART 871034

$\%N/\sqrt{\theta} = 90$

DATA PAGE A3

AIRESEARCH MANUFACTURING COMPANY

P 5406

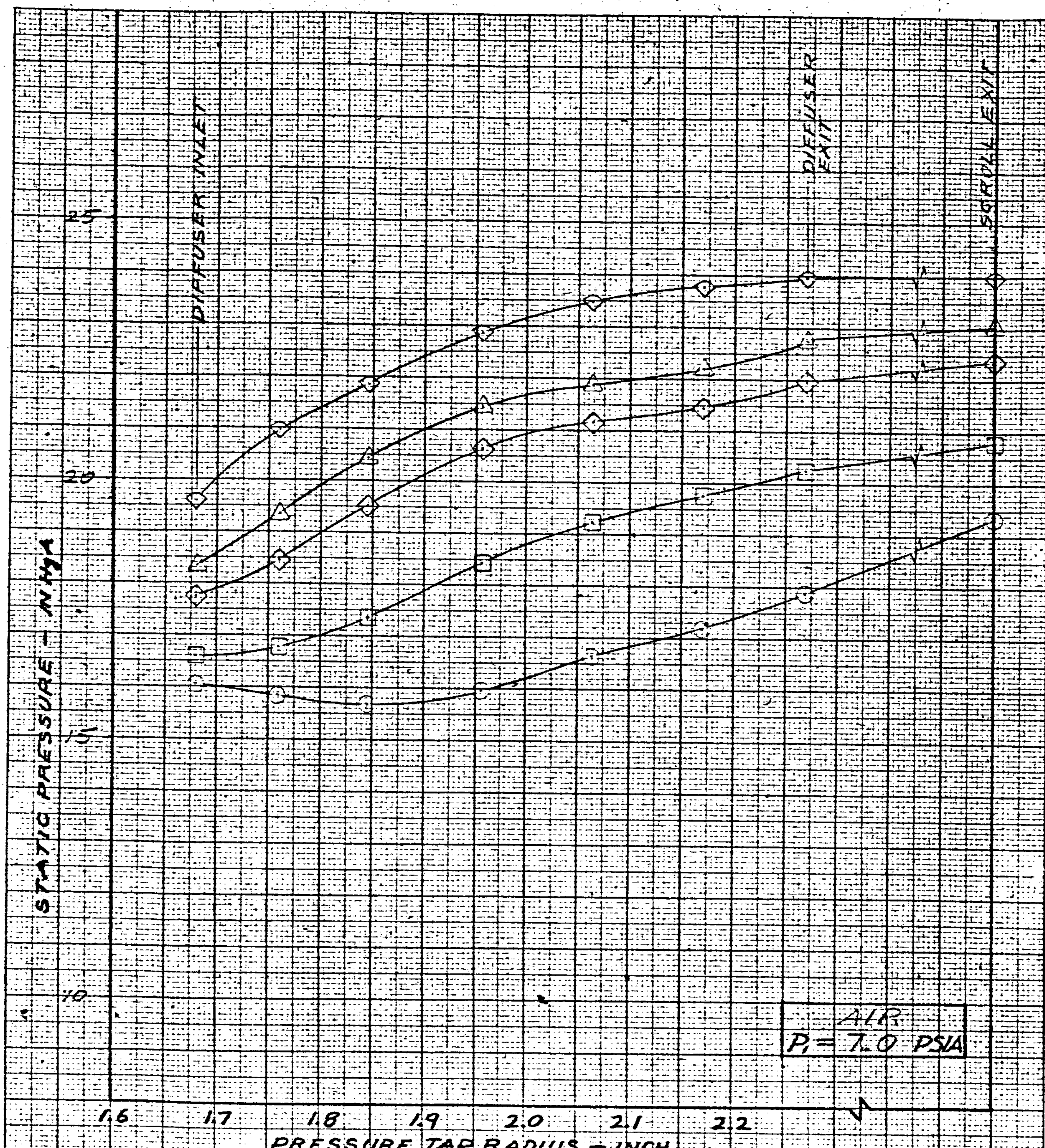

CALCULATED BY		
TRACED BY	Indwix	3-29-65
CHECKED BY		
APPROVED BY		
UNIT NO.		

STATIC PRESSURE DISTRIBUTION
ALONG DIFFUSER PART 871034

$\% \frac{N}{\sqrt{\theta}} = 100$

DATA FILE 43,60

AIRESEARCH MANUFACTURING COMPANY

P 5106

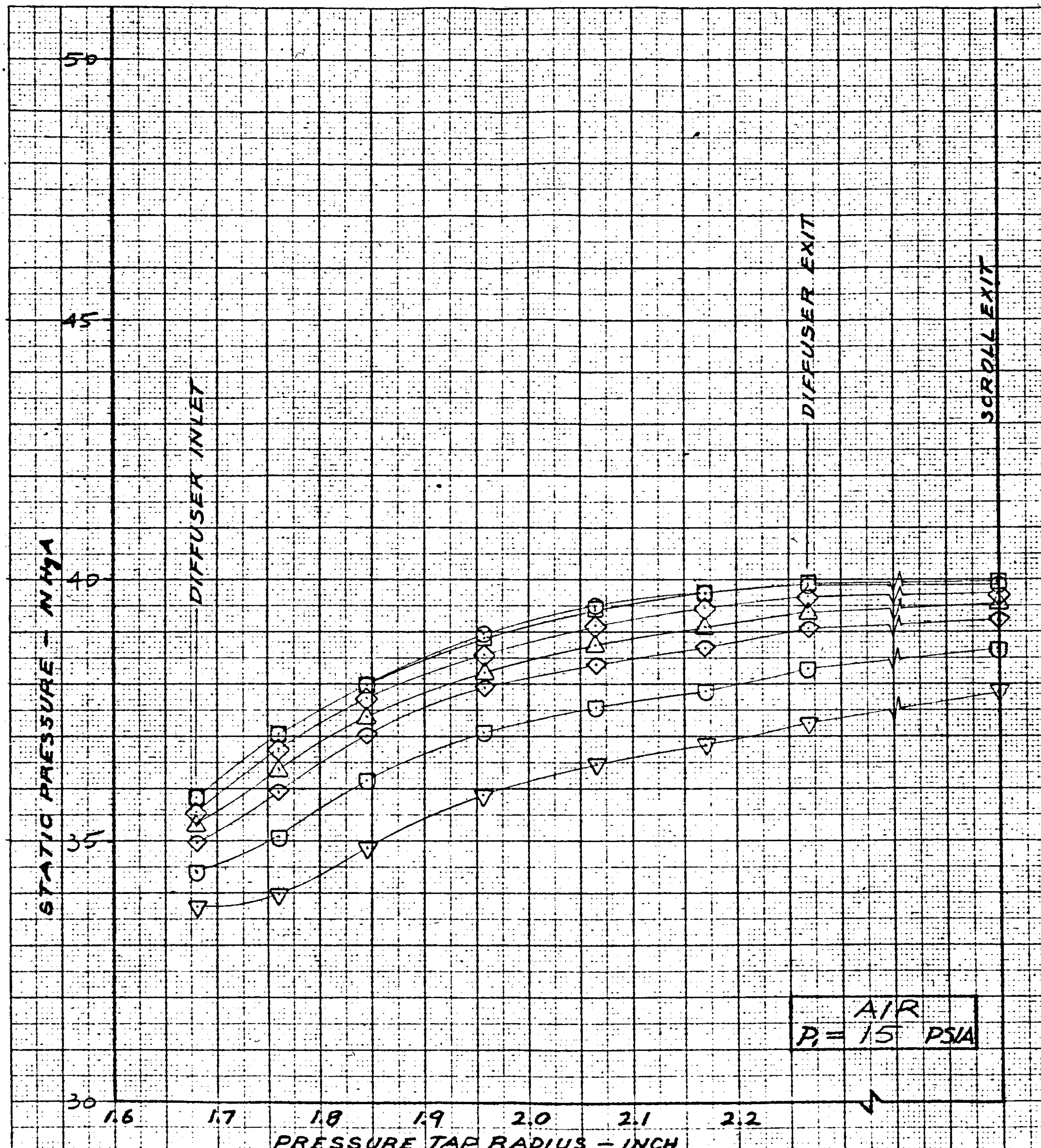

CALCULATED BY			STATIC PRESSURE DISTRIBUTION ALONG DIFFUSER PART 871034
TRACED BY		4-1-66	$\%\frac{N}{\sqrt{\theta}} = 70$
CHECKED BY			
APPROVED BY			AIRESEARCH MANUFACTURING COMPANY
UNIT NO.			

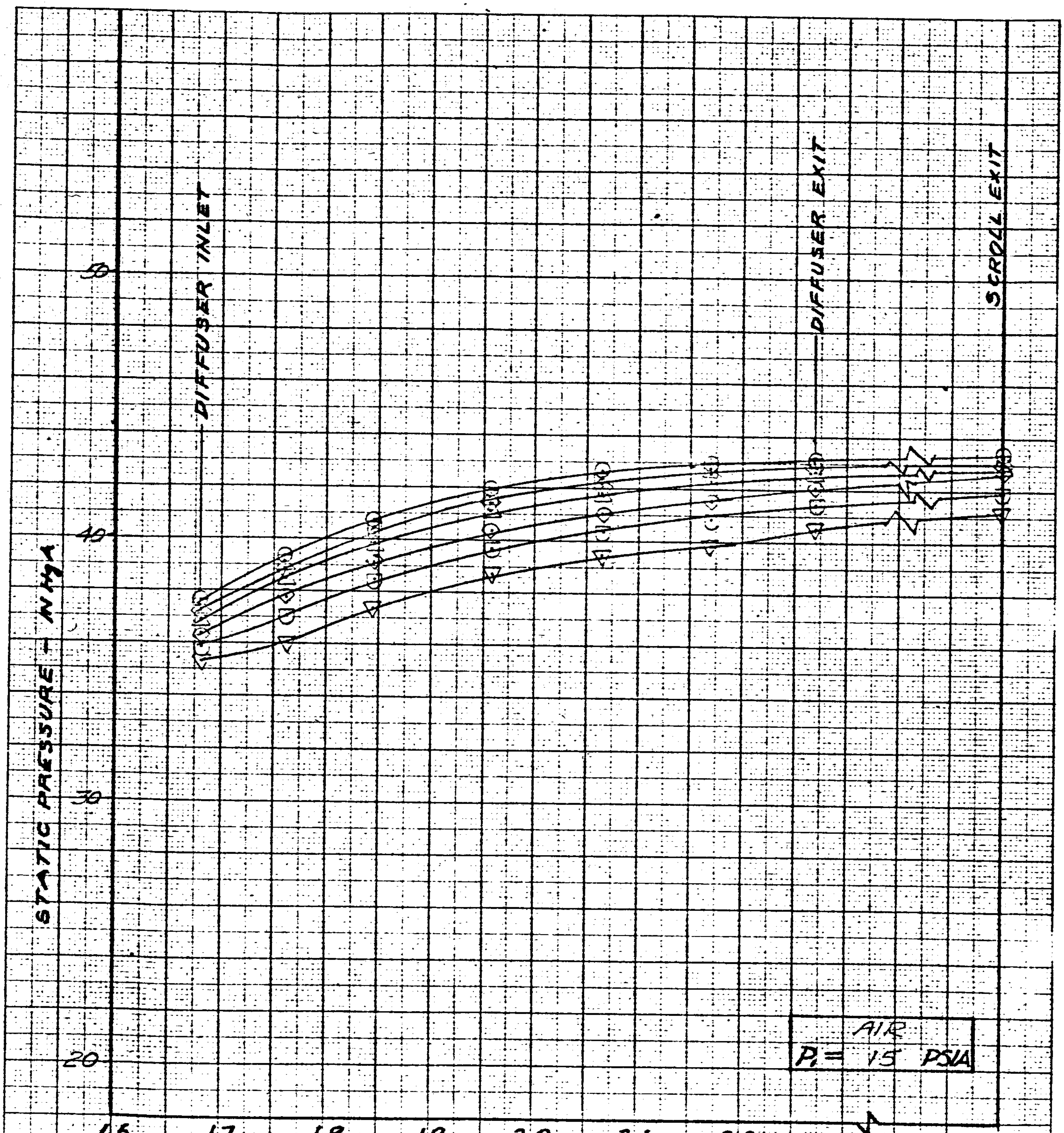

CALCULATED BY			STATIC PRESSURE DISTRIBUTION ALONG DIFFUSER PART 871034	$N/\sqrt{\theta}$ = 50
TRACED BY				
CHECKED BY				
APPROVED BY			AIRESEARCH MANUFACTURING COMPANY	DATA PAGE 61
UNIT NO.				

P 5106

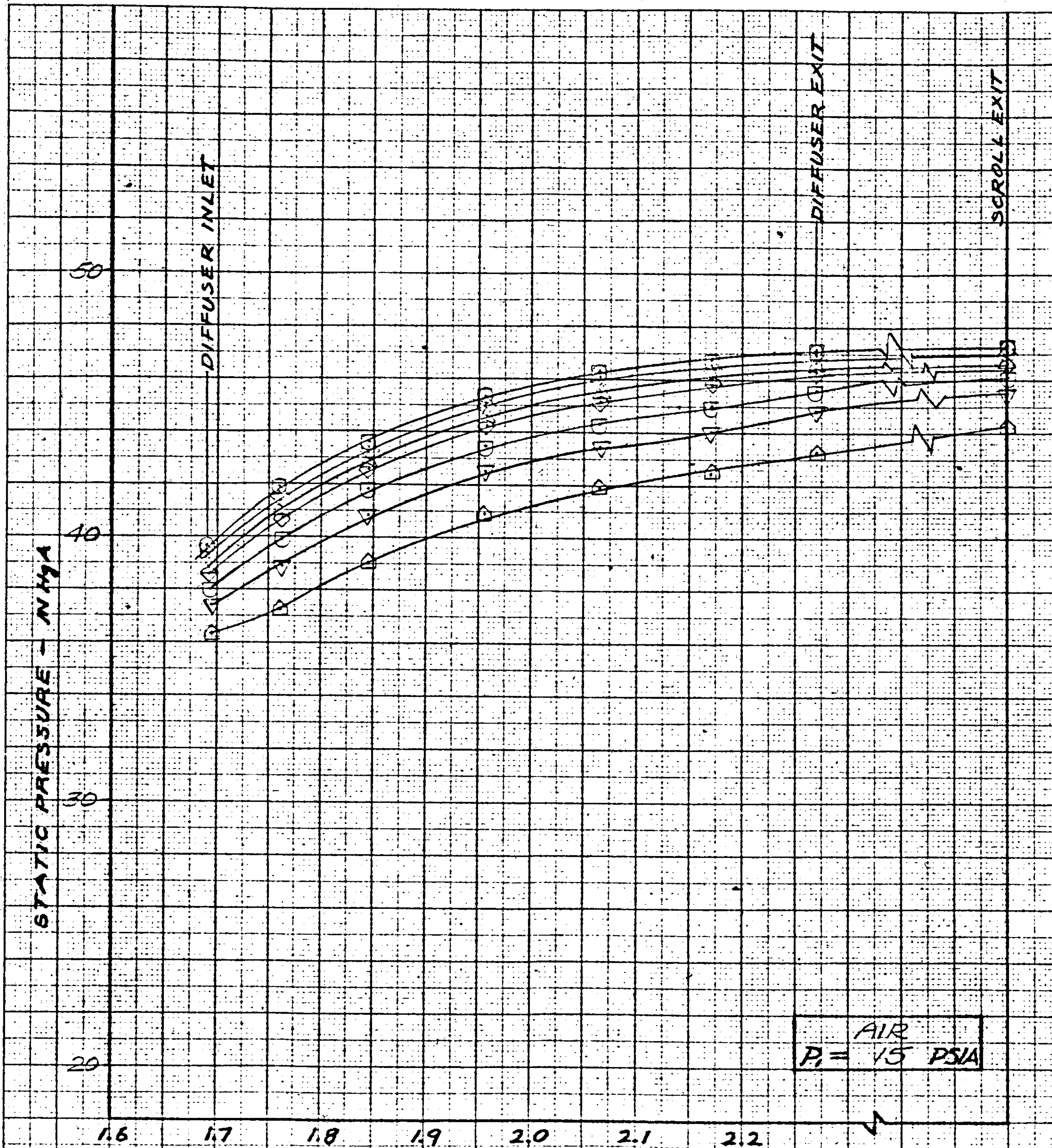

CALCULATED BY	
TRACED BY	
CHECKED BY	
APPROVED BY	
UNIT NO.	

STATIC PRESSURE DISTRIBUTION
ALONG DIFFUSER PART 871034

AIRESEARCH MANUFACTURING COMPANY

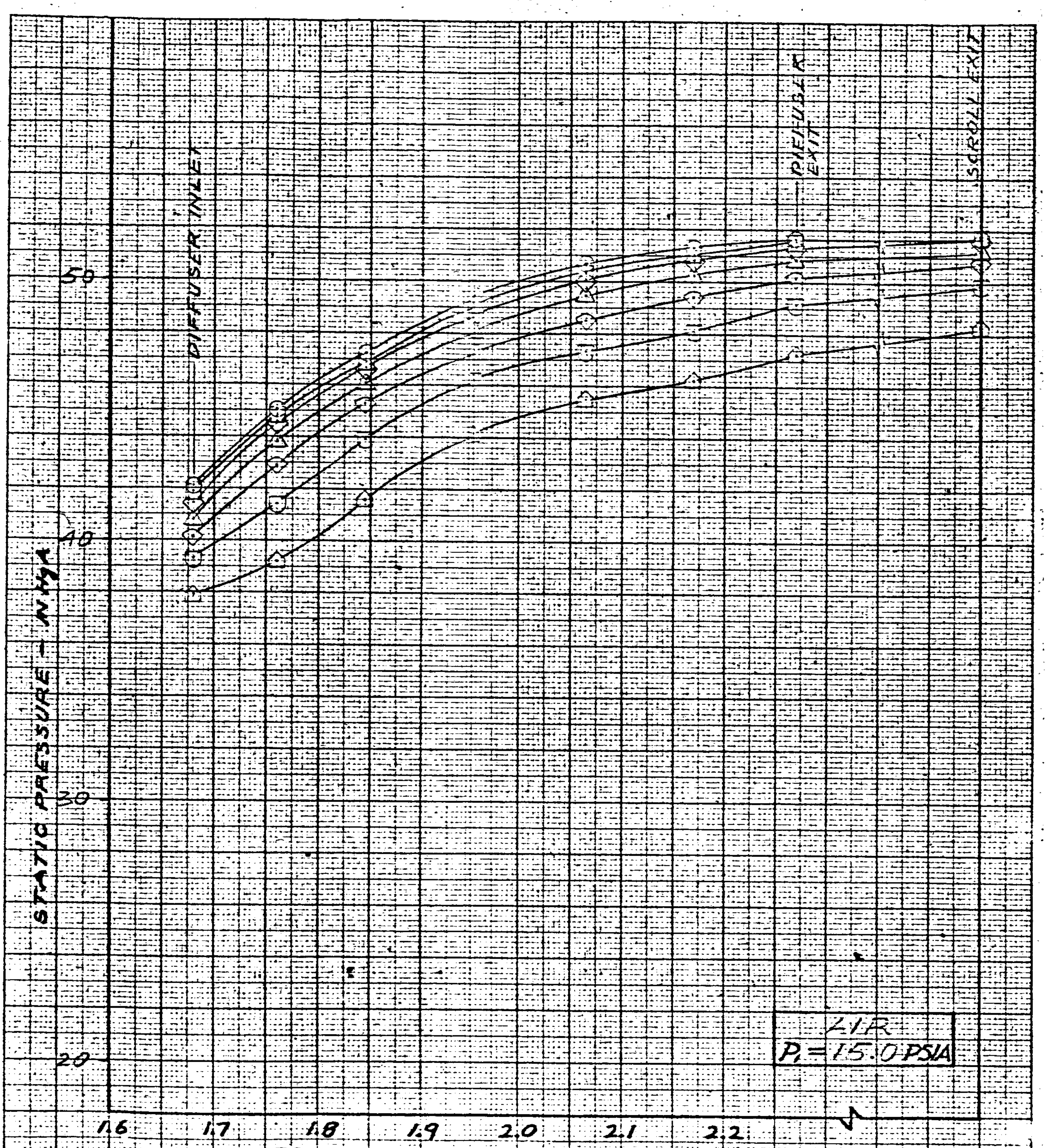

CALCULATED BY			STATIC PRESSURE DISTRIBUTION ALONG DIFFUSER PART 871034	$\%\frac{N}{\sqrt{\theta}}$ = 100
TRACED BY		3-29-50		
CHECKED BY				
APPROVED BY				DATA PAGE
UNIT NO.			AIRESEARCH MANUFACTURING COMPANY	60

P 5105

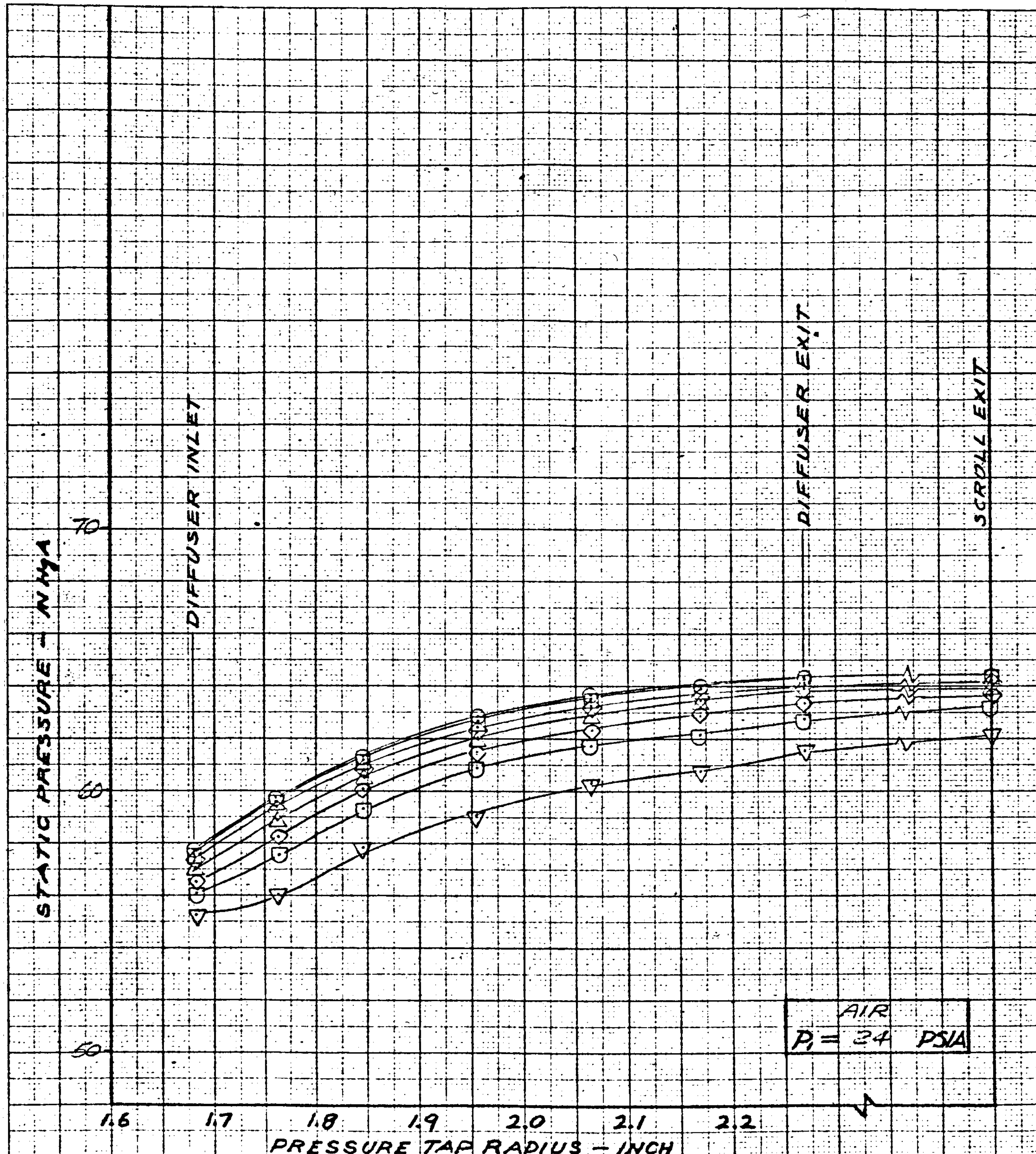

CALCULATED BY			STATIC PRESSURE DISTRIBUTION ALONG DIFFUSER PART 871034	$\% \frac{N}{\sqrt{\theta}} = 70$
TRACED BY				
CHECKED BY				DATA PAGE
APPROVED BY			AIRESEARCH MANUFACTURING COMPANY	52
UNIT NO.				

P 5106

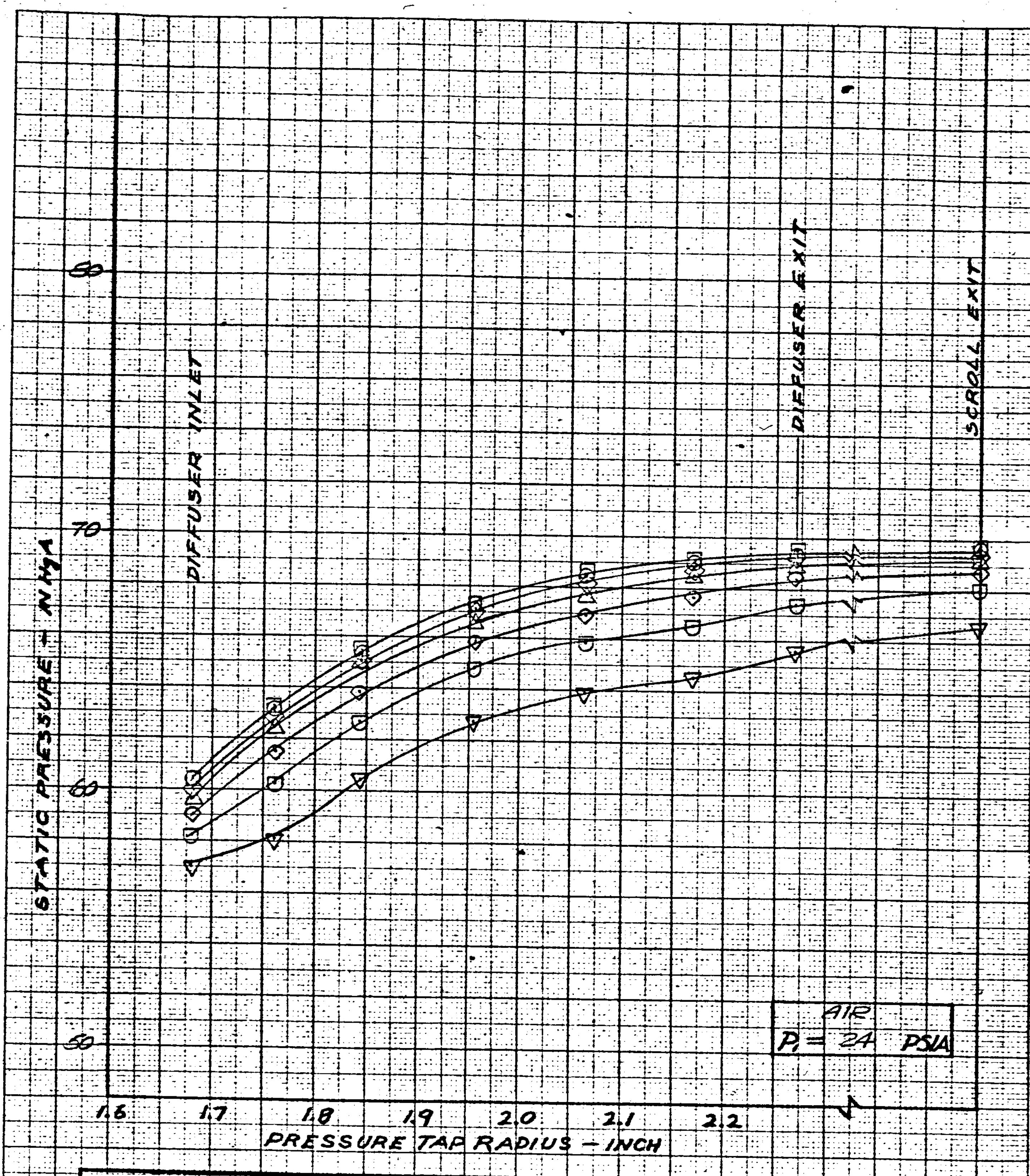

		STATIC PRESSURE DISTRIBUTION ALONG DIFFUSER PART 871034	$\frac{\%N}{\sqrt{\theta}}$ = 80
CALCULATED BY			
TRACED BY	SCL		
CHECKED BY			
APPROVED BY		AIRESEARCH MANUFACTURING COMPANY	DATA PAGE 63
UNIT NO.			

P 5106

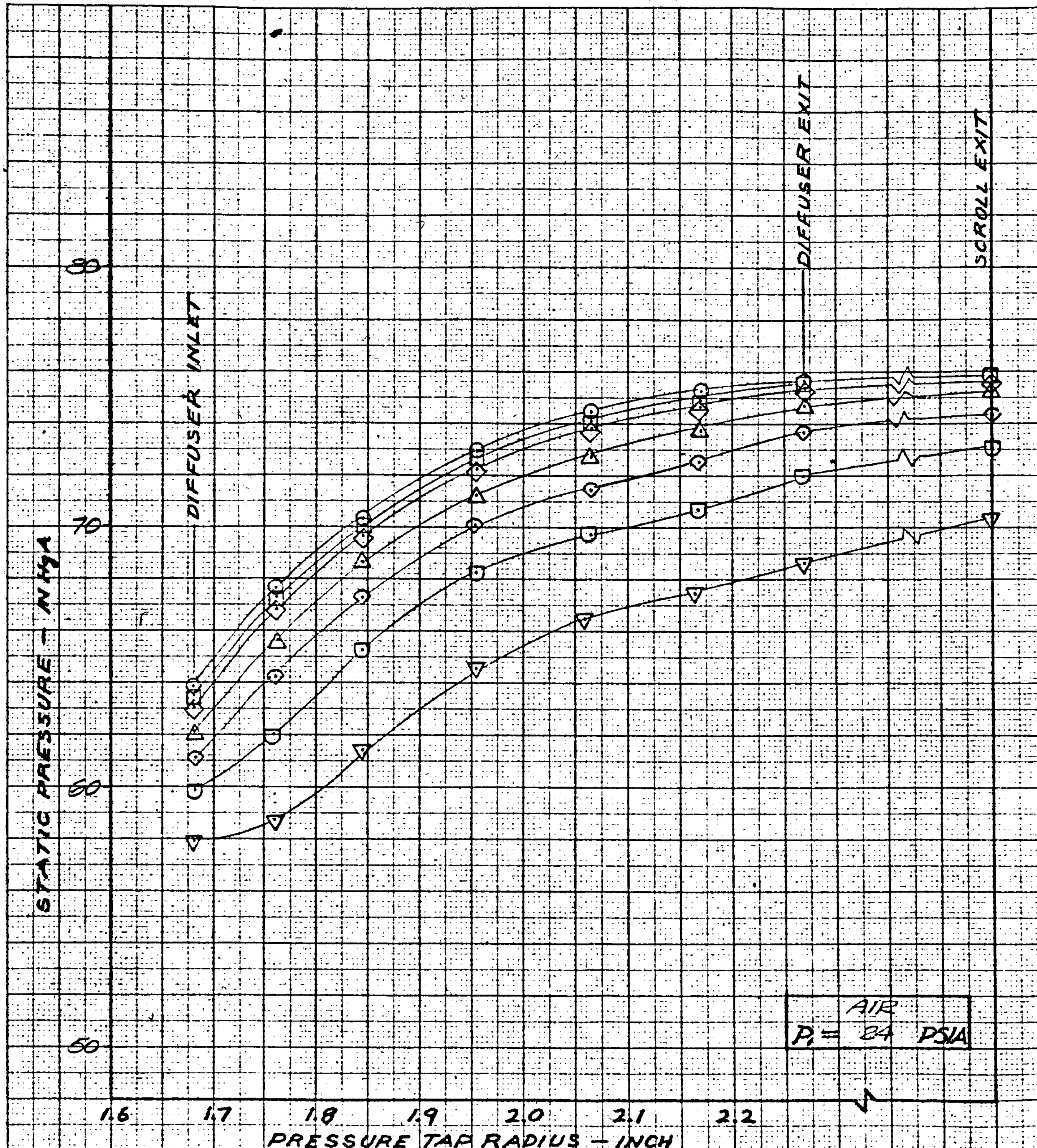

			STATIC PRESSURE DISTRIBUTION ALONG DIFFUSER PART 871034	$\% \frac{N}{\sqrt{\theta}}$ = 90
CALCULATED BY				
TRACED BY	HCL			
CHECKED BY				
APPROVED BY			AIRESEARCH MANUFACTURING COMPANY	DATA PAGE
UNIT NO.				63

P 5106

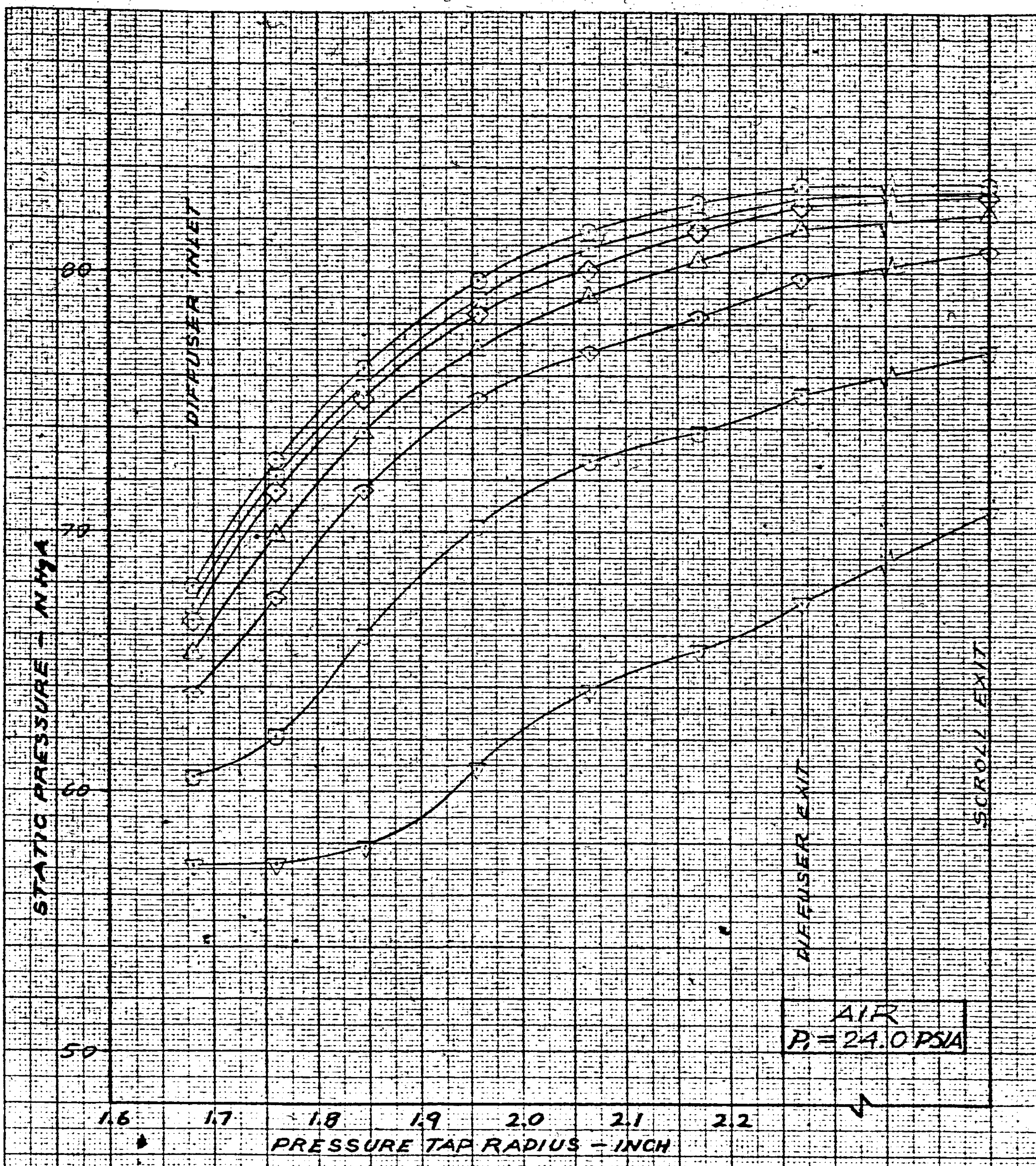

CALCULATED BY		
TRACED BY		
CHECKED BY		
APPROVED BY		
UNIT NO.		

STATIC PRESSURE DISTRIBUTION
ALONG DIFFUSER PART 871034

% $N/\sqrt{\theta}$ = 100

DATA PAGE

AIRESEARCH MANUFACTURING COMPANY

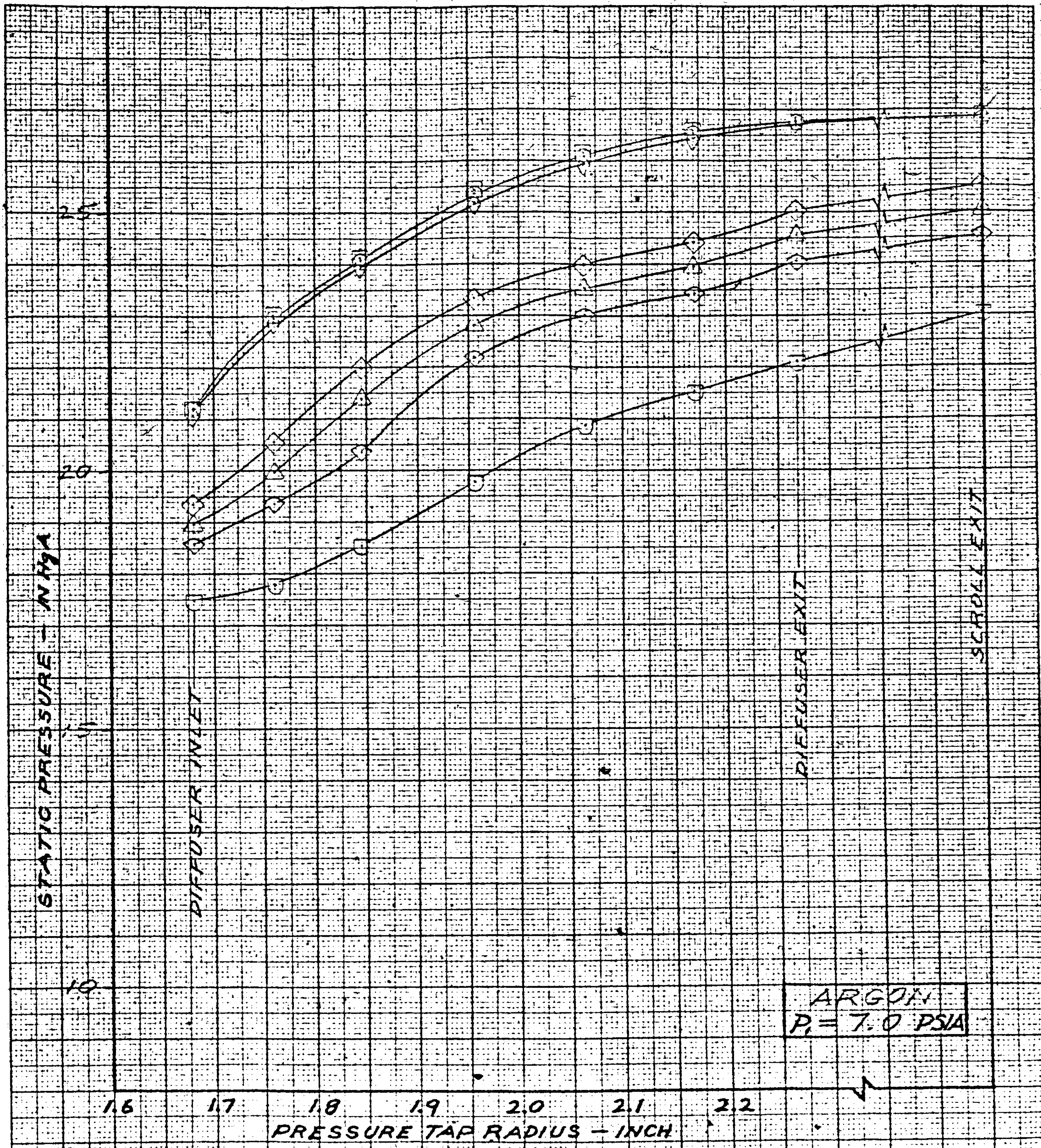

CALCULATED BY		
TRACED BY	Ludwig	3-29-62
CHECKED BY		
APPROVED BY		
UNIT NO.		

STATIC PRESSURE DISTRIBUTION
ALONG DIFFUSER PART 871034

$\% \frac{N}{\sqrt{\theta}} = 100$

AIRESEARCH MANUFACTURING COMPANY

65

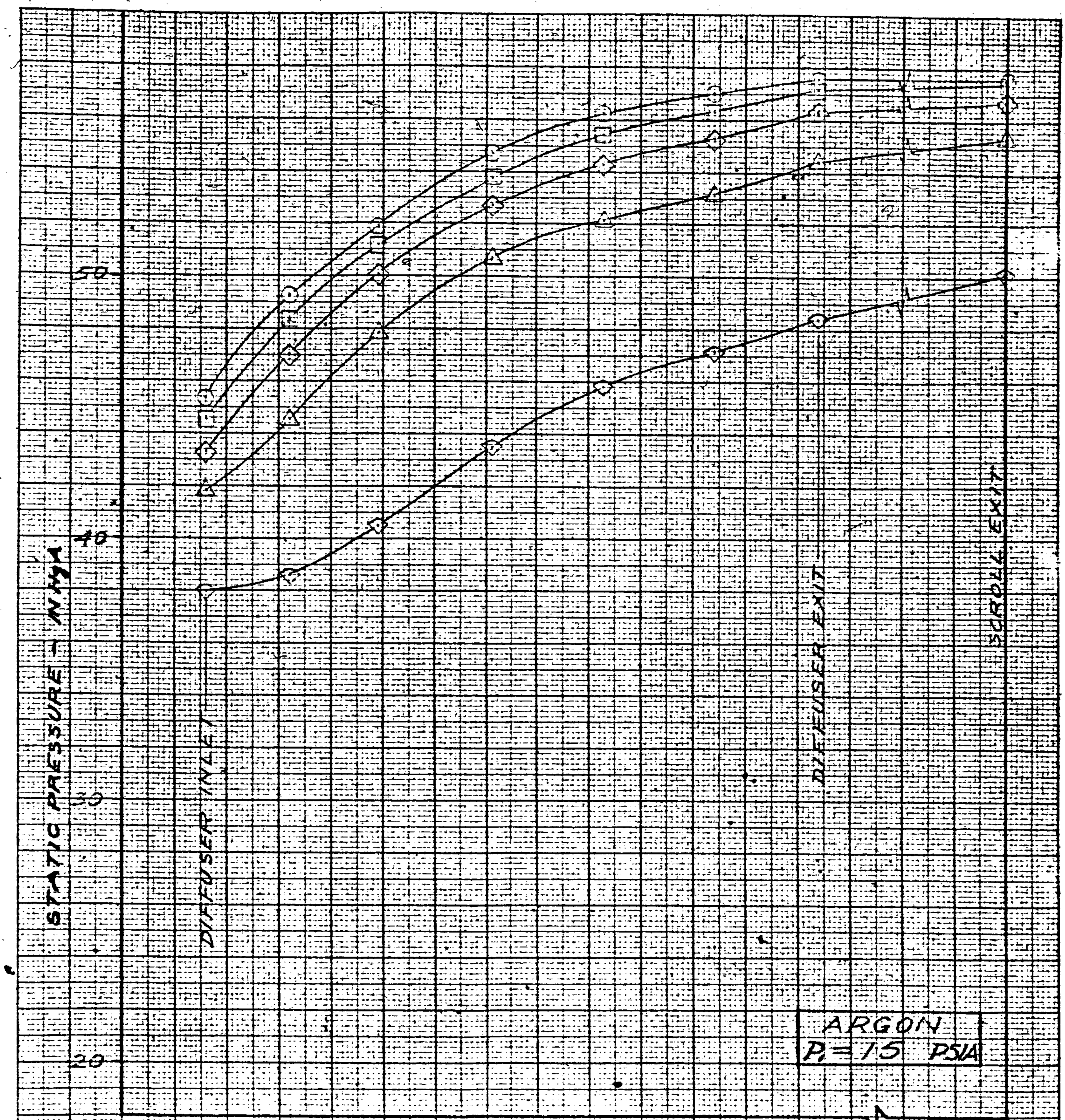

CALCULATED BY			STATIC PRESSURE DISTRIBUTION ALONG DIFFUSER PART 871034		$\frac{\% N}{\% \sqrt{\theta}}$ = 100
TRACED BY	[illegible]	3-30-66			
CHECKED BY					
APPROVED BY					DATA P.
UNIT NO.			AIRESEARCH MANUFACTURING COMPANY		65

P 5606

FINAL REPORT DISTRIBUTION LIST
FOR CONTRACT NAS3-6463
PERFORMANCE EVALUATION OF A 3.2-INCH DIAMETER RADIAL FLOW COMPRESSOR

NASA Lewis Research Center (1)
21000 Brookpark Road
Cleveland, Ohio 44135
Attn: Jack A. Heller
Mail Stop 500-201

NASA Lewis Research Center (1)
21000 Brookpark Road
Cleveland, Ohio 44135
Attn: Calvin L. Ball
Mail Stop 5-9

NASA Lewis Research Center (1)
21000 Brookpark Road
Cleveland, Ohio 44135
Attn: John E. Dilley
Mail Stop 500-309

NASA Lewis Research Center (1)
21000 Brookpark Road
Cleveland, Ohio 44135
Attn: Tech. Util. Office
John J. Weber
Mail Stop 3-19

NASA Scientific and Technical Information Facility (1 + 2 repro copies)
Post Office Box 33
College Park, Maryland
Attn: Acquisitions Branch
(SQT-34054)

NASA Lewis Research Center (1)
21000 Brookpark Road
Cleveland, Ohio 44135
Attn: Report Control Office
Mail Stop 5-5

NASA Lewis Research Center (2)
21000 Brookpark Road
Cleveland, Ohio 44135
Attn: Library
Mail Stop 60-3

NASA Lewis Research Center (1)
21000 Brookpark Road
Cleveland, Ohio 44135
Attn: Dr. B. Lubarsky
Mail Stop 500-201

NASA Lewis Research Center (1)
21000 Brookpark Road
Cleveland, Ohio 44135
Attn: I. I. Pinkel
Mail Stop 5-3

NASA Lewis Research Center (1)
21000 Brookpark Road
Cleveland, Ohio 44135
Attn: Melvin J. Hartmann
Mail Stop 5-9

NASA Lewis Research Center (1)
21000 Brookpark Road
Cleveland, Ohio 44135
Attn: Warner L. Stewart
Mail Stop 77-2

NASA Lewis Research Center (1)
21000 Brookpark Road
Cleveland, Ohio 44135
Attn: Donald C. Guentert
Mail Stop 500-201

NASA Lewis Research Center (1)
21000 Brookpark Road
Cleveland, Ohio 44135
Attn: Donald G. Beremand
Mail Stop 500-201

NASA Lewis Research Center (1)
21000 Brookpark Road
Cleveland, Ohio 44135
Attn: William A. Benser
Mail Stop 5-9

NASA Lewis Research Center (1)
21000 Brookpark Road
Cleveland, Ohio 44135
Attn: Daniel T. Bernatowicz

NASA Ames Research Center (1)
Moffett Field, California 94035
Attn: Library

NASA Flight Research Center (1)
Post Office Box 273
Edwards, California 93523
Attn: Library

NASA Goddard Space Flight Center (1)
Greenbelt, Maryland 20771
Attn: Library

Jet Propulsion Laboratory (1)
4800 Oak Grove Drive
Pasadena, California 91103
Attn: Library

NASA Langley Research Center (1)
Langley Station
Hampton, Virginia 23365
Attn: Library

NASA Manned Spacecraft Center (1)
Houston, Texas 77001
Attn: Library

NASA Marshall Space Flight Center (1)
Huntsville, Alabama 35812
Attn: Library

NASA Western Operations (1)
150 Pico Boulevard
Santa Monica, California 90406
Attn: Library

National Aeronautics and
Space Administration (3)
Washington, D. C. 20546
Attn: Herbert D. Rochen
Code RNP

National Aeronautics and
Space Administration (1)
Washington, D. C. 20546
Attn: Dr. Fred Schulman
Code RNP

NASA Manned Spacecraft Center (1)
Houston, Texas 77001
Attn: W. E. Rice
Power Generation Branch

U.S. Army Engineer R & D Labs.
Gas Turbine Test Facility (1)
Fort Belvoir, Virginia
Attn: W. Crim

Department of the Air Force (3)
Air Force Aero Propulsion
Laboratory
Wright-Patterson Air Force Base
Ohio 45433
Attn: George E. Thompson
Aerospace Power Division

Office of Naval Research (1)
Department of the Navy
Washington 25, D. C.
Attn: Dr. Ralph Roberts

Bureau of Naval Weapons (1)
Department of the Navy
Washington 25, D. C.
Attn: Code RAPP

Air Force Systems Command (1)
Aeronautical Systems Division
Wright-Patterson Air Force Base
Ohio 45433
Attn: Librarian

Power Information Center (1)
University of Pennsylvania
Moore School Building
200 South 33rd Street
Philadelphia, Pennsylvania
19104

AIRESEARCH MANUFACTURING COMPANY OF ARIZONA
A DIVISION OF THE GARRETT CORPORATION
PHOENIX, ARIZONA

Aerojet-General Corporation (1)
Azusa, California 91703
Attn: Librarian

The Boeing Company (1)
Aero-Space Division
Box 3707
Seattle, Washington 98124
Attn: Librarian

Continental Aviation & Engineering
Corp. (1)
12700 Kercheval Avenue
Detroit, Michigan 48215
Attn: Librarian

Curtiss-Wright Corporation (1)
Wright Aero Division
Main & Passaic Streets
Woodridge, New Jersey 07075
Attn: Librarian

General Electric Company (1)
FPLD
Cincinnati, Ohio 45215
Attn: Librarian

General Electric Company (1)
Lynn, Massachusetts 01905
Attn: Librarian

Massachusetts Institute of
Technology (1)
Cambridge, Massachusetts 02139
Attn: Librarian

Mechanical Technology Inc. (1)
968 Albany-Shaker Road
Latham, N. Y. 12110
Attn: Librarian

Northern Research & Engineering Co. (1)
219 Vassar Street
Cambridge, Massachusetts 02139
Attn: Librarian

Pratt & Whitney Aircraft (1)
400 Main Street
East Hartford, Connecticut
06108
Attn: Peter Bolan, APS-2J

Solar, Division of
International Harvester (1)
2200 Pacific Highway
San Diego, California 92212
Attn: Librarian

TRW Space Power Group (1)
7209 Platt Avenue
Cleveland, Ohio 44104
Attn: Librarian

United Aircraft Research
Lab. (1)
East Hartford, Connecticut
06108
Attn: Librarian

Westinghouse Electric Corp. (1)
Aerospace Electrical Division
Post Office Box 989
Lima, Ohio 45802
Attn: AED Librarian